

DEPOSITIONAL ENVIRONMENT, PETROLOGY, AND
DIAGENESIS OF THE LAVERTY-HOOVER SAND-
STONE IN BEAVER, HARPER, ELLIS, AND
WOODWARD COUNTIES, OKLAHOMA AND
LIPSCOMB COUNTY, TEXAS

By

Douglas Lynn Yelken
Bachelor of Science
in Arts and Science
Oklahoma State University
Stillwater, Oklahoma

1982

Submitted to the Faculty of the
Graduate College of the
Oklahoma State University
in partial fulfillment of
the requirements for
the Degree of
MASTER OF SCIENCE
May, 1985

Thesis
1985
Y43d
cop. 2



DEPOSITIONAL ENVIRONMENT, PETROLOGY, AND
DIAGENESIS OF THE LAVERTY-HOOVER SAND-
STONE IN BEAVER, HARPER, ELLIS, AND
WOODWARD COUNTIES, OKLAHOMA AND
LIPSCOMB COUNTY, TEXAS

Thesis Approved:

Zuhair al-Sharrah
Thesis Adviser

Arthur W. Cleaves

Gary F. Stewart

Norman N. Dushan
Dean of the Graduate College

1216430

ACKNOWLEDGMENTS

I would like to thank Phillips Petroleum Company for its financial support of this study. Phillips provided electric logs, x-ray diffraction data, scanning electron microscope analysis, and thin sections for the project. Individuals within the Exploration Projects Section of Phillips devoted a tremendous amount of time and effort into the study and this is deeply appreciated.

Bailey Rascoe suggested the topic and provided numerous helpful suggestions throughout the study. Dr. Zuhair Al-Shaieb served as my adviser, and was a tremendous support throughout the study. Drs. Arthur Cleaves and Gary Stewart served on my advisory committee and I would like to thank them for editing the thesis and for their helpful suggestions.

The Oklahoma Core Library provided the opportunity to describe and sample the cores, Heinz Hall photographed the cores, and Pat Birdsall patiently typed the manuscript.

TABLE OF CONTENTS

Chapter	Page
I. ABSTRACT.	1
II. INTRODUCTION.	3
Location	3
Production Characteristics	3
Objectives	5
Methods of Investigation	5
III. GEOLOGIC SETTING.	8
Introduction	8
Regional Tectonics	8
Regional Structural Setting.	12
Local Structural Geology	15
IV. STRATIGRAPHIC FRAMEWORK	16
Introduction	16
Regional Stratigraphy of the Virgilian Series	16
Douglas Group	18
Shawnee Group	20
Wabaunsee Group	20
Genetic Units.	22
Facies and Stratigraphic Boundaries of P.V.U. 4.	25
V. DEPOSITIONAL ENVIRONMENT.	30
Introduction	30
Transgressive Phase.	31
Shelf Limestone-Shale System.	31
Shelf Edge Carbonate Bank System.	31
Basinal Limestone System.	33
Depositional Model for the Trans- gressive Phase.	33

Chapter	Page
Regressive Phase	35
Source of Clastic Material.	35
Sand Trends, Boundaries, and Thickness	35
Interpretation of Electric Log Characteristics.	36
Fluvial Facies	36
Deltaic Facies	36
Discussion of Cores.	39
Shell Oil Co., Bedell No. 1-20	39
Gulf Oil Co., McClung No. 1.	39
Internal Features.	47
Interstratification.	47
Small-Scale Cross Bedding.	47
Bioturbation	51
Ripple and Horizontal Laminations.	51
Rip up Clasts.	51
Channel Lag.	51
Classification of the Laverty- Hoover Delta	54
Depositional Model for the Regressive Phase	56
VI. PETROLOGY	58
Composition.	58
Detrital Constituents.	58
Diagenetic Constituents.	67
VII. DIAGENESIS.	79
Introduction	79
Silica	79
Dissolution of Feldspar.	80
Dissolution of Detrital Matrix	80
Carbonates	80
Authigenic Clays	86
Other Diagenetic Constituents.	94
Diagenetic History	94
VIII. POROSITY.	97
Introduction	97
Primary Porosity	97
Secondary Porosity	98
IX. CONCLUSIONS	103
BIBLIOGRAPHY.	105

LIST OF TABLES

Table	Page
I. Average Mineralogic Composition of the Lavery Hoover Sandstone	61

LIST OF FIGURES

Figure	Page
1. Location Map of Study Area	4
2. Structural Geologic Map of Basement Rocks, Showing the Major Tectonic Features of the Mid-continent Region	9
3. Structural Setting of the Area of Study.	13
4. Structure of the Haskell Limestone Throughout the Northern Shelf	14
5. General Stratigraphy of Permo-Carboniferous Rocks Throughout the Mid-continent Region.	17
6. Isopach Map of the Virgilian Series in the Mid- continent.	19
7. Correlation Chart of Upper Pennsylvanian Rocks in the Anadarko Basin.	21
8. Diagrammatic Illustrations of Genetic Increment of Strata.	24
9. Electric Log Characteristics of Shelf-edge Carbonate Bank and Shelf Limestone-shale Systems.	32
10. Depositional Model for the Transgressive Phase . .	34
11. Electric-Log Characteristics of Fluvial and Deltaic Facies	37
12. Core Description of Shell Bedell No. 1-20. Depth: 4390-4466 ft	40
13. Photograph of Shell Bedell No. 1-20 Core. Depth: 4390-4429 ft	41
14. Photograph of Shell Bedell No. 1-20 Core. Depth: 4429-4466 ft	42

Figure	Page
15. Core Description of Gulf McClung No. 1. Depth: 4163-4266 ft 6 in	43
16. Photograph of Gulf McClung No. 1 Core. Depth: 4163-4199 ft	44
17. Photograph of Gulf McClung No. 1 Core. Depth: 4199-4235 ft	45
18. Photograph of Gulf McClung No. 1 Core. Depth: 4235-4266 ft 6 in	46
19. Interdistributary Bay Deposit. Gulf McClung No. 1 Core. Depth: 4230-4231 ft.	48
20. Interstratification of Sandstone and Shale	49
21. Small-Scale Cross Beds and Rip Up Clasts	50
22. Bioturbated Sandstone.	52
23. Channel-Lag Deposit.	53
24. Characteristics of High Constructive Lobate Deltas	55
25. Depositional Model of the Regressive Phase	57
26. Classification of Samples from Shell Bedell No. 1-20 Core.	59
27. Classification of Samples from Gulf McClung No. 1 Core	60
28. Photomicrograph of Dust Rims Showing the Original Outline of Detrital Quartz Grains.	63
29. Photomicrograph of Monocrystalline and Poly- crystalline Quartz	63
30. Photomicrograph of Polycrystalline Quartz.	64
31. Photomicrograph of Stained Potassium Feldspar Grains	64
32. Photomicrograph Showing Several Stained Potassium-Feldspar Grains.	65
33. Photomicrograph of Several Twinned Plagioclase Feldspar Grains.	65

Figure	Page
34. Photomicrograph of Several Low-Rank Metamorphic-Rock Fragments	66
35. Photomicrograph of Sedimentary Rock Fragment	66
36. Photomicrograph of Several Detrital Mica Grains.	68
37. Photomicrograph of Opaque Mineral Grains	68
38. Photomicrograph of an Elongate Detrital Chert Grain.	69
39. Photomicrograph of a Glauconite Grain.	69
40. Photomicrograph of Detrital Zircon	70
41. Photomicrograph, Fragment of a Fossil.	70
42. Photomicrograph of Detrital Matrix Material.	71
43. SEM Micrograph Showing Abundance of Quartz Overgrowths.	71
44. Photomicrograph of Calcium-Carbonate Cement.	72
45. Photomicrograph of Siderite Concentrated in Detrital Matrix.	72
46. Photomicrograph of Siderite-Lined Edges of Calcite Cement.	73
47. Photomicrograph of Dolomite-Surrounded Detrital Grains.	73
48. Photomicrograph of Iron Oxides	75
49. SEM Micrograph of Framboidal Pyrite.	75
50. Photomicrograph of Pore-Filling Kaolinite.	76
51. Photomicrograph of Detrital Grains Coated With Authigenic Illite.	76
52. Photomicrograph of Psuedomatrix Material	77
53. Photomicrograph of Psuedomatrix Material	77
54. SEM Micrograph Showing Ductile Deformation of Micaceous Material	78

Figure	Page
55. SEM Micrograph of a Corroded Quartz Grain Lined with Authigenic Clays	81
56. Photomicrograph of Calcite-Invaded Detrital Grains	81
57. Photomicrograph of Grain Molds	82
58. Photomicrograph of Partly Dissolved Feldspar	82
59. SEM Micrograph of Quartz Overgrowth, Feldspar Dissolution and Framboidal Pyrite.	83
60. SEM Micrograph of a Partially Dissolved Feldspar Grain	83
61. SEM Micrograph of Dissolved Feldspar	84
62. SEM Micrograph of Partly Dissolved Feldspar and Authigenic Chlorite.	84
63. Photomicrograph of Dissolved Detrital Matrix	85
64. SEM Micrograph Showing Evidence of Dissolution of Silica by Calcite.	85
65. SEM Micrograph of Authigenic Pore-Filling Kaolinite.	88
66. SEM Micrograph of Quartz Overgrowth, Authigenic Kaolinite, and Framboidal Pyrite	88
67. SEM Micrograph of Pore-Filling Authigenic Kaolinite.	89
68. SEM Micrograph of Pore-Filling Kaolinite and Quartz Overgrowths	89
69. SEM Micrograph of Pore-Filling Kaolinite and Quartz Overgrowths	90
70. SEM Micrograph of Grain-Coating Authigenic Illite and Chlorite.	90
71. SEM Micrograph of Authigenic Illite.	91
72. SEM Micrograph of Illite-Lined Quartz Grain and Chlorite-Bridged Pore Space	91

Figure	Page
73. SEM Micrograph of Illite-Lined Corroded Quartz Grain.	92
74. SEM Micrograph of Authigenic Chlorite.	92
75. SEM Micrograph of Authigenic Chlorite.	93
76. SEM Micrograph of Quartz Overgrowth and Authigenic Chlorite Occupying Pore Space	93
77. Diagenetic History of the Lavery-Hoover Sandstone.	95
78. Photomicrograph Showing Reduced Primary Intergranular Porosity.	99
79. Photomicrograph of Enlarged Intergranular Porosity	99
80. Photomicrograph Showing Grain Molds.	101
81. Photomicrograph Showing Dissolved Detrital Matrix	101
82. Photomicrograph of Microporosity	102

LIST OF PLATES

Plate	
I.	Lithofacies Map of Pennsylvanian Virgilian Upper Unit 4 containing the Lavery-Hoover Sandstone In Pocket
II.	Isopach Map of Pennsylvanian Virgilian Upper Unit 4 containing the Lavery-Hoover Sandstone In Pocket
III.	Sandstone Isolith Map of the Lavery-Hoover Sandstone. In Pocket
IV.	Structural Contour Map on top of the Lavery-Hoover Sandstone. In Pocket
V.	SP-Resistivity Characteristics of the Lavery-Hoover Sandstone. In Pocket
VI.	Cross Section Location Map. In Pocket
VII.	Stratigraphic Cross Section A-A'. In Pocket
VIII.	Stratigraphic Cross Section B-B'. In Pocket
IX.	Stratigraphic Cross Section C-C'. In Pocket
X.	Stratigraphic Cross Section D-D'. In Pocket
XI.	Stratigraphic Cross Section E-E'. In Pocket
XII.	Stratigraphic Cross Section F-F'. In Pocket
XIII.	Stratigraphic Cross Section G-G'. In Pocket
XIV.	Stratigraphic Cross Section H-H'. In Pocket

CHAPTER I

ABSTRACT

The Lavery-Hoover Sandstone of Virgilian (Pennsylvanian) age is a fluvial-deltaic complex with fluvial sandstones in the eastern part of the study area and deltaic deposits in the western part. Clastic deposition was initiated by a regressive episode which allowed the clastic material to be transported from the Ouachita source area, westward into the Anadarko Basin. Minor wave action appears to have reworked the delta fronts, and the delta can best be classified as a high-constructive lobate delta. This delta has produced large amounts of gas from a northern, updip, stratigraphic trap.

Most of the sandstones within the Lavery-Hoover are classified as sublitharenites. The sandstone typically is dominated by quartz, contains small amounts of feldspar, and is fairly abundant in low rank metamorphic rock fragments.

Authigenic cements are present in the Lavery-Hoover Sandstone and include calcite, siderite, and minor amounts of dolomite. Authigenic clays include kaolinite, illite, and chlorite which probably were derived primarily from the dissolution of feldspar grains. Other diagenetic constit-

ments are quartz overgrowths, pyrite, and hematite.

Primary intergranular porosity is of minor importance in the Lavery-Hoover Sandstone. Secondary porosity is very abundant; dissolution of calcite cement and feldspar grains are considered to have created most of the secondary porosity.

CHAPTER II

INTRODUCTION

Location

The study area is located on the northern shelf of the Anadarko Basin in northwestern Oklahoma and includes small portions of the Texas and Oklahoma panhandles (Figure 1). It includes approximately 2160 square miles consisting of 36 townships (T.22-27 N., R.21-26W.) in Harper, Ellis, and Woodward Counties, Oklahoma, and 16 townships (T.1-4 N., R.25-28 E.C.M.) in Beaver County, Oklahoma. The study area also includes the northeastern corner of Lipscomb County, Texas. The Laverty-Hoover Sandstone is the primary unit of interest in this study; it is within the Wabaunsee Group, Virgilian Series, Pennsylvanian System.

Production Characteristics

The Laverty-Hoover Sandstone produces gas from an updip, stratigraphic trap in the Laverne gas area of Beaver and Harper Counties, Oklahoma. This producing zone was discovered in 1955 and by 1962 there were 154 wells producing from an average depth of 4,250 feet below ground

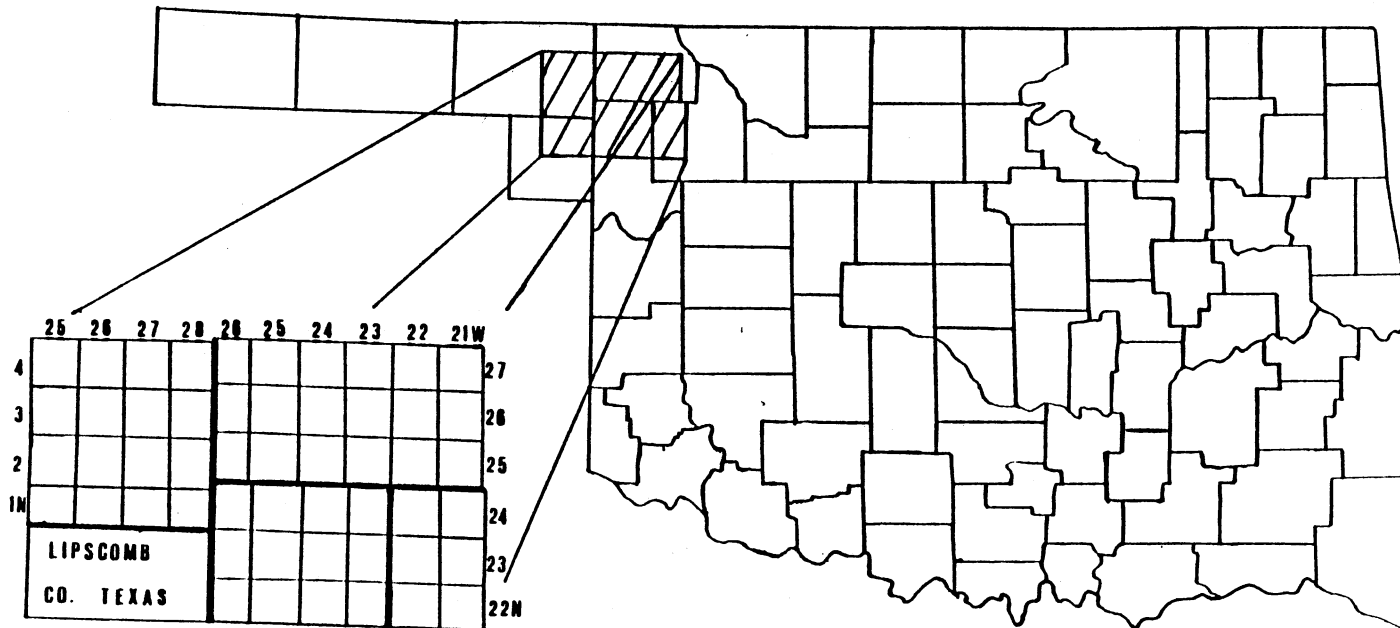


Figure 1. Location Map of the Study Area.

level. Recovery efficiency of the Lavery-Hoover gas is 80%, and the average well has an estimated total production of 10.56 billion cubic feet of gas. These wells have an estimated total proved reserve of 1,626 billion feet of gas in the Lavery-Hoover reservoir (Pate, 1962).

Objectives

The primary objectives of this study are: (1) to provide an interpretation concerning the depositional environment of the Lavery-Hoover Sandstone; (2) to define the overall geometry of the Lavery-Hoover sand body; (3) to show the average petrologic composition of the Lavery-Hoover Sandstone; (4) to determine the diagenetic events that have effected the Lavery-Hoover Sandstone since its burial and the relative time frame in which these events took place; and (5) to determine porosity types and their abundances in the Lavery-Hoover Sandstone.

Methods of Investigation

A search of literature was conducted in order to find material written about the thesis area or thesis topic that might benefit the study.

Selected electric well logs were used in the preparation of eight stratigraphic cross sections, which established a grid network throughout the study area. The Wabaunsee Group was divided into format units and these units were correlated. The format unit containing the Lavery-Hoover Sandstone was assigned the name of

Pennsylvanian Virgilian Upper 4 (P.V.U. 4) by Rascoe (1978).

Lithologic and structural data were used in this study; they were obtained through examination of more than 1200 electric well logs. Data sheets were used to record the parameters for mapping within P.V.U. 4, such as depth of sandstone (top), thickness of P.V.U. 4, sandstone isolith, percentage of sandstone, limestone isolith, percentage of limestone, shale isolith, and percentage of shale. A sandstone-isolith map was constructed to describe the trends, boundaries, and thicknesses of the Lavery-Hoover sandstone. An isopach map of P.V.U. 4 was constructed to estimate the paleotopographic surface and the basin configuration that were present during deposition of the Lavery-Hoover Sandstone. A structural contour map of the top of the Lavery-Hoover Sandstone was constructed in order to illustrate the present day structural setting of the sand body. A lithofacies map showed the different facies and their boundaries within genetic unit P.V.U. 4 and aided in the environmental interpretation of the unit. A log signature map of the Lavery-Hoover Sandstone illustrated thickness of the sand and aided in interpretation of depositional environments by illustrating the spontaneous potential-resistivity characteristics.

Two Lavery-Hoover cores were examined in detail for variations in grain size, lithologic variations, and sedimentary structures. Fifty thin sections were made from

the Shell Oil Company, Bedell No. 1-20 (sec. 20, T.3N., R.28 E.C.M.), and the Gulf Oil Company, R. C. McClung No. 1 (sec. 23, T.26N., R.25W.).

The thin sections were examined by making a standard 300-point count for each sample to determine mineral-constituent percentages, average grain sizes of the total rock, porosity types and percentages, cement types and percentages, and an estimate of the types and percentages of clays that are present in the rock. Thin sections were re-examined to determine average grain sizes of individual mineral constituents, to determine the diagenetic events that effected the rock, and to estimate the relative time frame in which these changes took place.

Eight samples were prepared and viewed in the scanning electron microscope in order to determine the presence of authigenic clays and their positions within the pore spaces. This technique also aided the study concerning the diagenetic events that effected the Lavery-Hoover and the relative time frame in which these events took place.

X-ray diffraction analyses were made of 24 samples from the two cores. The untreated samples were run from 2 to 60 theta in order to determine the mineral constituents. Clay was extracted from the samples and natural, heated, and glycolated runs were made from 2 to 30 theta. These data provided information concerning the presence and relative abundance of detrital and authigenic clays that are in the Lavery-Hoover Sandstone.

CHAPTER III

GEOLOGIC SETTING

Introduction

During the Pennsylvanian Period, the Mid-continent region was affected by two major episodes of tectonism. Prior to the Pennsylvanian Period, a widespread uplift centered around the Transcontinental Arch gave rise to the Central Kansas Uplift. From late Morrowan through early Desmoinesian, the Wichita orogeny took place, which is believed to be responsible for several tectonic features in Oklahoma. Arbuckle orogeny took place in the late Pennsylvanian, however, it was confined to the Ardmore Basin and adjacent features. Figure 2 shows the major tectonic features of the Mid-continent region. The following discussion is based primarily on the work of Frezon and Dixon (1975), Stewart (1975), and Rascoe and Adler (1983).

Regional Tectonics

Shortly before Morrowan time, a widespread cratonic emergence centering around the Transcontinental Arch

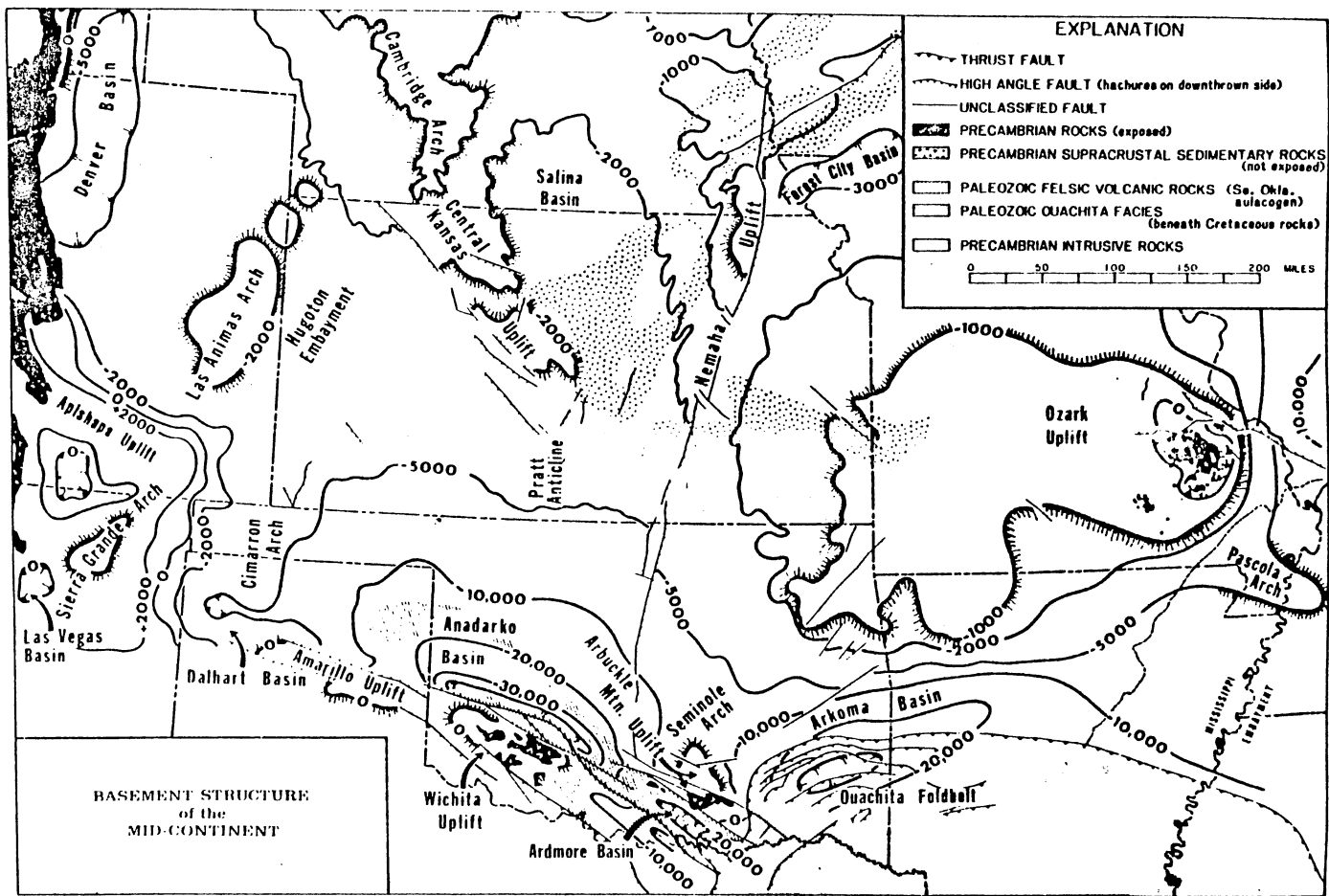


Figure 2. Structural Geologic Map of Basement Rocks, Showing the Major Tectonic Features of the Mid-continent Region (After Adler, 1971, Fig. 3).

occurred, resulting in the formation of the Central Kansas Uplift, which bounds the Anadarko Basin to the northeast (Figure 2). This epeirogenic movement caused the erosion of Mississippian and older rocks from part of Kansas and Upper Mississippian rocks from the northern shelf areas bordering the Anadarko and Arkoma Basins in Oklahoma. This erosion created the pre-Pennsylvanian unconformity onto which Morrowan through Missourian rocks overlapped rocks ranging from Precambrian to Upper Mississippian in age in the Mid-continent region. The Central Kansas Uplift was rejuvenated during Missourian time to form a large shelf platform throughout Kansas.

From late Morrowan through early Desmoinesian time, a collision took place between the North American plate and Gondwanaland. This collision is thought to be responsible for the folding and faulting of the Ouachita Foldbelt, the drastic subsidence of the Arkoma Basin, the emergence of the Amarillo-Wichita, Apishipa, and Nemaha Uplifts, and the uplift of the Cimarron Arch and small structures along the Las Animas Arch (Figure 2).

The Ouachita Foldbelt lies to the southeast of the northern shelf area of the Anadarko Basin (Figure 2). It does not bound the basin directly; however, it was an important tectonic feature during Late Pennsylvanian. Rascoe (1978) concluded that the Ouachita Mountains provided the main supply of clastic material to the Anadarko Basin during Missourian and Virgilian time.

The Amarillo-Wichita uplift bounds the study area to the south - southwest (Figure 2). As the North American Plate and Gondwanaland collided near the end of early Pennsylvanian time, the Amarillo-Wichita Mountains were uplifted and eroded. The eroded material was deposited on the flanks of the Amarillo-Wichita uplift in the form of large clastic wedges composed of arkosic sand, granite wash, and related clastics from pre-Desmoinesian through Virgilian time (Totten, 1956).

The northward-trending Nemaha Uplift bounds the Anadarko Basin to the east (Figure 2). Morrowan and Atokan rocks are absent from the crest of this structure, indicating that it probably was a positive tectonic feature during this time. Desmoinesian through Virgilian rocks unconformably overlie pre-Pennsylvanian rocks near the crest of this structure.

The study area is bounded by the Cimarron Arch-Keys Dome, the Apishapa Uplift, and the Las Animas Arch to the west and northwest (Figure 2). The Cimarron Arch-Keys Dome began rising near the end of the Mississippian and was strongly uplifted near the end of Desmoinesian time, recorded by the appreciable amounts of sediments that were spread from it. On the Apishapa uplift, located in southeastern Colorado, redbeds of probable late Pennsylvanian age unconformably overlie Precambrian through Ordovician rocks. The Las Animas Arch is located in East-central Colorado. Desmoinesian rocks unconformably overlie

Morrowan rocks on several anticlinal features of this uplifted area indicating the structures are Atokan in age.

The Ozark Dome is located to the east of the study area in Northeastern Oklahoma, Northern Arkansas and Missouri. In late Pennsylvanian time, the Ozark Dome was probably a broad, low-lying land area which may have supplied minor amounts of clastic material to the Anadarko Basin (Huffman, 1958).

Sediments that had accumulated in the Ardmore Basin were subjected to deformation near the close of Pennsylvanian time. This orogenic event created the Arbuckle Mountains which are located to the southeast of the study area.

Regional Structural Setting

The area of study is located on the northern shelf of the Anadarko Basin (Figure 3). This is a relatively stable platform area in which Pennsylvanian sediments dip southerly into the deep Anadarko Basin. Figure 4 shows the structure of the Haskell Limestone throughout the northern shelf area. The Haskell Limestone is a regionally persistent thin marker bed that directly overlies the Tonkawa Sandstone of the Missourian Series. The structure on top of this limestone shows generally a southerly Homoclinal dip of approximately 30 feet per mile and very little faulting.

-
=
-

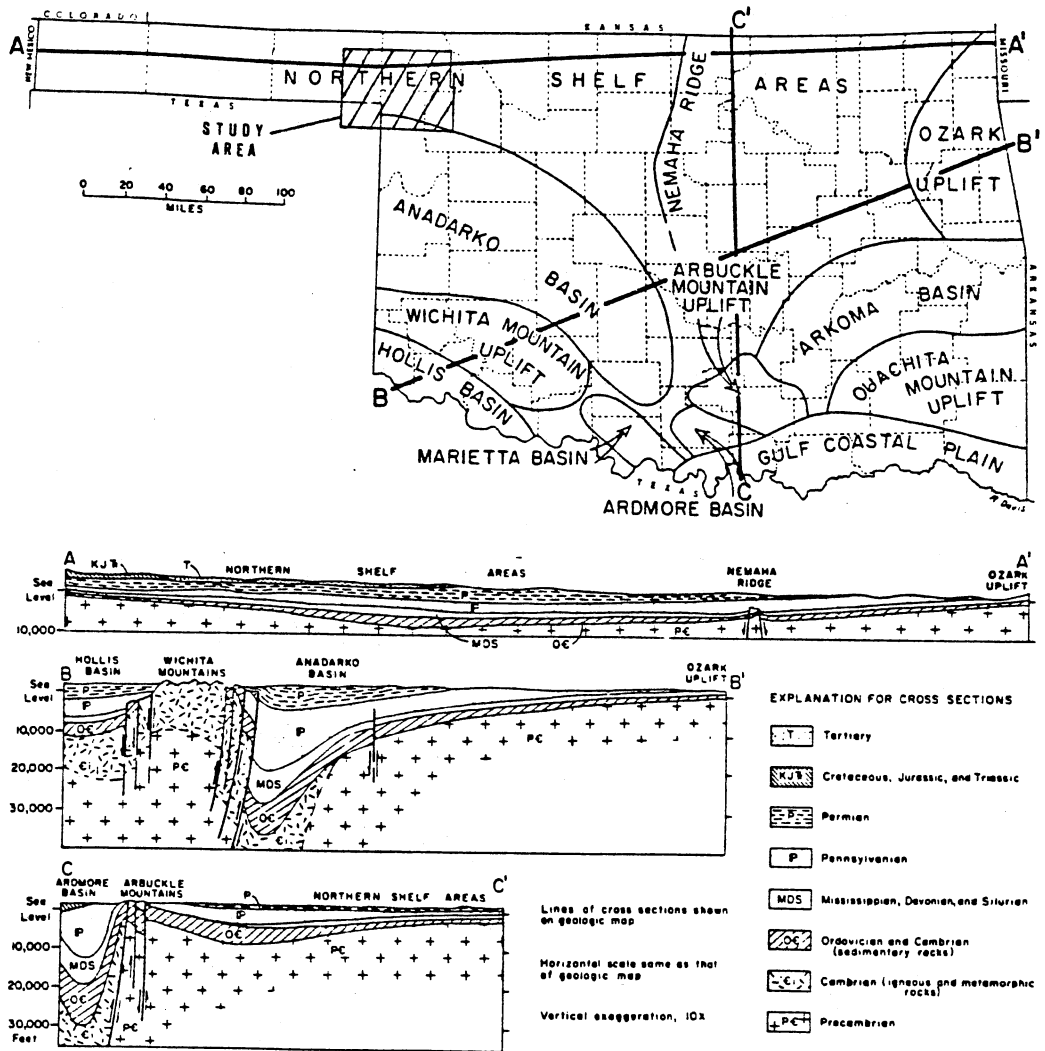


Figure 3. Structural Setting of the Area of Study (Oklahoma Geologic Survey).

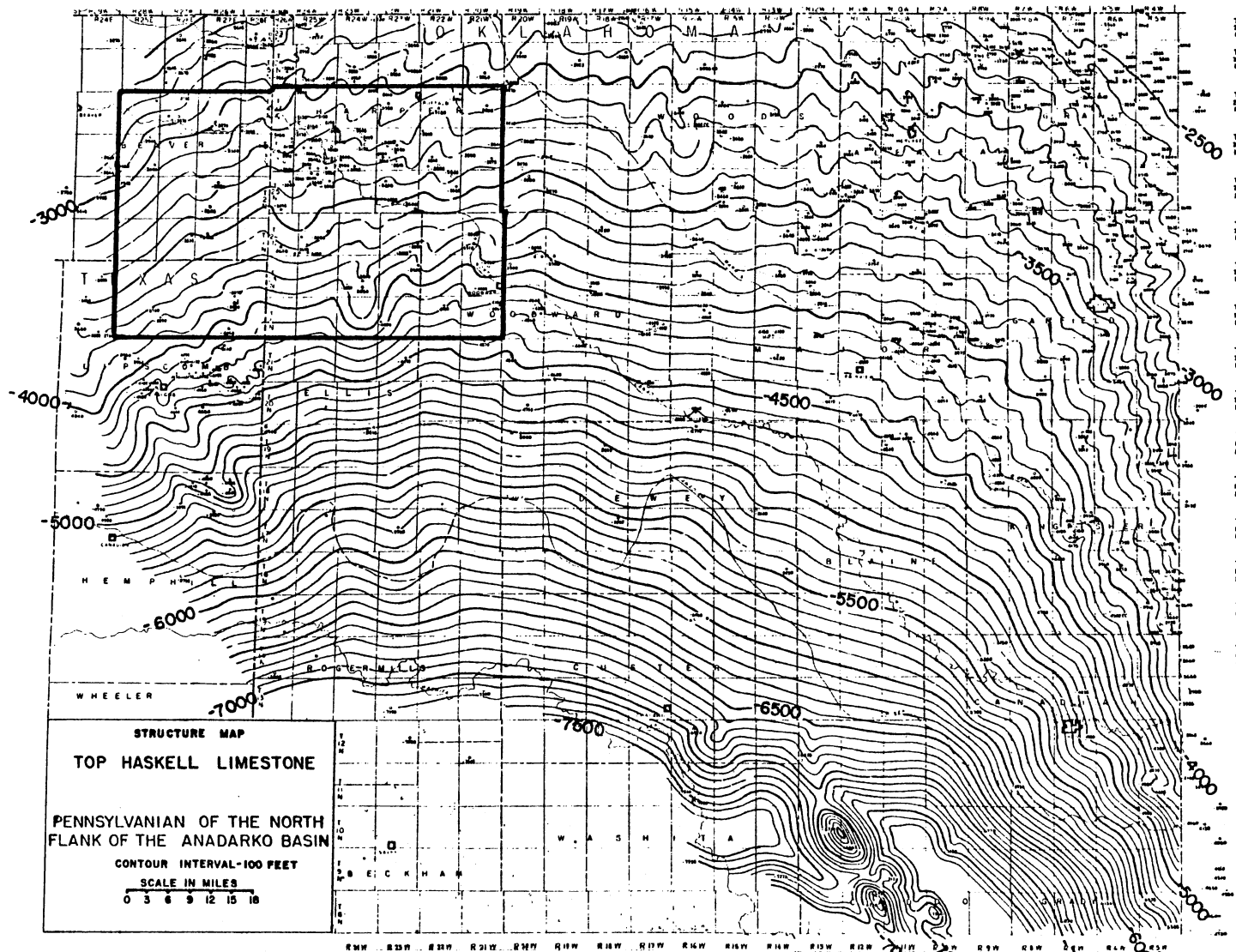


Figure 4. Structure of the Haskell Limestone Throughout the Northern Shelf (From Gibbons, 1960, panel 2, map 2).

Local Structural Geology

The top of the Lavery-Hoover Sandstone was contoured to determine the present structural setting of the sand body (Plate IV). The sand shows a homoclinal, southerly dip of about 20 feet per mile. In the study area, the top of the sand ranges from 1950 feet below sea level in the north, to 2800 feet below sea level in the south. A few minor structural anticlines and synclines are evident, however, no faulting of the sand body was recognized.

CHAPTER IV

STRATIGRAPHIC FRAMEWORK

Introduction

In the Mid-continent region, the Pennsylvanian System is divided into Morrowan, Atokan, Desmoinesian, Missourian, and Virgilian Series in ascending order (Figure 5). The primary unit of investigation in this study is the Lavery-Hoover Sandstone which is included in format unit P.V.U. 4 of the Wabaunsee Group, Virgilian Series, Pennsylvanian System. The Lavery-Hoover Sandstone was first discovered in 1955 by An-Son Petroleum Corporation No. 1 Lavery (sec. 26, T.26N., R.25W.). This sandstone was miscorrelated and mistakenly identified as being equivalent to the Hoover Sandstone of the Shawnee Group, which is predominantly in north-central Oklahoma. After its discovery, the sandstone was first called the Lavery-Hoover by Jordan, Pate, and Williamson (1959).

Regional Stratigraphy of the Virgilian Series

The Virgilian Series is the uppermost series of the Pennsylvanian System of the Mid-continent region; it

SYSTEM		SERIES	STAGE	GROUP	FORMATION
PERMIAN		GUADALUPIAN			
		LEONARDIAN			Red Cave Ss.
	WOLFCAMPIAN	UPPER	Chase	Pontotoc	Brown Dol.
LOWER		Council Grove Admre	Pontotoc		
CARBONIFEROUS	PENNSYLVANIAN	UPPER	VIRGILIAN	Wabunsee Shawnee Douglas	Laverty-Hoover Ss. Endicott Ss.
			MISSOURIAN	Lansing- Kansas City	Tonkawa Ss. Medrano Ss.
	MIDDLE	DESMOINESIAN		Marmaton	Oswego-Fort Scott Ls.
				Cabaniss Krebs	Cherokee Deese Bartlesville Ss.
		ATOKAN		Thirteen-finger Ls.	
	LOWER	MORROWAN		Wapanucka Ls. Wapanucka Sh. Union Valley-Cromwell Ss.	Upper Morrow Ss. Keyes Ss.
	MISSISSIPPIAN	CHESTERIAN			Springer-Penn. Caney Fm.
		MERAMECIAN			Mississippi Chat Mississippi Ls.
		OSAGIAN			
		KINDERHOOKIAN			

Figure 5. General Stratigraphy of Permo-Carboniferous Rocks Throughout the Mid-continent Region (From Rascoe and Adler, 1983, p. 982).

includes rocks between the top of the Missourian Series and the base of the Permian System. Rocks of the Virgilian Series are divided into the Douglas, Shawnee, and Wabaunsee Groups.

An isopach map of the Virgilian Series throughout the western Mid-continent region shows a line in which the series shows abrupt thickening (Figure 6). This is the Virgilian "hinge line" which marks the division between sedimentary shelf and basin. On the shelf, the Virgilian thickens at about six feet per mile toward the axis of the Anadarko Basin. Basinward from the hinge line, the rocks thicken towards the axis at approximately 22 feet per mile (Rascoe, 1962).

According to Gibbons (1962, p. 85),

Virgilian rocks grade from granite and carbonate wash at the Wichita Mountain front northward to limestones and shales. Northwestward towards Beaver County, Oklahoma, Virgilian rocks grade to an increasingly high percentage of carbonates, with an attendant decrease in the percentage of shales. Northeastward, toward Garfield County, Oklahoma, Virgilian rocks are essentially shales with thin limestones. Eastward from the Wichita Mountains, and extending northward along the west flank of the Nemaha ridge, Virgilian rocks are essentially shales and sandstones.

Douglas Group

The Douglas Group includes rocks from a disconformity at the base of the Virgilian Series up to the base of the Toronto Limestone member (Pate, 1962). A regionally-correlatable shale was deposited over the disconformity at the base of the Virgilian Series and was overlain by the

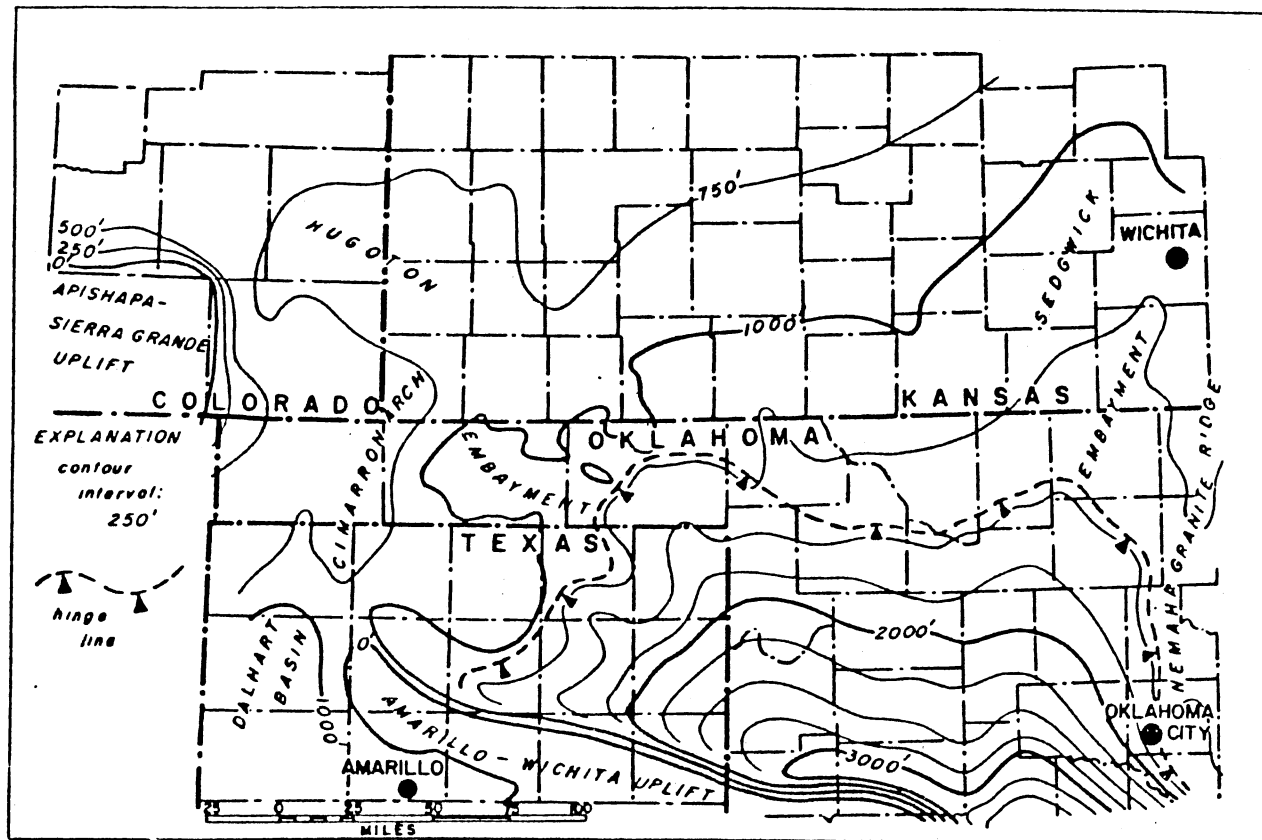


Figure 6. Isopach Map of the Virgilian Series in the Mid-continent.
 C.I.: 250 ft. (From Rascoe, 1962, p. 1363).

Lovell Limestone. Throughout much of Western Oklahoma, a fluvial sandstone, the Endicott Sandstone directly overlies the Lovell Limestone.

Shallow water conditions probably prevailed in the Anadarko Basin during deposition of the Douglas Group (Rascoe, 1978). The individual formations of the Douglas Group show very little lateral variation, possibly indicating that subsidence was negligible in the Anadarko Basin during deposition of the group.

Shawnee Group

Rascoe (1978) divided the Shawnee Group into two format units. Pennsylvanian Virgilian Middle 1 and 2 (P.V.M. 1 and 2) were designated to correlate through facies changes in the Shawnee Group from shelf to basinal areas (Figure 7). P.V.M. 1 was defined by the Elgin Limestone below to the top of the Topeka Limestone. P.V.M. 2 is the format bounded by the Heebner Shale below and the Elgin Limestone above.

Wabaunsee Group

Rascoe recognized 11 cycles of sedimentation in the Wabaunsee Group of the Anadarko Basin, which were defined as Pennsylvanian Virgilian Upper 1 through 11 (P.V.U. 1-11) (Figure 7). Each format consists of a transgressive and regressive phase of deposition. The transgressive phase contains a shallow marine shelf limestone-shale

SYSTEM	SERIES	STAGE	GROUP	FORMAT
PENNSYLVANIAN	UPPER	VIRGIL	WABAUNSEE	PVU 1 • 2 • 3 • 4 • 5 • 6 • 7 • 8 • 9 • 10 • 11
			SHAWNEE	PVM 1
				PVM 2
		DOUGLAS		
		MISSOURI		

Figure 7. Correlation Chart of Upper Pennsylvanian Rocks in the Anadarko Basin (From Rascoe, 1978).

system, and a shelf-edge carbonate-bank system. The regressive phase contains a deltaic shale-sandstone system.

As many as nine of these Wabaunsee cycles were recognized on cross-sections A-A' through H-H' (Plates VII through XIV) located within the study area. The Lavery-Hoover Sandstone is located within format unit P.V.U. 4, and the remainder of this chapter will focus on the stratigraphic boundaries and facies of this unit.

Genetic Units

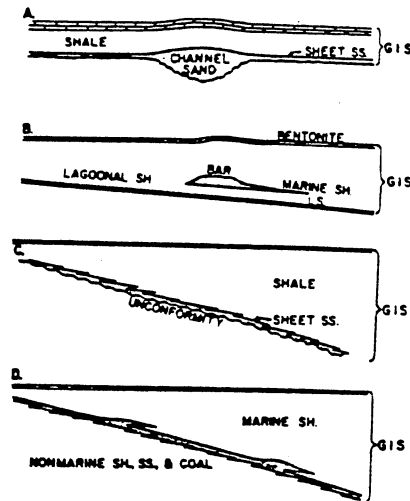
For detailed regional stratigraphic work, as in this study, it is necessary to map laterally continuous rocks through facies changes. This can be accomplished in the subsurface by defining the tops and bottoms of these units on the basis of electric-log markers that are laterally persistent through facies changes. The term format was defined by Forgotson (1957) as "marker defined operational units that are segregations of strata sandwiched between markers which can be traced through facies changes effecting the enclosed strata". He also stated that the isopach and lithofacies pattern shown by this type of unit are the most significant factors to be considered in the interpretation of the paleogeography, the tectonic framework, and the regional environmental pattern which existed during the deposition of the unit.

Busch (1971, p. 1137) defined the term "Genetic Increment of Strata (G.I.S.)" as

a vertical sequence of strata in which each lithologic component is related to all others. It is defined at the top by a time lithologic marker bed, and at the base by an unconformity, or a facies change from marine to nonmarine beds. In defining the G.I.S., the lithologic time marker bed is critical because it represents contemporaneity of deposition. The most commonly used marker beds are a thin limestone or bentonite bed (Figure 8).

Rascoe (personal communication, 1984) explained that boundaries of genetic units are not the marker beds themselves, but the depositional surfaces associated with those beds. The critical factor in determining the significance of the marker bed whatever its lithology, depends on whether the upper or lower boundary (or both), represent a continuous depositional surface. He also stated that "thin" marker beds are not a prerequisite to delineation of genetic units, making it possible to recognize genetic units in areas where thin marker beds are not present at all.

In this study, the term "format" applies to a complete transgressive-regressive cycle. The base of format unit P.V.U. 4 is recognized by a thin limestone marker bed throughout the deep sedimentary basin. In the shallower parts of the basin, fluvial channels have created an unconformable surface which marks the base of the unit. In the clastic filled basin, the top of the unit is recognized by the depositional surface between clastic shales of P.V.U. 4 and the persistent shelf limestone-shale system of P.V.U. 3. In the shelf limestone-shale and shelf edge carbonate bank systems within P.V.U. 4, depositional



Diagrammatic illustrations of Genetic Increments of Strata (GIS).

- A. Channel and sheet sandstones with overlying shale and limestone; upper limit of GIS is defined by time-lithologic marker bed, base by unconformity.
- B. Sandstone bar bordered by lagoonal shale on one side and by marine shale on other; upper and lower limits of GIS are defined by time-lithologic marker beds (bentonite and limestone).
- C. Sheet sandstone, resulting from cyclic subsidence, overlain by basinward-diverging marine shale; upper limit of GIS is defined by time-lithologic marker bed, base by unconformity.
- D. Sheet sandstone showing two areas of locally thicker sandstone at former stillstand positions of shoreline; upper boundary is defined by time-lithologic marker bed, base by facies change from continental to marine beds.

Figure 8. Diagrammatic Illustrations of Genetic Increment of Strata (After Busch, 1971, p. 1138).

surfaces can be recognized which mark the top and base of the unit. These depositional surfaces were created during regressive phases at a time in which no carbonate deposition took place.

Facies and Stratigraphic Boundaries of P.V.U. 4

Cross section A-A' (Plate VII) shows the relationships between shelf limestone-shale, shelf edge carbonate bank, and basinal deltaic sandstone-shale systems within P.V.U. 4. Shelf limestones are represented in wells 12 and 13 where the unit is about 90 feet thick, and contains interbedded shales and thin, tight limestones. The unit thickens to about 160 ft. in well 11, and contains a highly porous limestone. Wells 9 through 11 mark the transition zone between limestone shelf edge and sedimentary basin which consists primarily of a fill of sandstones and shales. In the basin, the base of P.V.U. 4 is delineated by a very thin (3-10') limestone marker bed that is persistent throughout the basin. The top of the unit was overlain by the shelf limestone-shale system of P.V.U. 3.

P.V.U. 4 contains both sandstones of fluvial origin and the more distal deltaic deposits, in cross section B-B' (Plate VIII). Fluvial sandstones are represented in wells 22 through 26, where an erosive contact exists between P.V.U. 4 and the underlying format units. The fluvial

sandstones appear to have replaced the shelf limestone systems within the unit and cut into the underlying P.V.U. 5, partially removing the unit. In well 25, P.V.U. 5 was completely removed by the downcutting fluvial channel. The erosive basal contact is replaced by the limestone marker bed of the basin between wells 21 and 22. This transition zone marks the boundary between fluvial and deltaic environments of the Lavery-Hoover Sandstone. P.V.U. 4 is about 250 feet thick in the fluvial dominated area of this cross section, and thickens to a maximum of about 580 feet in the basin.

Cross section C-C' (Plate IX) is similar to cross section A-A' in the respect that both show the complete transition of P.V.U. 4 from limestone shelf to sedimentary basin. In well 39, the unit is only about 50 feet thick and is believed to represent the shelf limestone-shale system. The unit thickens to almost 100 feet in well 38, to a porous limestone representing a shelf edge carbonate bank deposit. The transition between shelf and basin can be seen between wells 37 and 38. In this cross section, the basinal area during the deposition of P.V.U. 4 consists primarily of shale. Only wells 30, 33, and 34 contain deltaic sandstone deposits in P.V.U. 4. The base of the unit in the basin is bounded by the thin limestone marker bed and P.V.U. 4 is overlain by shelf limestones of P.V.U. 3. In cross section C-C', the unit reaches a maximum thickness of about 600 feet in the basin.

Cross section D-D' (Plate X) shows the deep basinal area during the deposition of P.V.U. 4. The unit is consistently 550 to 600 feet thick throughout the cross section and consists primarily of shales. The base of the unit lies just below the limestone marker format and the top is overlain by limestones of P.V.U. 3. Sandstones are present only in wells 3, 41, and 45 within P.V.U. 4 in cross section D-D'.

Cross section E-E' (Plate XI) intersects the basinal area that was established during the deposition of P.V.U. 4. However, the wells in this cross section are closer to the clastic source, and there is a much greater percentage of deltaic sand in the unit. The sandstone body pinches out to the north and south, and is completely enclosed by shale. P.V.U. 4 is consistently about 500 feet thick throughout this cross section, and is bounded by the limestone marker bed below, and shelf limestones of P.V.U. 3 above.

The transition zone between shallow sedimentary basin and adjacent carbonate shelf edge, which bounds the basin to the north and south, is illustrated in cross section F-F' (Plate XII). To the north, the shelf edge facies is represented in wells 54 and 55, where P.V.U. 4 is approximately 100 feet thick, and in the south this facies is represented by well 62, in which the unit is about 130 feet thick. The transition between shelf edge and sedimentary basin is shown in the north by wells 55,

10, and 56, and in the south by wells 61 and 62. In cross section F-F', the deepest part of the basin is about 350 feet thick. The base of the basin is marked by the limestone marker bed and the format unit here was overlain by shelf limestones. The Laverly-Hoover reaches a maximum thickness of about 190 feet in well 21 of this cross section, and pinches out in well 56 to the north and well 60 to the south.

Cross section G-G' (Plate XIII) is similar to F-F' in the respect that it shows the complete transition of P.V.U. 4 from shelf limestone to shallow sedimentary basin, both in the north and south. However, in this cross section, the northern half of the basin was dominated by fluvial systems which cut through underlying rocks, creating an unconformable surface. Fluvial sandstones are recognized in wells 66, 23, and 67. The basal limestone marker bed was not removed by fluvial channels in the southern half of the basin and can be seen in wells 68, 70, 71, and 36. To the north, the carbonate shelf area is recognized by wells 2, 63, and 64, and in the south by well 72. A thick, porous limestone is seen in well 64, which is interpreted as a carbonate bank deposit.

Cross section H-H' (Plate XIV) shows the relationship between the shelf limestone-shale system and the fluvial dominated system of P.V.U. 4 located in wells 76, 25, 77, and 78. These fluvial channels replaced the preceding limestone-shale system of P.V.U. 4 and cut into the

underlying units, creating an unconformable surface that marks the base of the unit in wells 76, 25, 77, and 78. The shelf limestone-shale system is about 50 feet thick in the north and is represented by wells 73, 74, and 75. This system is only about 40 feet thick in the south, and can be seen in wells 79, 80, and 39.

Throughout the basin near the top of P.V.U. 4, there is a thin limestone unit which was overlain by shale. This is considered to represent a minor transgressive-regressive cycle. However, the basal limestone is not laterally persistent and the interval can not be delineated as a genetic unit.

CHAPTER V

DEPOSITIONAL ENVIRONMENT

Introduction

In the study area, P.V.U. 4 shows the transition from limestone shelf to sedimentary basin. This area of transition has been called the hinge line and has proved to be a prolific hydrocarbon producing zone in many areas. Therefore, an understanding of the common relationships that can be expected in these areas is essential to the petroleum geologist. This chapter will provide a depositional model for P.V.U. 4, describing the facies that are present along with the factors that controlled their deposition.

Cyclic sedimentation has been recognized in the Pennsylvanian Period in many areas of the Mid-continent region. According to Wilson (1975, p. 202),

the persistence of platforms situated just at sea level, the tectonic activity which provided periodic incursions of clastics, and the enhanced possibilities of eustatic sea level fluctuations (either glacially or tectonically induced) all concided to make this time in earth history favorable for cyclic sedimentation.

P.V.U. 4 shows one complete transgressive-regressive cycle of sedimentation. As sea level rose, conditions were

favorable for the deposition of limestones on the shelf area, and as sea level fell, fluvial-deltaic clastics prograded into the basin.

Transgressive Phase

Shelf Limestone-Shale System

In the Northeast and Southeast corners of the study area, and further to the east, P.V.U. 4 thins to about 50 feet thick (see Plate II). In these areas, the unit is dominated by relatively thin limestones interbedded with shales. Figure 9 shows the typical electric log characteristics associated with the shelf limestone-shale system.

These sediments are thought to have been deposited on a stable shelf platform in a shallow marine environment. Rascoe (1978, p. 159) stated that,

the shelf carbonates are generally limestones that are often oolitic and commonly fossiliferous with fusulinids, brachiopods, crinoid fragments, bryozoans, and algal remains.

Shelf-Edge Carbonate Bank System

The thin limestones and shales of the shelf platform thicken to more than 100 feet near the shelf edge, which is dominated by limestones. The shelf-edge carbonate bank system is represented primarily by lithology A on the lithofacies map of P.V.U. 4 (see Plate I). Figure 9 shows some typical electric-log responses for the shelf-edge carbonate bank system.

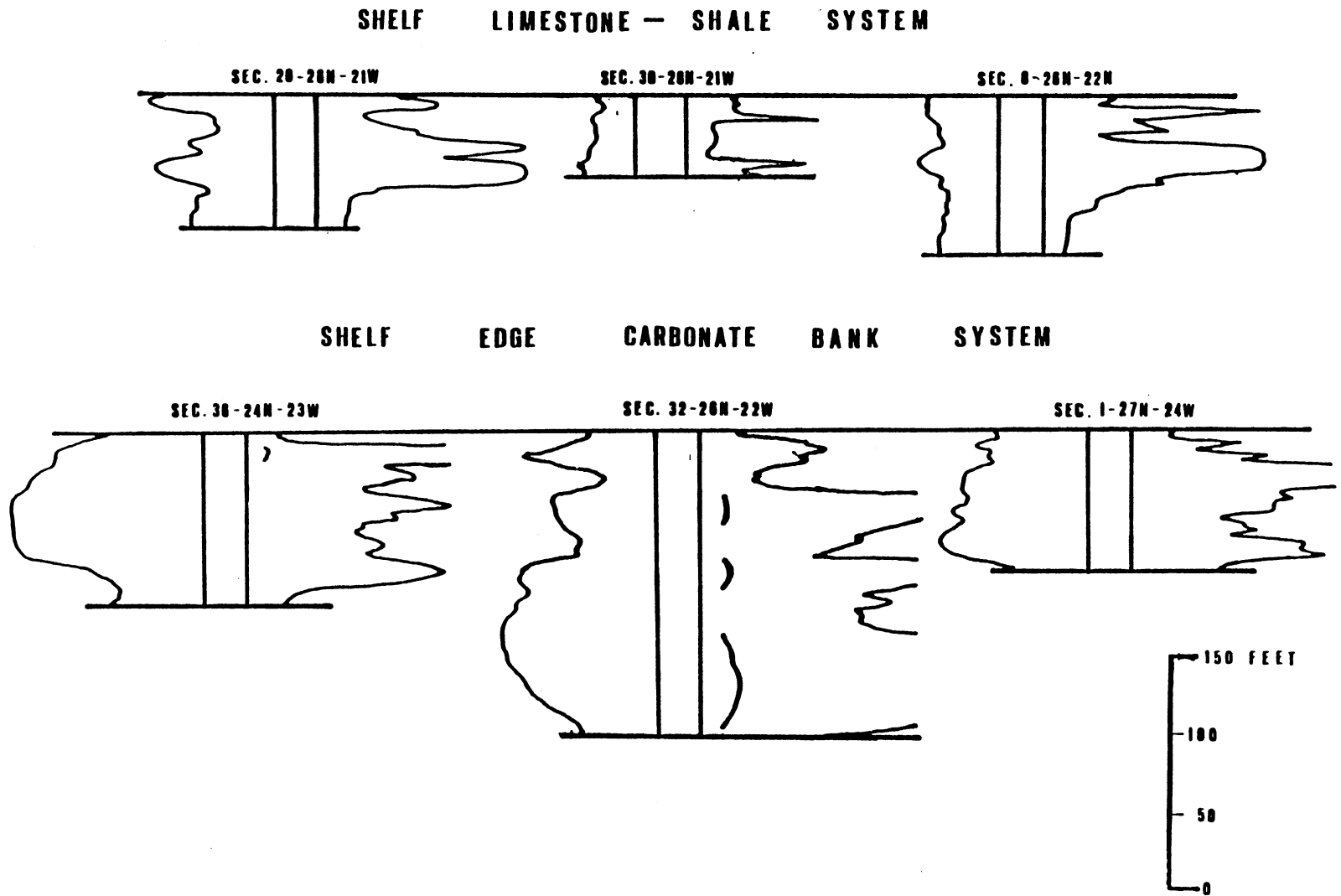


Figure 9. Electric-Log Characteristics of Shelf-edge Carbonate Bank and Shelf Limestone-Shale Systems.

Very few frame-building organisms were present during the Late Paleozoic, and shelf margin buildups consisted of abundant algal plates along with foraminifera, sponges, and stromatoporoids (Wilson, 1975). Rascoe (1978) noted the banks contain many tens of feet of oolites which indicates the banks were deposited in a high energy environment in shallow, warm waters which were bordered by deeper, cooler, waters basinward. The tremendous porosity that developed in the thick shelf edge carbonates of the unit probably resulted from vadose diagenesis which was created by meteoric waters during the following regressive phase.

Basinal Limestone System

On the basin floor, a thin (3-10'), silty limestone was deposited. The fine grained carbonate material within this bed was probably deposited below wave base in the deep, quiet waters of the basin. It is persistent throughout the basin, and serves as the lower boundary for P.V.U. 4.

Depositional Model for the Transgressive Phase

During the transgressive phase of deposition, the shelf-edge carbonate bank system extended across the study area (Figure 10). In the northeast and southeast corners of the study area, thin limestones and shales were deposited in a shallow-marine environment. Small submarine

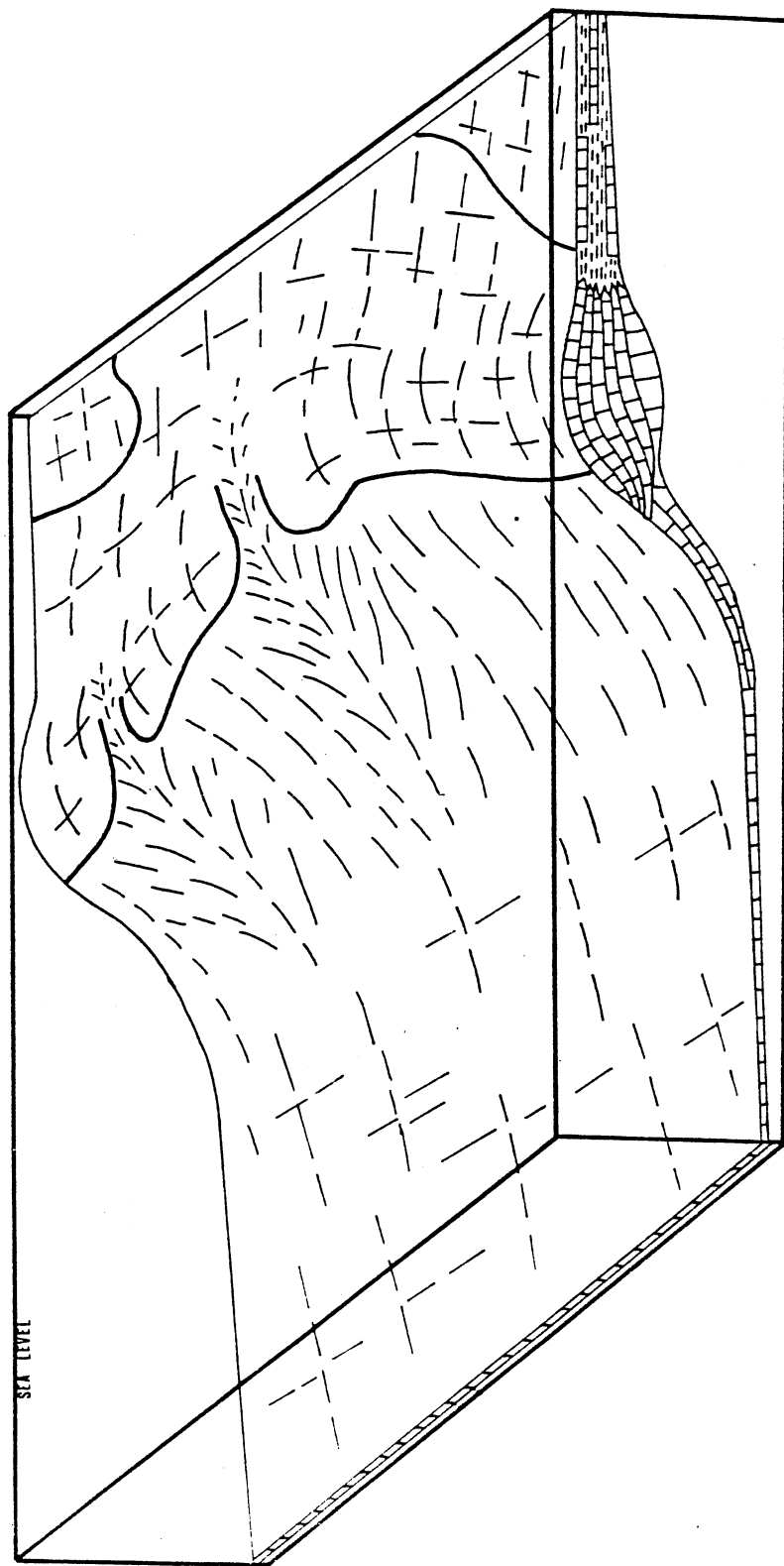


Figure 10. Depositional Model for the Trigravitative Phase.

canyons probably were on the shelf slope, which allowed a thin layer of carbonaceous siltstone to be deposited in the deep basin.

Regressive Phase

Source of Clastic Material

The Lavery-Hoover sand body is oriented in an east-west fashion, with fluvial sandstones on the shelf to the east and deltaic sands in the basin to the west, indicating an eastern source for the clastic material. The Lavery-Hoover Sandstone contains abundant mica flakes and metamorphic rock fragments which provides evidence for a metamorphic source area for the sand. Rascoe (1978) concluded that the Ouachita foldbelt was the principal source of the clastic material for the Anadarko Basin during Missourian and Virgilian time.

Sand Trends, Boundaries, and Thickness

The Lavery-Hoover sand body is generally oriented in an east-west direction, and this corresponds to the major channel direction during deposition (see Plate III). To the east, the sand body is as narrow as one mile and widens to the west to a maximum of about 20 miles. The sand body has a maximum length of about 50 miles. The southern limit of sand in the study area is T.23N. in Ellis County, except for a thin, elongate sand body in Lipscomb County, Texas.

The northern limit of sand is T.27N. in Harper County. The sand reaches a maximum thickness of about 230 feet in section 26, T.26N., R.25W. of Harper County. The major sand body is lenticular in form, and sands appear to be interconnected.

Interpretation of Electric Log

Characteristics

By comparing electric-log signatures of the Lavery-Hoover Sandstone with examples proposed from previous authors, along with determining the position of each well within the fluvial-deltaic complex, individual facies may be recognized. An SP-Resistivity Map of the Lavery-Hoover Sandstone was constructed for this reason (Plate V).

Fluvial Facies

Fluvial sandstones are present in the eastern part of the study area, primarily in T.25N., R.21 and 22W. These sands are thought to have been deposited by a fine grain meanderbelt system, in which channel fill, point bar, and flood plain deposits can be recognized by log signatures (Figure 11). The channels are multistoried, and as many as three individual channel units can be seen in one well.

Deltaic Facies

Deltaic sandstones and shales are dominant throughout the basin within the study area. Several deltaic facies

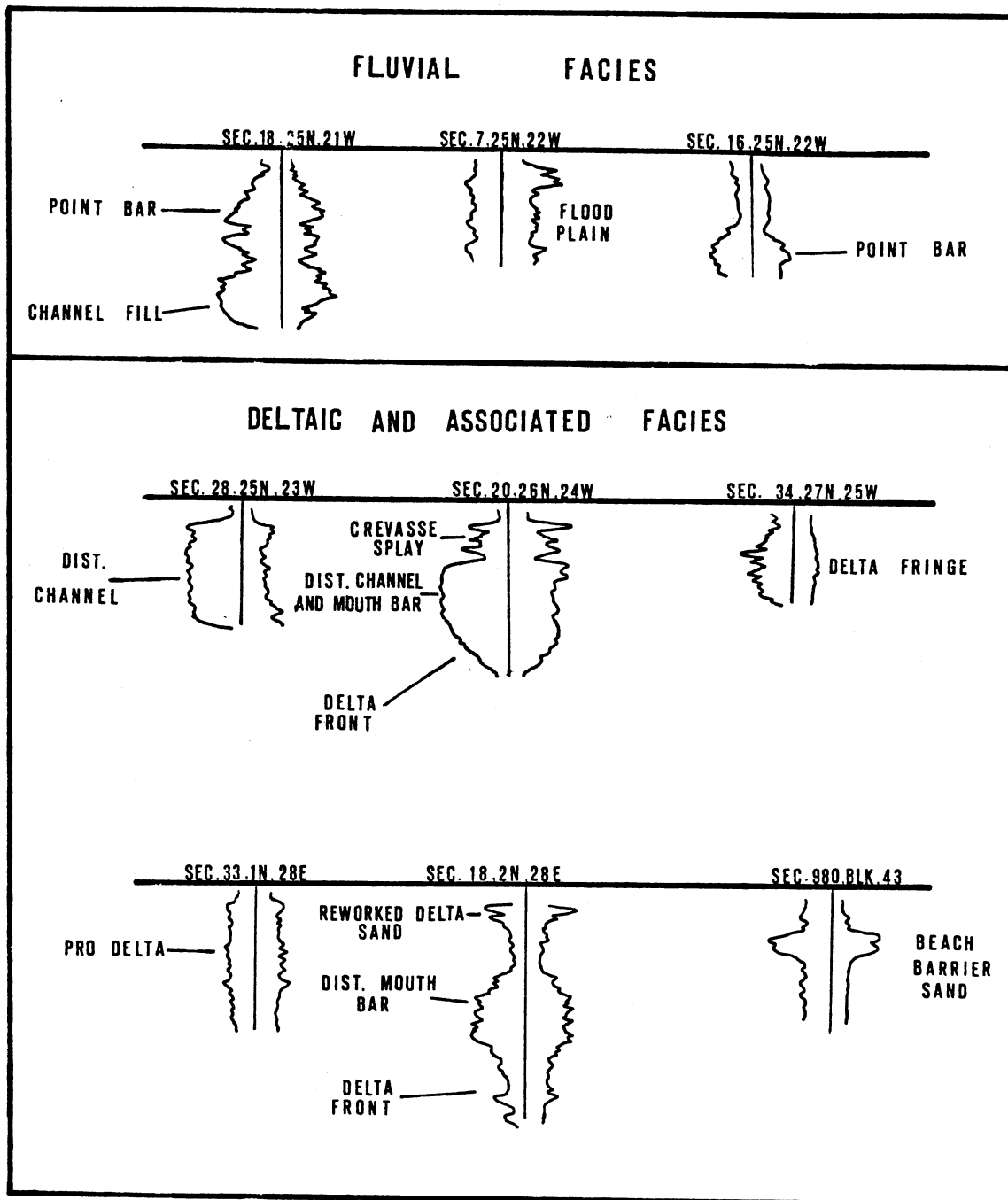


Figure 11. Electric-Log Characteristics of Fluvial and Deltaic Facies.

have been interpreted from electric-log characteristics of the Lavery-Hoover Sandstone (Figure 11). The basal marker bed of P.V.U. 4 was overlain by rocks which show poor SP-resistivity development. These rocks are believed to represent pro-delta shales deposited distally to the delta front. The base of the Lavery-Hoover Sandstone throughout most of the basin contains a coarsening upward sequence which is believed to represent the delta front. This is overlain by a distributary mouth bar and channel complex which contains the cleanest sand accumulation. On the southern and northern flanks of the delta, delta fringe sands are recognized which contain thin, interbedded sandstones and shales. Interdistributary bay shales are present in several wells and directly overlie distributary channel deposits. Crevasse splay facies are recognized in many wells near the top of the sandstone sequence.

A sandstone deposit is present in Lipscomb County, Texas, which is oriented approximately parallel to deltaic depositional strike. This sand body shows log signatures resembling a beach barrier facies. The sand is believed to have been derived from the delta front environment and transported by longshore currents to the south. Near the top of the sandstone sequence and surrounding the delta front, are sandstones which were probably reworked deltaic deposits. These sands were probably deposited after deltaic progradation had ceased, during a minor transgressive phase.

Discussion of Cores

Shell Oil Co., Bedell No. 1-20

This core contains interbedded sandstones and shales that are considered to have been deposited in a delta front environment (Figures 12, 13, and 14). From the base of the core up to a depth of 4402 feet, the core consists of sandstone beds from 1/2 to 5 inches thick that are interbedded with dark shales. The sandstone beds contain small scale cross beds throughout the core. Bioturbation is also present throughout the entire core and rip up clasts can be seen, especially near 4413 feet. From 4402 feet to the top of the core, dark shales are dominant with occasional sandstone lenses which are about one centimeter thick, and contain small scale cross beds.

Gulf Oil Co., McClung No. 1

From the base of this core up to about 4232 feet, very fine to fine grained sandstones with small scale cross beds are present along with a few interbedded shales (Figures 15, 16, 17, and 18). Mica flakes are present in between bedding planes and siltstone rock fragments are present but not abundant. Combining the electric log characteristics along with the sedimentary features contained within the sand, this interval is believed to represent a deltaic distributary channel deposit.

Company SHELL OIL CO., BEDELL NO. 1-20
 Well Location SEC. 20, T. 3 N., R. 20 E. C.M.

Petrologic Log

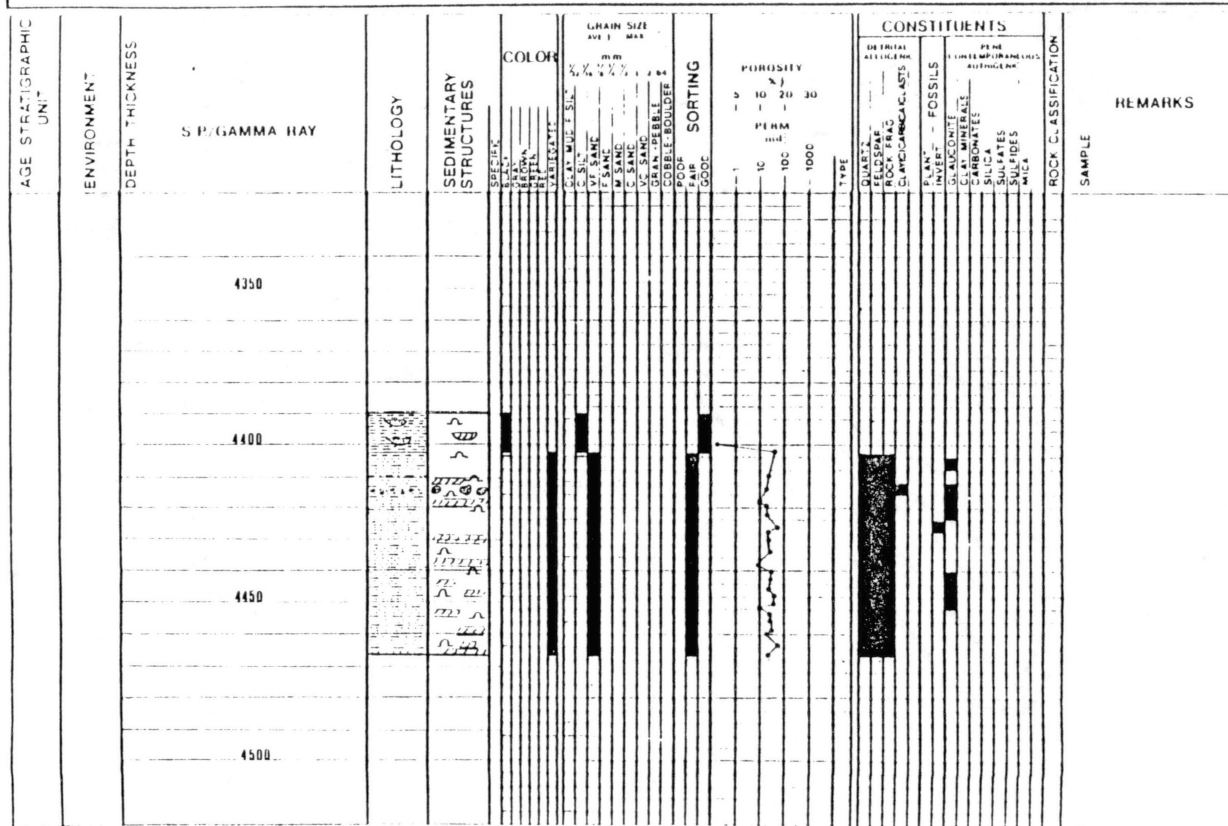


Figure 12. Core Description of Shell Bedell No. 1-20. Depth: 4390-4466 ft.

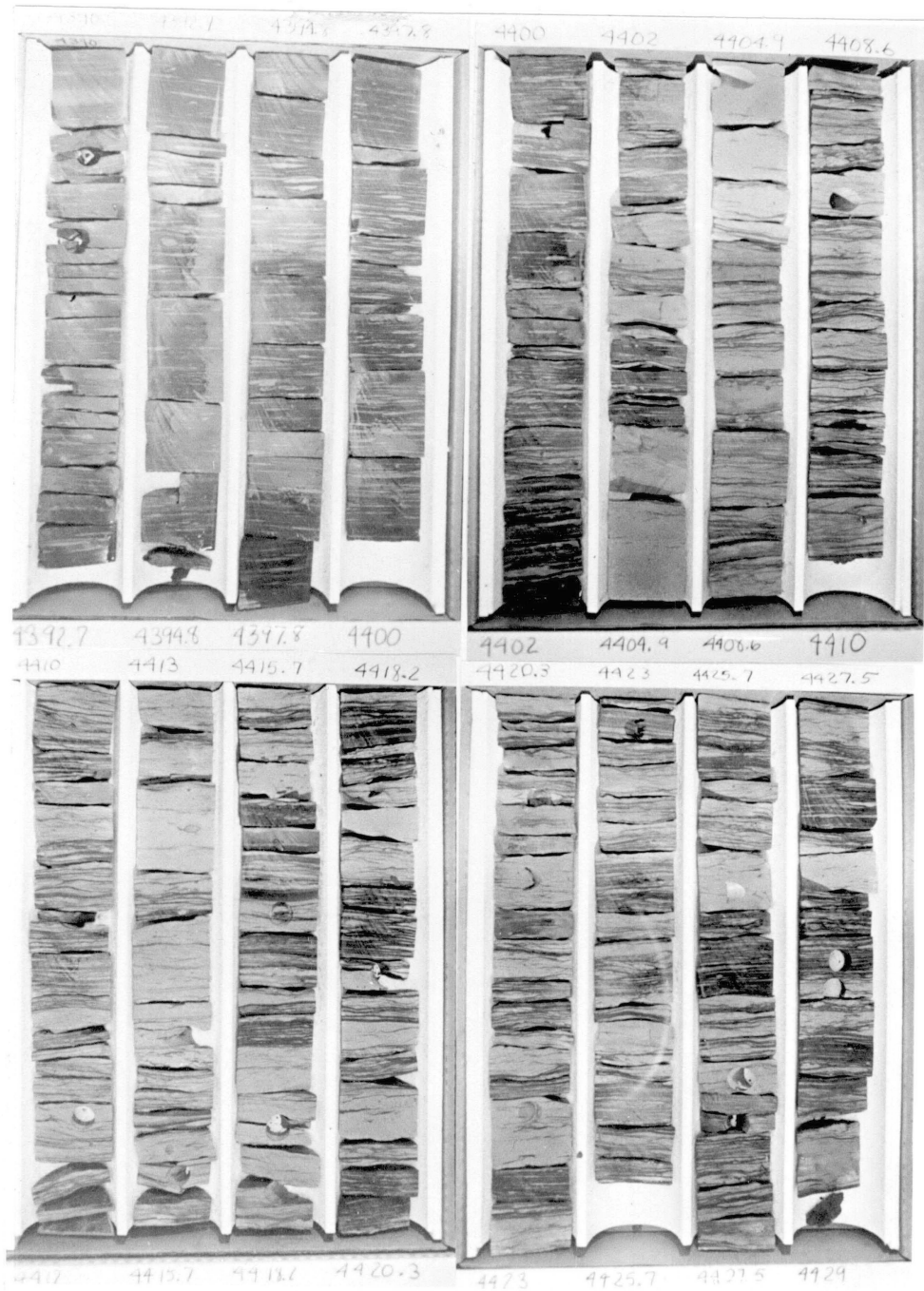


Figure 13. Photograph of Shell Bedell No. 1-20 Core. Depth: 4390-4429 ft.

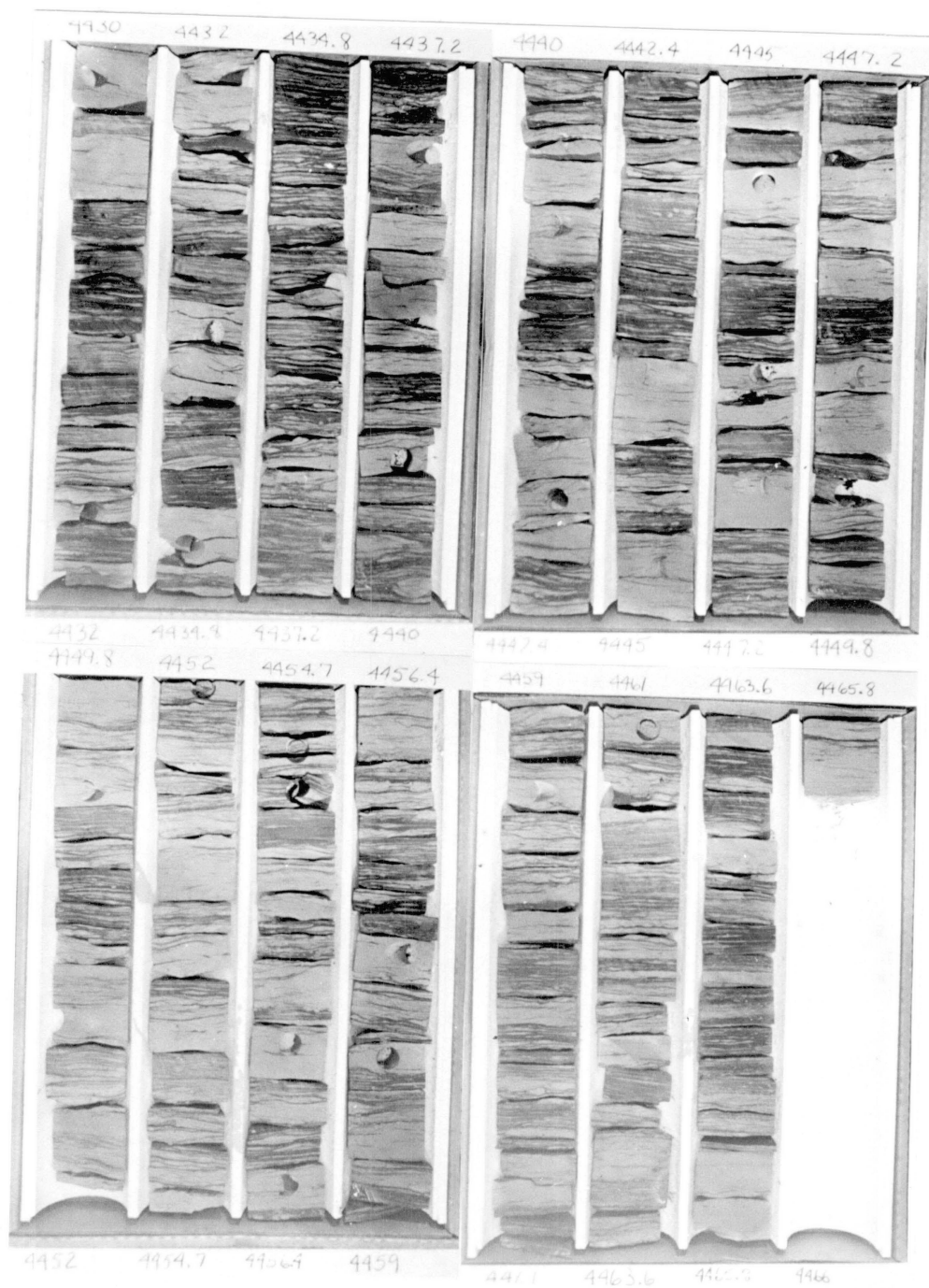


Figure 14. Photograph of Shell Bedell No. 1-20 Core. Depth: 4429-4466 ft.

Company GULF OIL CO., McCLUNG NO. 1
 Well Location SEC. 23, T.26N., R.25W.

Petrologic Log

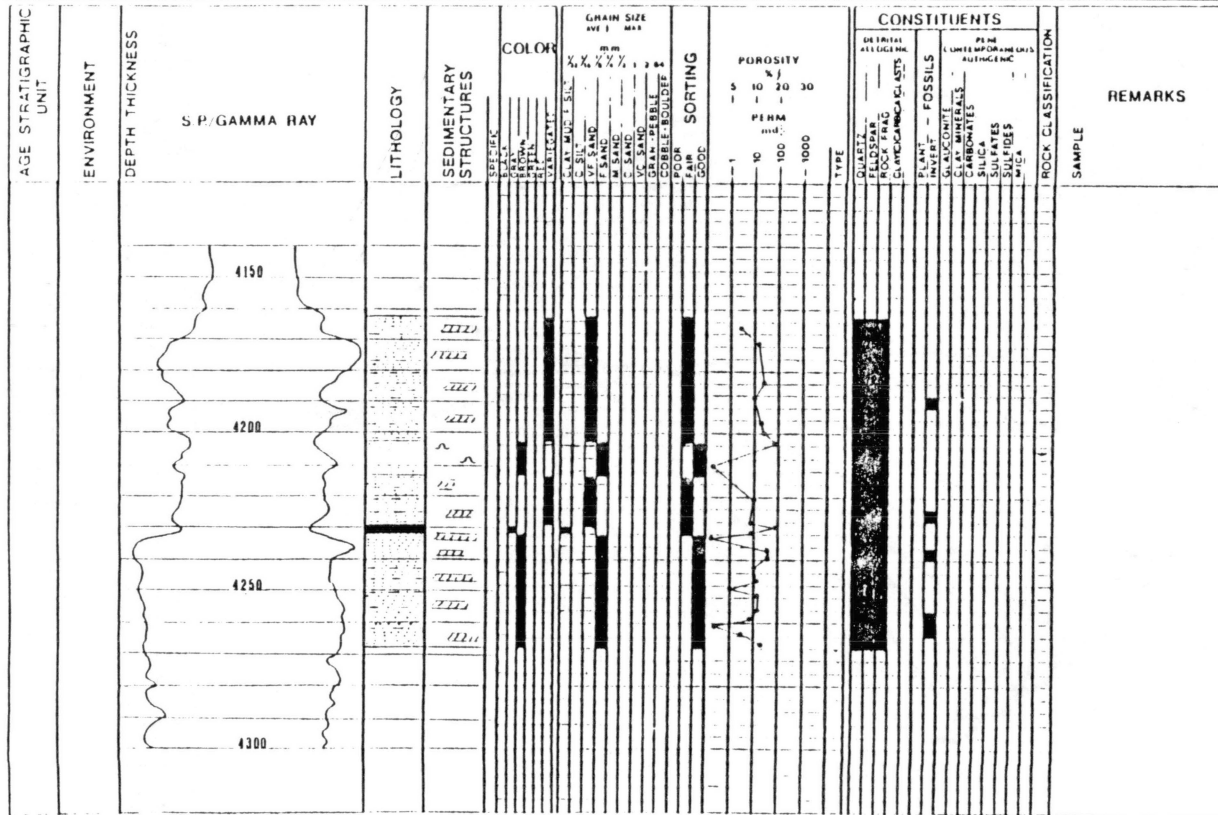


Figure 15. Core Description of Gulf McClung No. 1. Depth: 4163-4266 ft. 6 in.



Figure 16. Photograph of Gulf McClung No. 1 Core. Depth: 4163-4199 ft.

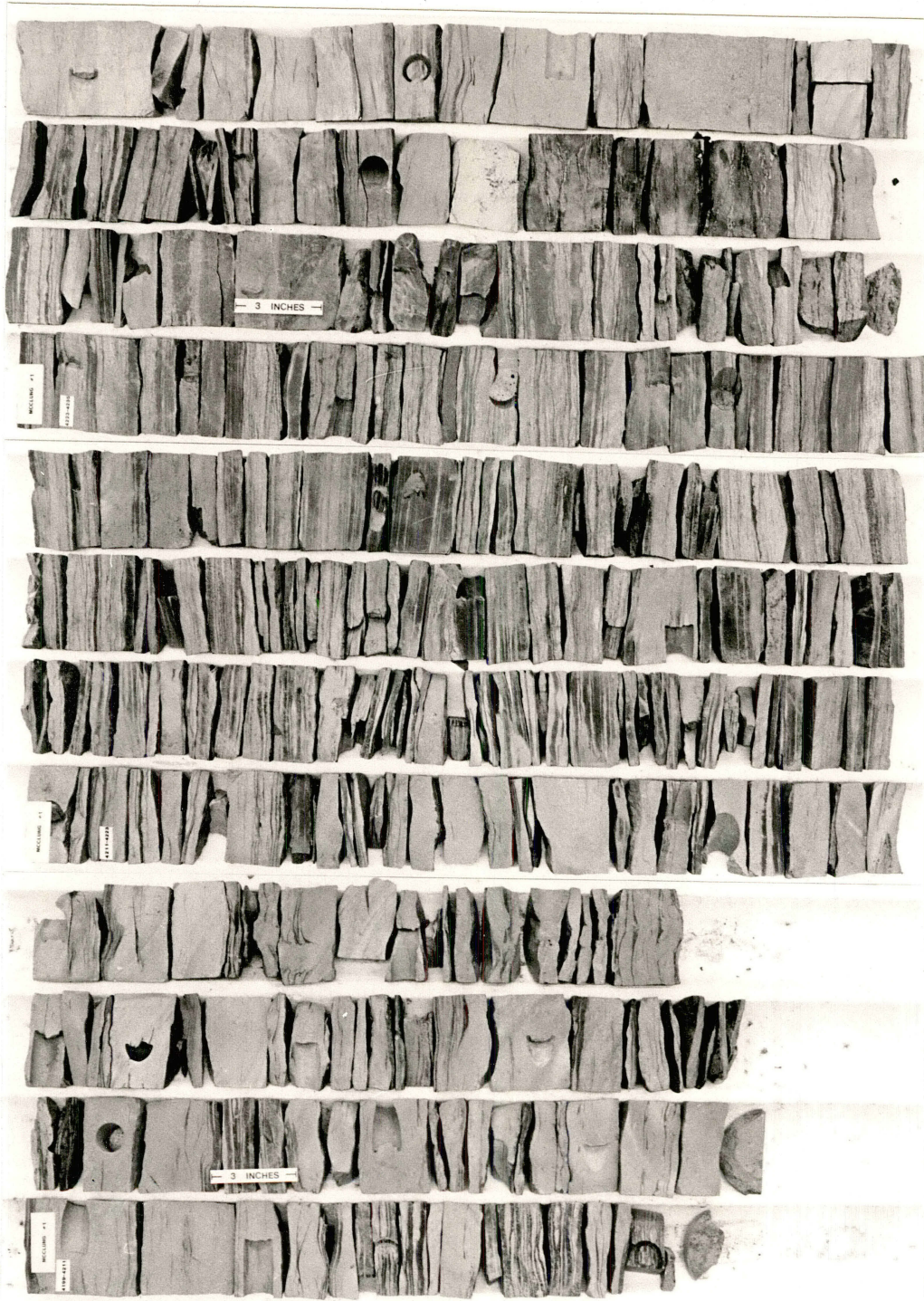


Figure 17. Photograph of Gulf McClung No. 1 Core. Depth: 4199-4235 ft.

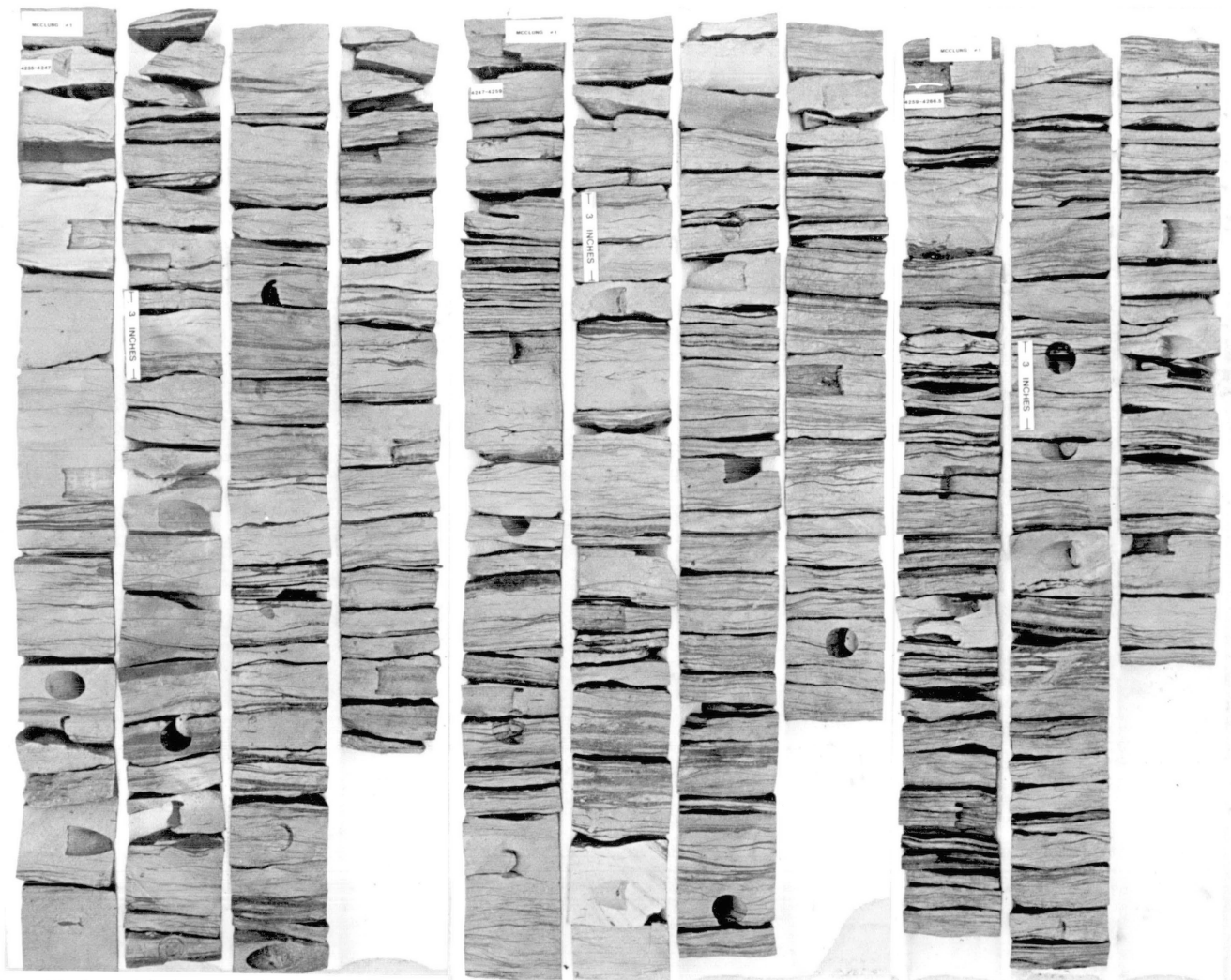


Figure 18. Photograph of Gulf McClung No. 1 Core. Depth:
4235-4266 ft. 6 in.

After the distributary channel was abandoned, it was overlain by an interdistributary bay deposit which is only a few feet thick. This deposit consists of organic rich muds and sideritic zones (Figure 19).

From 4229 feet to the top of the core, the rocks are primarily interbedded sandstones and shales. The sandstone beds are generally from about 2 - 10 centimeters thick and contain small scale cross beds. Bioturbated rocks can be seen in this interval near 4207 feet, however, burrowing organisms must not have been as abundant as they were near the Shell Bedell locality. This interval is believed to represent a crevasse splay deposit, most of the sediment having been deposited during periodic floods.

Internal Features

Interstratification

Interstratification of sandstone and shale is very common in the Lavery-Hoover Sandstone (Figure 20). The sandstone beds range from lensoidal bodies less than 1 centimeter thick up to a maximum thickness of about 20 centimeters. Within these interstratified sequences, the lower and upper contacts are generally sharp.

Small Scale Cross Bedding

Small Scale cross bedding is very abundant in the Lavery-Hoover Sandstone (Figure 21).

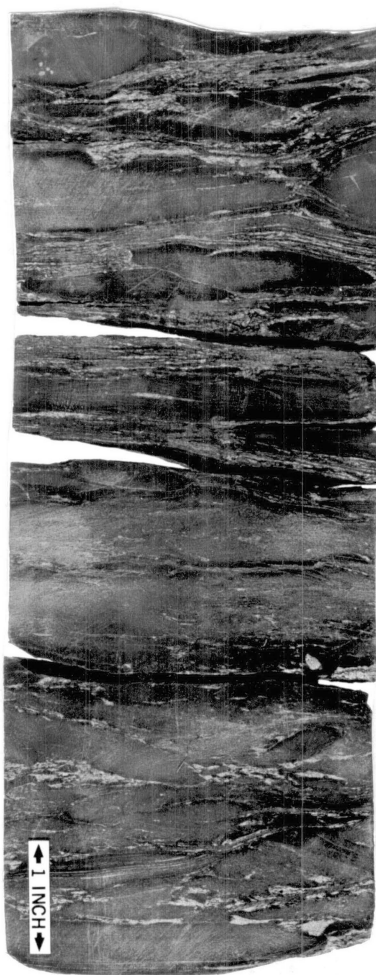


Figure 19. Interdistributary Bay Deposit. Gulf McClung No. 1
Core. Depth: 4230-4231 ft.

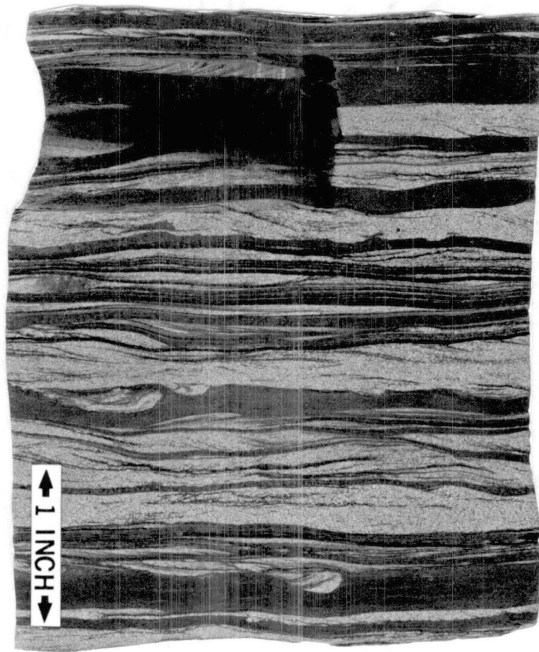


Figure 20. Interstratification of Sandstone and Shale. Gulf McClung No. 1 Core. Depth: 4186 ft.

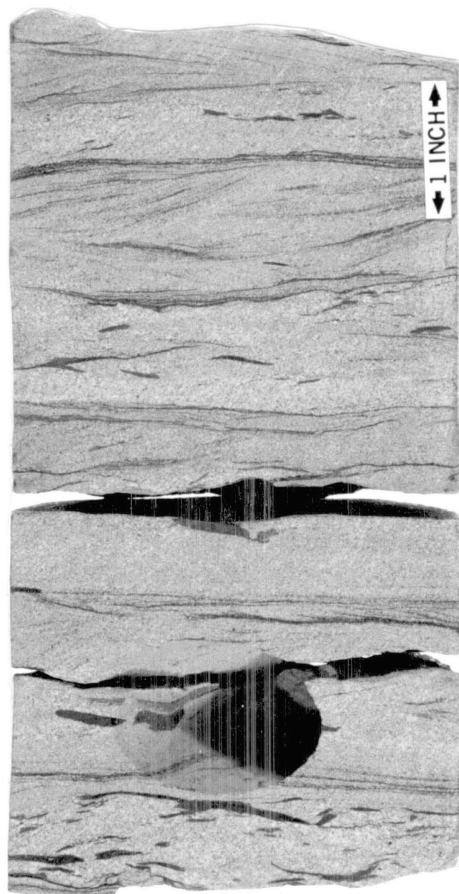


Figure 21. Small Scale Cross Beds and Rip Up Clasts.
Shell Bedell No. 1-20 Core. Depth:
4414 ft.

Bioturbation

Bioturbation can be seen in both of the cores that were examined, however, it is much more abundant in the Shell Bedell core (Figure 22). This indicates that in the delta front environment, there was a great deal of biological activity.

Ripple and Horizontal Laminations

Both ripple and horizontal laminations are in the cores of the Lavery-Hoover Sandstone. Ripple laminations are most common on the bedding planes of interstratified sandstone-shale sequences. Horizontal laminations are more common within the thin sandstone beds of the major channel deposits.

Rip Up Clasts

Rip up clasts are in the cores, however, they are not abundant (Figure 21). These clasts are composed of silt and clay sized material.

Channel Lag

A channel lag deposit was recognized in the Gulf McClung core at a depth of 4229 feet (Figure 23).

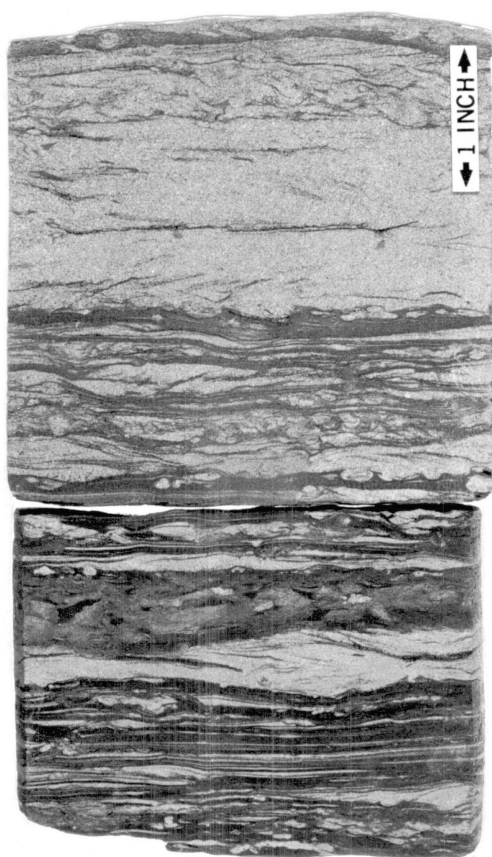


Figure 22. Bioturbated Sandstone. Shell Bedell
No. 1-20 Core. Depth: 4463 ft.

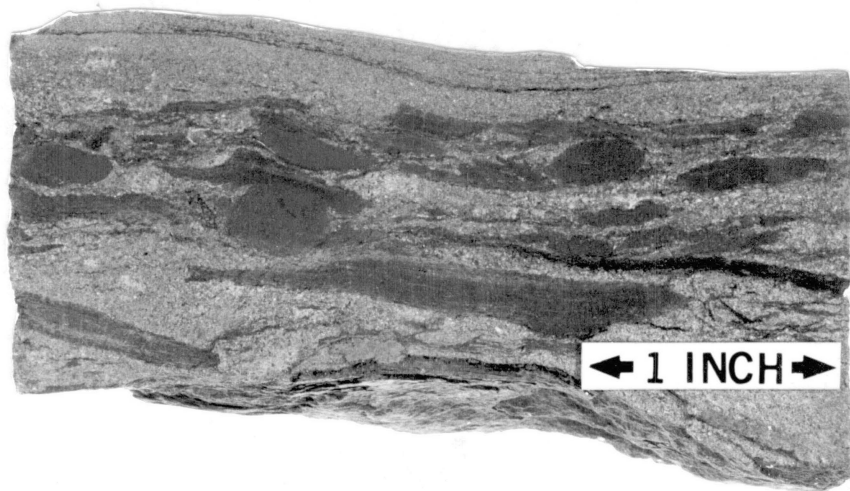


Figure 23. Channel Lag Deposit. Gulf McClung No. 1
Core. Depth: 4229 ft.

Classification of the Lavery- Hoover Delta

The overall geometry of the Lavery-Hoover delta best fits the high constructive lobate model described by Fisher (1969). These deltas prograde into shallow water and deposit relatively thin pro-delta shale facies. Sand facies prograde over the thin mud sequences. Upon abandonment, the upper part of the prograded delta mass is reworked by marine processes and undergoes relatively little compactional subsidence (Fisher, Brown, Scott, and McGowen, 1969). Figure 24 shows the general characteristics expected with high constructive lobate deltas.

According to Fisher (1969), the Lower Wilcox of the Gulf coast contains three facies which characterizes high constructive lobate deltas. These facies are: (1) an extensive delta plain facies made up of thick distributary channel sands, (2) a downdip delta front facies consisting mostly of sands forming a lobate fringe to the delta plain facies, and (3) a pro-delta facies consisting of dark, organic rich, laminated muds. Holocene examples of high constructive lobate deltas are the Lafourche, Saint Bernard, and Teche deltas of the Mississippi system, all of which are abandoned.

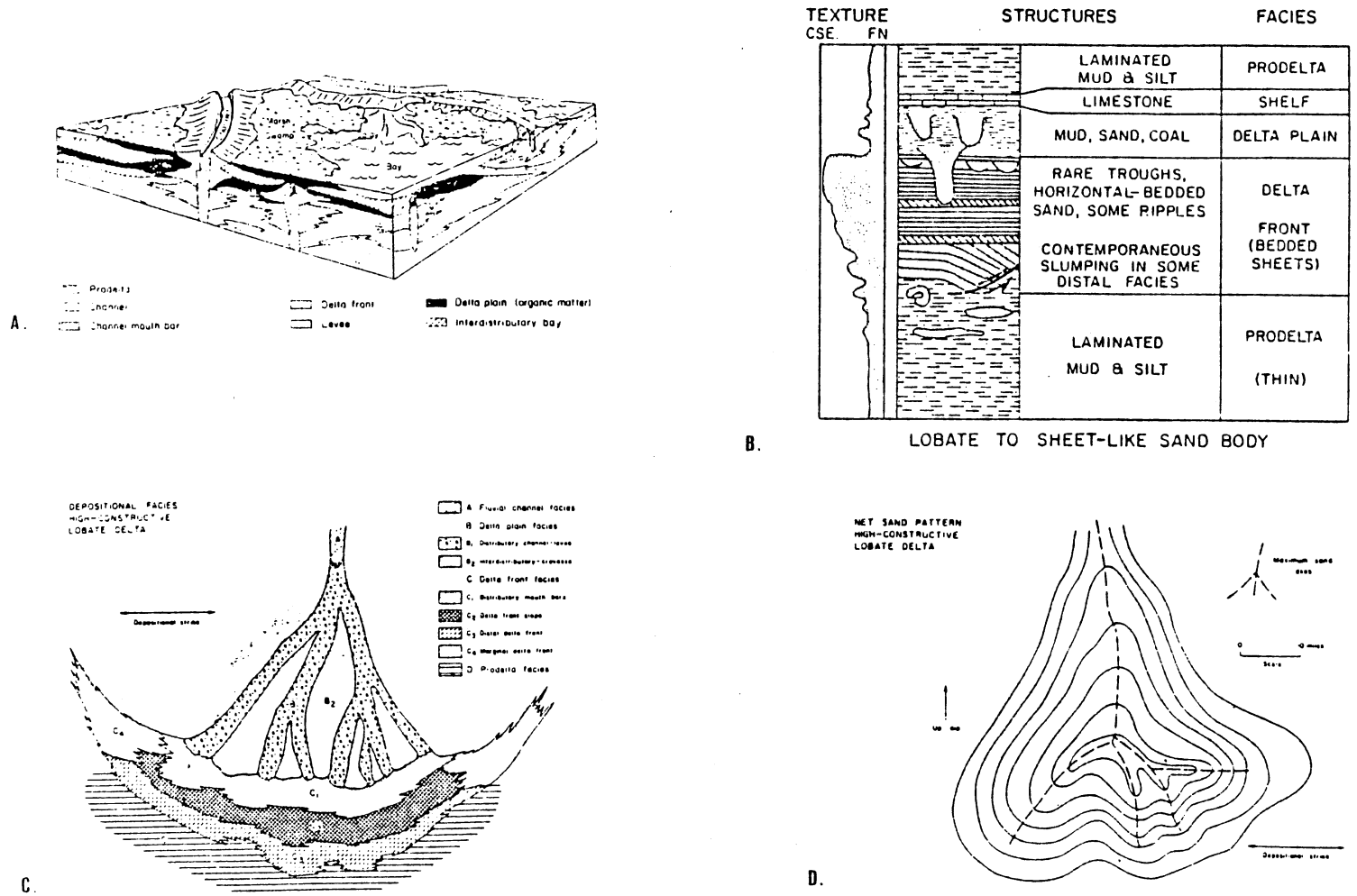


Figure 24. Characteristics of High Constructive Lobate Deltas.
 A. After Frazier, (1967) B. After Brown, Cleaves and Exleben, (1973) C. After Fisher, (1969), D. After Fisher, (1969).

Depositional Model of the Regressive Phase

A lowering of sea level initiated the regressive phase of deposition, which allowed the advance of clastic material into the basin (Figure 25). The lowering of base level caused fluvial channels to cut through the carbonate bank and shelf systems which were exposed at this time and created an unconformable surface throughout the mid-eastern part of the study area. Pro-delta shales prograded into the basin and were overlain by delta front, distributary mouth bar, and distributary channel deposits. Interdistributary bays and marshes were created as distributary channels shifted and were abandoned. Crevasse splays were present in many areas and became active during occasional flooding.

Longshore currents transported deltaic clastic material southward, and wave action created a barrier bar system which is oriented parallel to the depositional strike of the deltaic system. Near the end of deltaic deposition, the delta front was reworked by wave action, and the reworked sands were deposited at the top of the deltaic sequence, during a minor transgressive event.

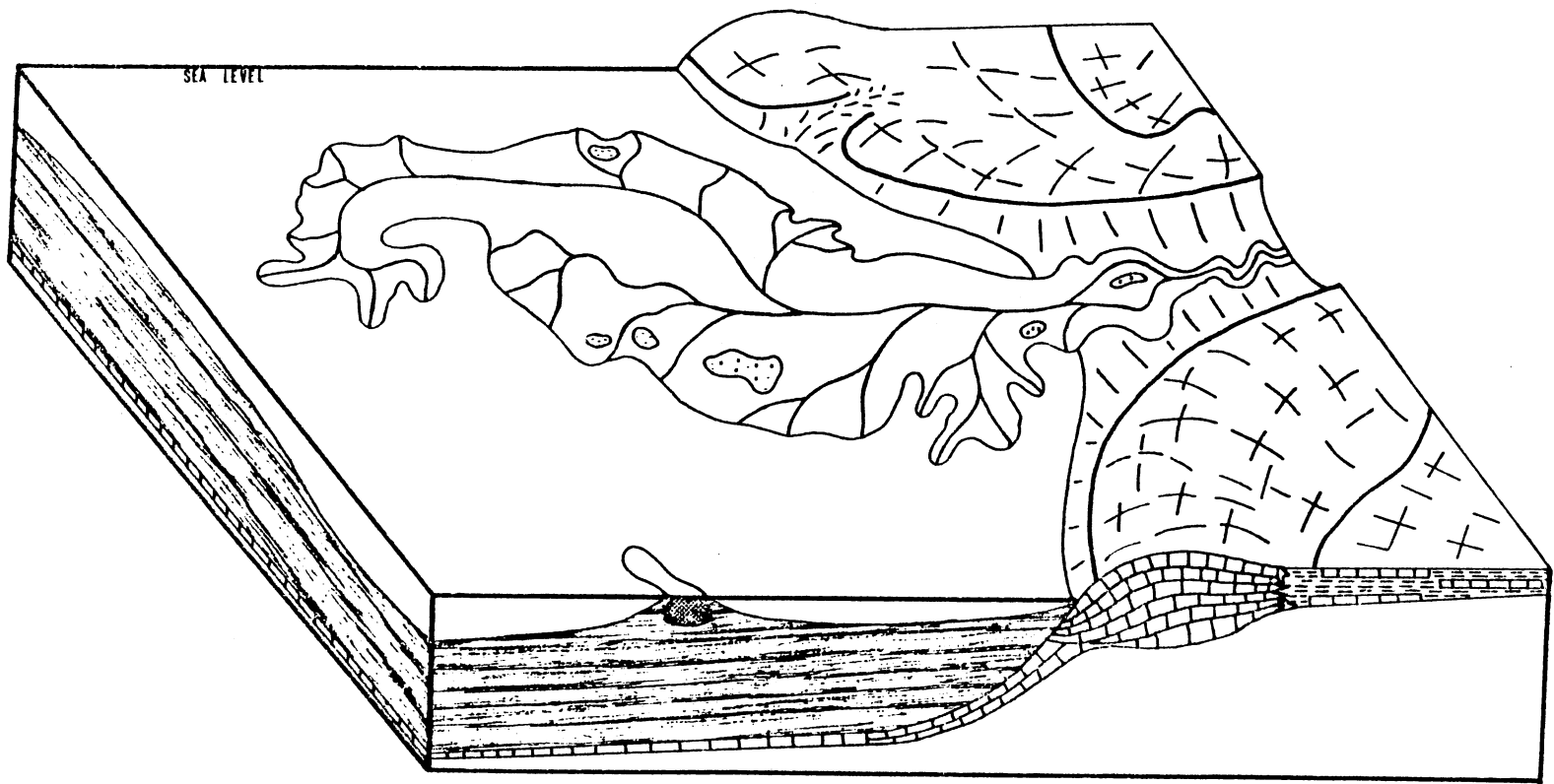


Figure 25. Depositional Model of the Regressive Phase.

CHAPTER VI

PETROLOGY

Composition

The Lavery-Hoover Sandstone is a very fine to fine grained sandstone composed of moderately well sorted, subangular, detrital grains. Figures 26 and 27 show the compositional plots for samples of the Gulf McClung No. 1 and Shell Bedell No. 1-20 wells based on relative abundance of quartz (monocrystalline and polycrystalline), rock fragments (including chert), and feldspars. The average composition of the Lavery-Hoover Sandstone is about 77% quartz, 18% rock fragments, 5% feldspars. Most of the samples plot as sublitharenites because of an abundance of metamorphic rock fragments, and a few of the samples plot as litharenites and feldspathic litharenites. Table I shows the average composition of the Lavery-Hoover Sandstone based on thin section examination.

Detrital Constituents

Monocrystalline quartz is by far the most abundant detrital constituent, accounting for slightly more than 45% of the total rock. Quartz grains typically are subangular

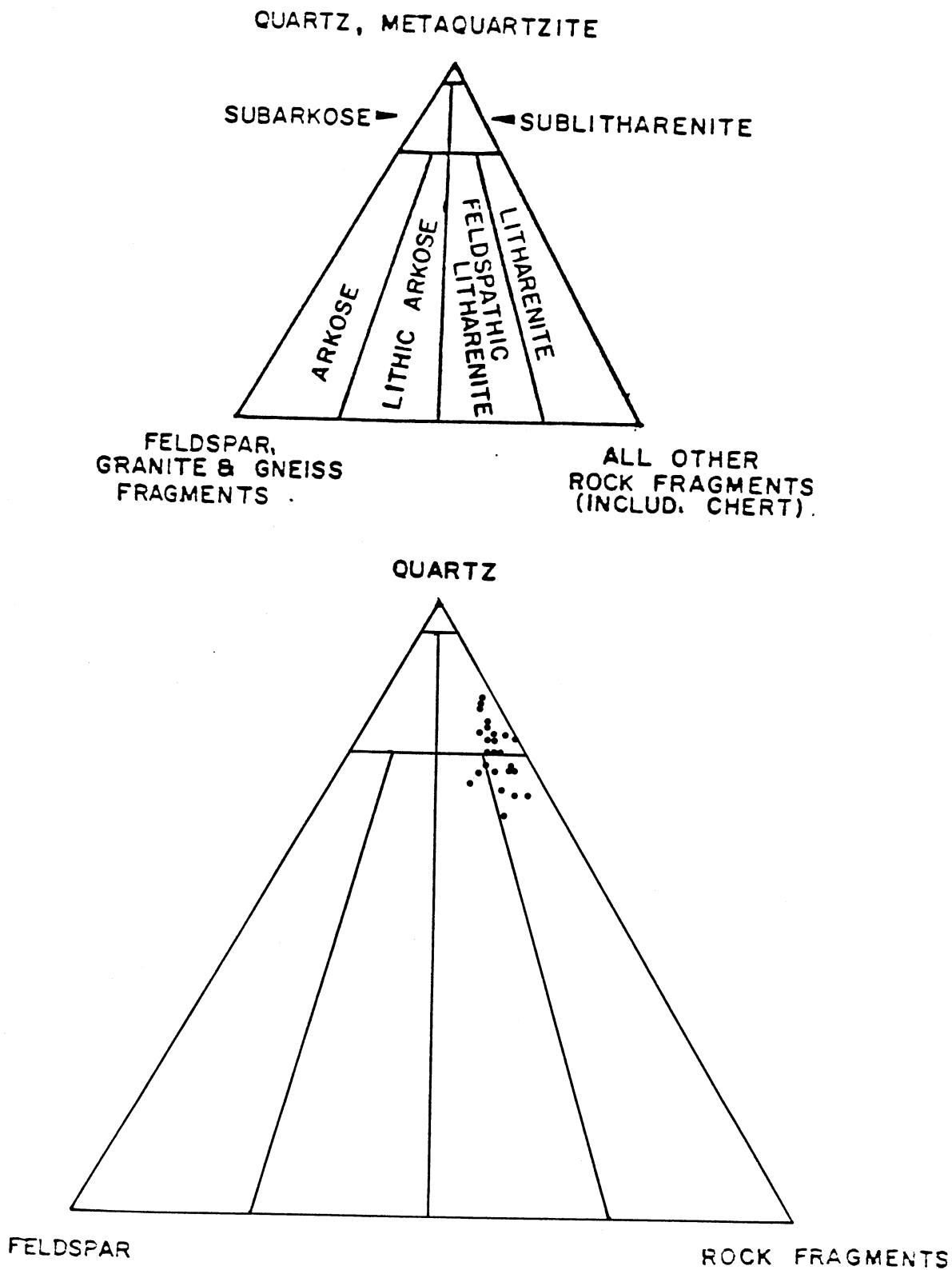


Figure 26. Classification of Samples from Shell Bedell No. 1-20 Core.

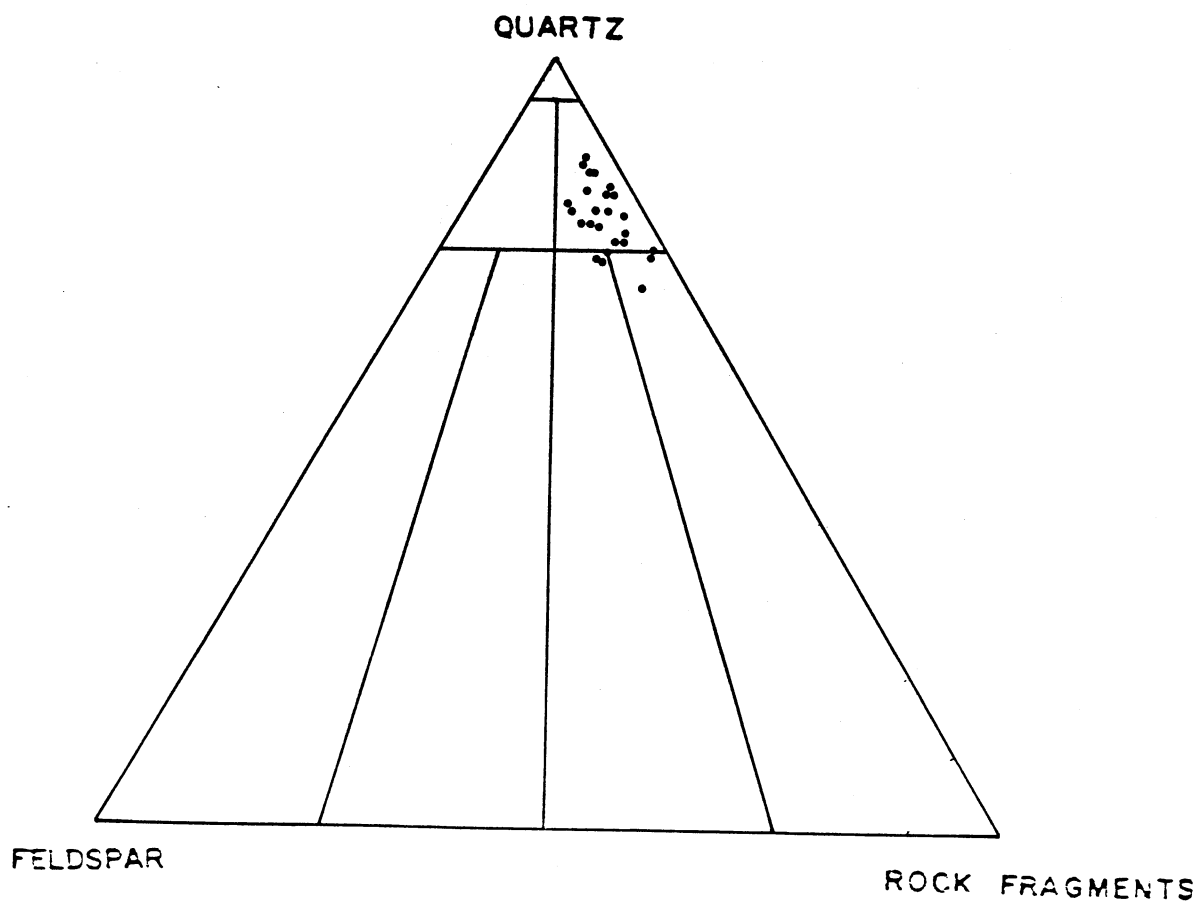
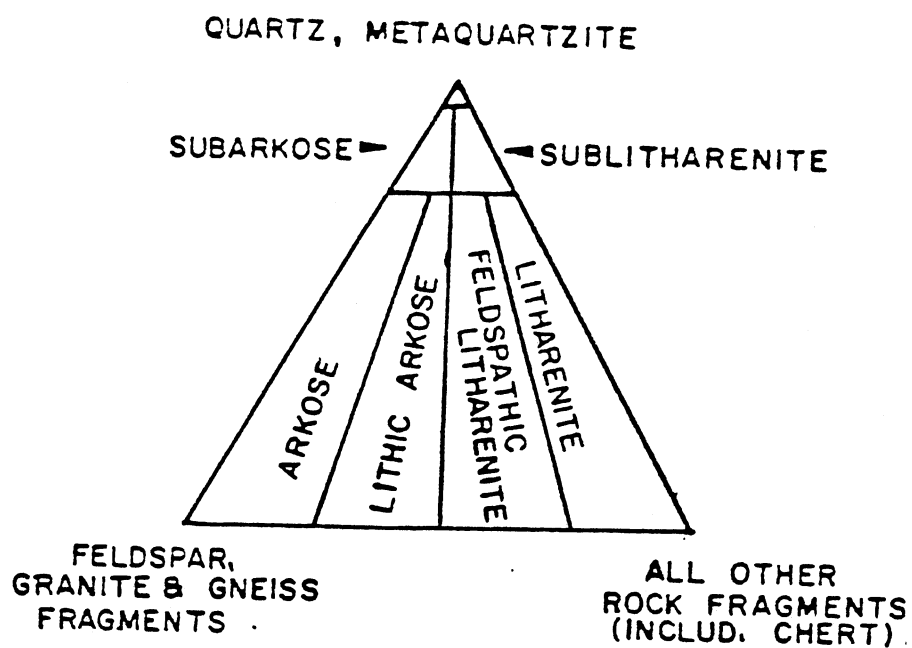


Figure 27. Classification of Samples from Gulf McClung No. 1 Core.

TABLE I
 AVERAGE MINERALOGIC COMPOSITION
 OF THE LAVERTY-HOOVER SANDSTONE

<u>DETRITAL CONSTITUENTS</u>	
QUARTZ	PERCENTAGE
MONOCRYSTALLINE	45.5
POLYCRYSTALLINE	3.5
FELDSPAR	
UNDIFFERENTIATED	2.2
ORTHOCLASE	.2
PLAGIOCLASE	.6
MICROCLINE	.1
ROCK FRAGMENTS	
LOW RANK METAMORPHIC	10.7
SEDIMENTARY	.4
IGNEOUS	Tr
OTHER DETRITAL CONSTITUENTS	
MICAS	4.6
CHERT	.4
OPAQUE MINERAL	.7
GLAUCONITE	.1
ZIRCON	Tr
TOURMALINE	Tr
HORNBLende	Tr
FOSSIL FRAGMENT	Tr
DETRITAL MATRIX	2.9
<u>DIAGENETIC CONSTITUENTS</u>	
CEMENT	
SYNTAXIAL QUARTZ OVERGROWTHS	.3
CALCITE	7.1
SIDERITE	.4
DOLOMITE	Tr
AUTHIGENIC CLAY	
KAOLINITE	1.9
ILLITE	2.6
CHLORITE	.3
SMECTITE	Tr
OTHER	
IRON OXIDES	1.3
PYRITE	Tr
PSUEDOMATRIX	2.4

due to quartz overgrowths, but the original grain shapes can occasionally be recognized by dust rims which outline the original shape of the detrital grain (Figure 28). During deposition, these quartz grains probably were subrounded. The monocrystalline quartz of the Lavery-Hoover Sandstone shows slightly undulose extinction. Polycrystalline quartz averages about 3.5% of the total rock, and contains composite quartz grains. This type of quartz is probably of metamorphic origin (Figures 29 and 30).

Feldspars are not extremely abundant in the Lavery-Hoover Sandstone, accounting for only about 3% of the total rock. The thin sections were stained for detection of potassium rich feldspars (Figures 31 and 32). Plagioclase feldspars were distinguished by their characteristic twinning (Figure 33). Feldspar dissolution is abundant in the samples and the percentage of feldspars may have been slightly higher during deposition.

Rock fragments are fairly abundant in the rock averaging just over 11%. The most abundant of these are low rank metamorphic rock fragments (Figure 34), which account for more than 10% of the total rock. The metamorphic rock fragments consist of fine grained mica aggregates and very fine grained quartz grains which are polycrystalline. Other rock fragments include sedimentary rock fragments (Figure 35), which are composed of illitic material, and igneous rock fragments which were seen only in trace amounts.

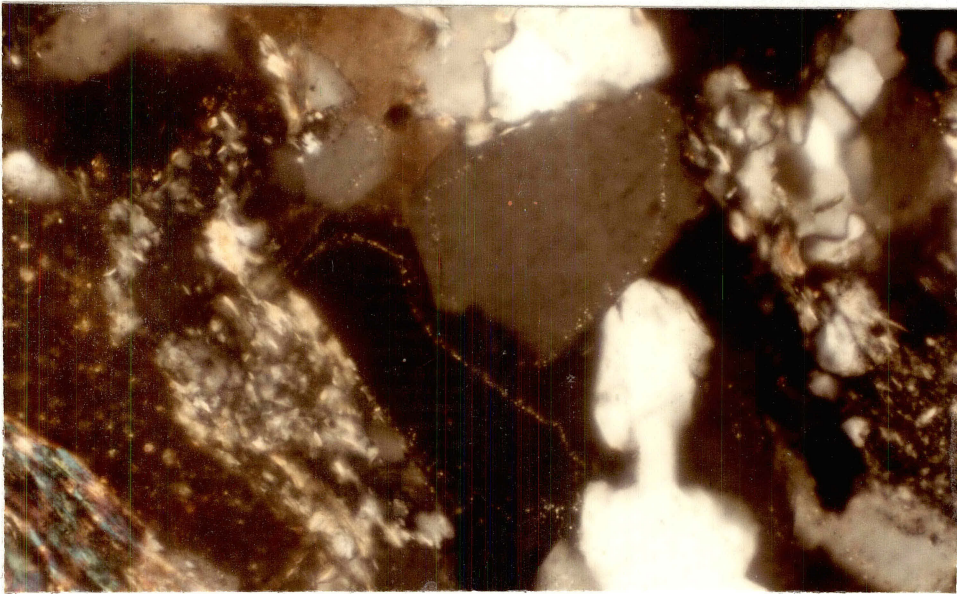


Figure 28. Photomicrograph of Dust Rims Showing the Original Outline of Detrital Quartz Grains. 200X, CN, Gulf McClung, Depth: 4166 ft.

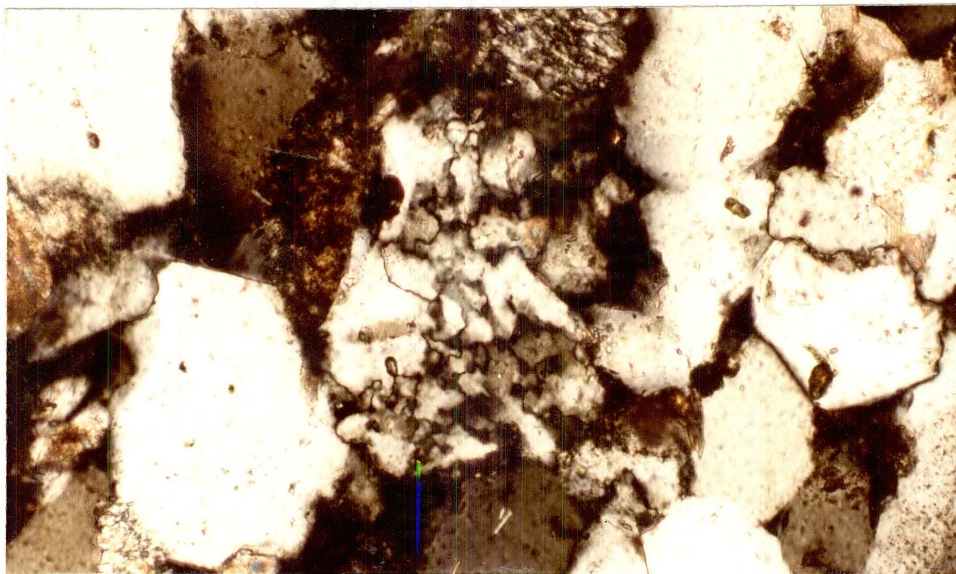


Figure 29. Photomicrograph of Monocrystalline and Polycrystalline Quartz. 200X, CN, Shell Bedell, Depth: 4419 ft.

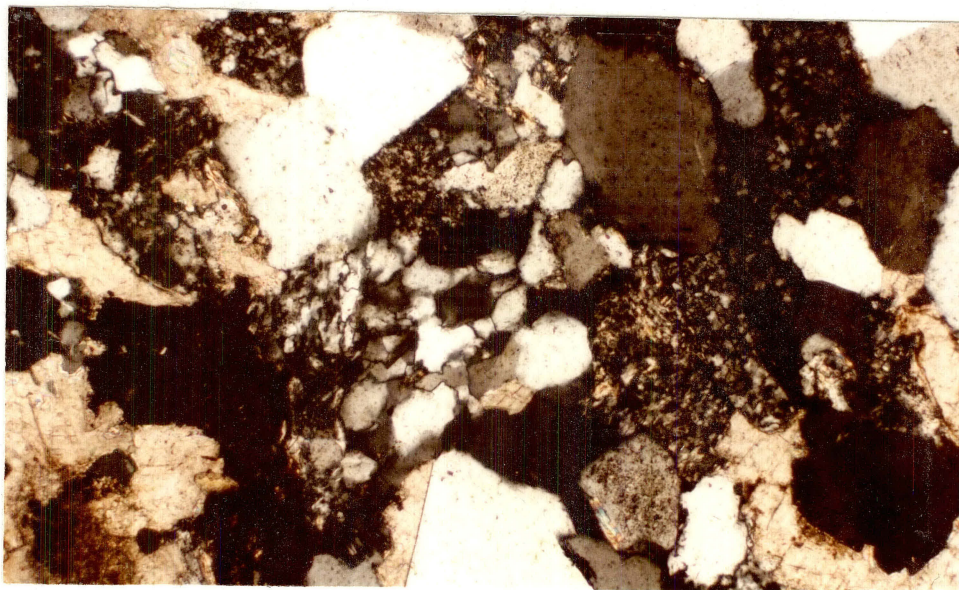


Figure 30. Photomicrograph of Polycrystalline Quartz.
100X, CN, Gulf McClung, Depth: 4221 ft.

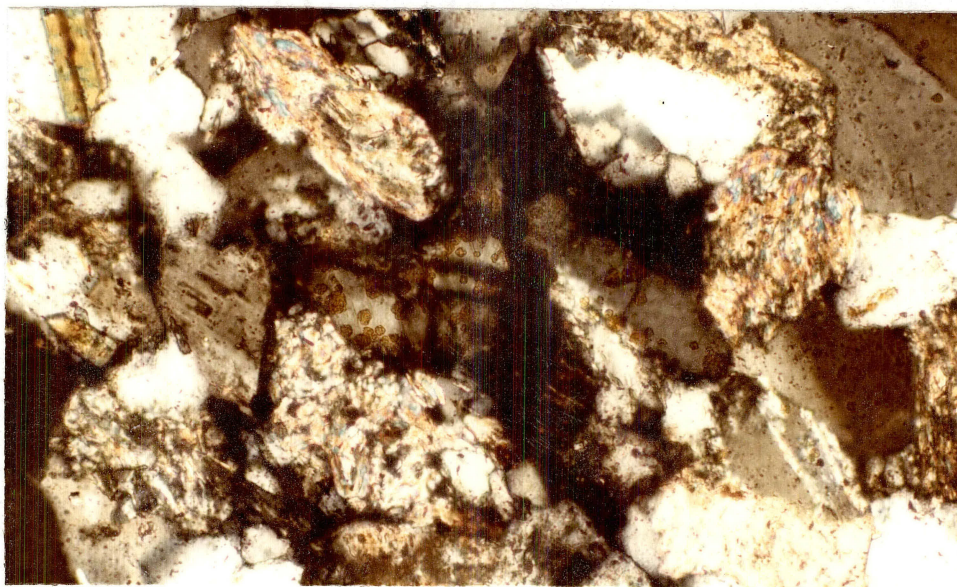


Figure 31. Photomicrograph of Stained Potassium Feldspar
Grains. 200X, CN, Shell Bedell, Depth:
4437 ft.

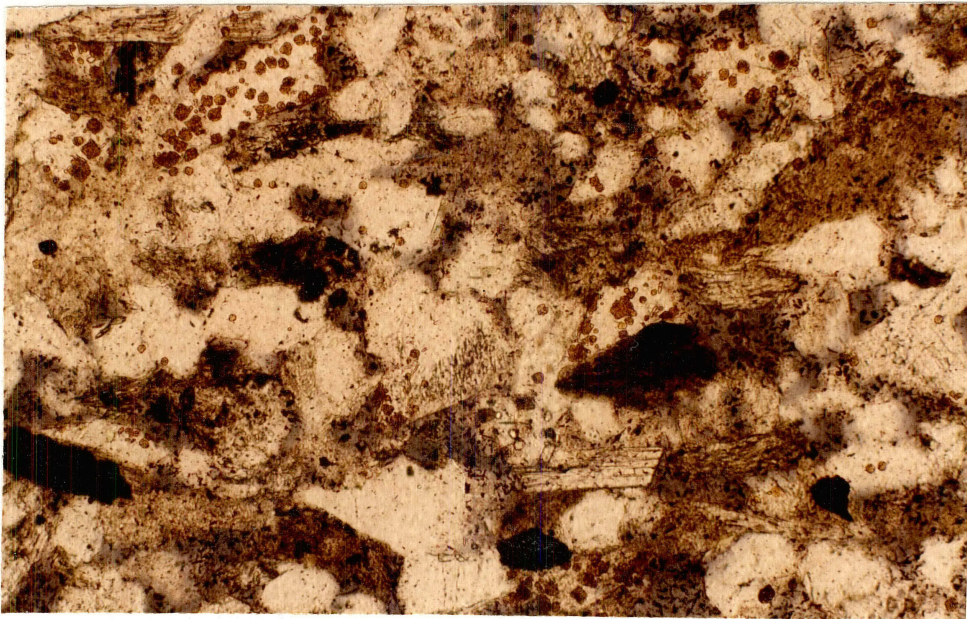


Figure 32. Photomicrograph Showing Several Stained Potassium-Feldspar Grains. 100X, PP, Shell Bedell, Depth: 4437 ft.

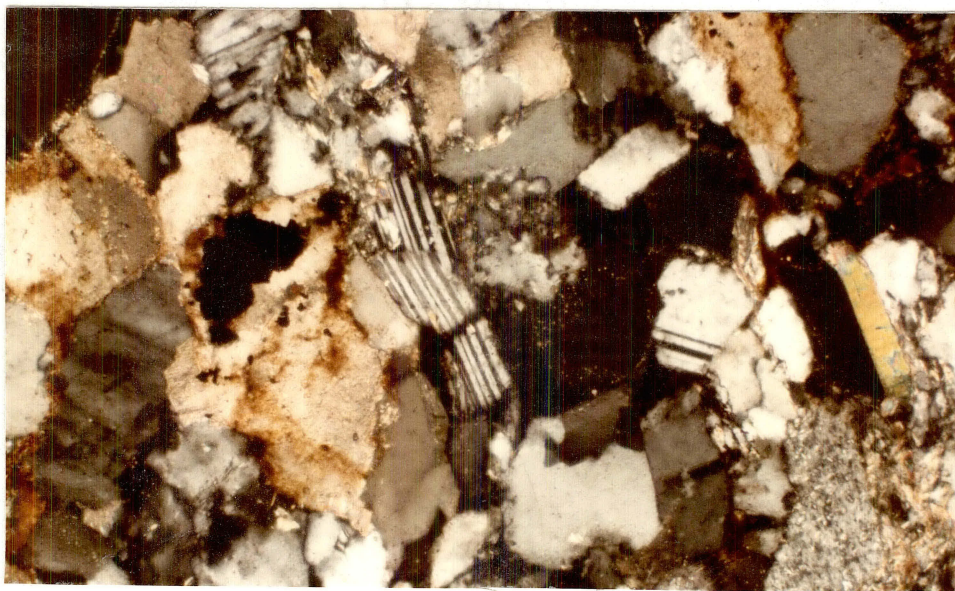


Figure 33. Photomicrograph of Several Twinned Plagioclase Feldspar Grains. 100X, CN, Gulf McClung, Depth: 4171 ft.

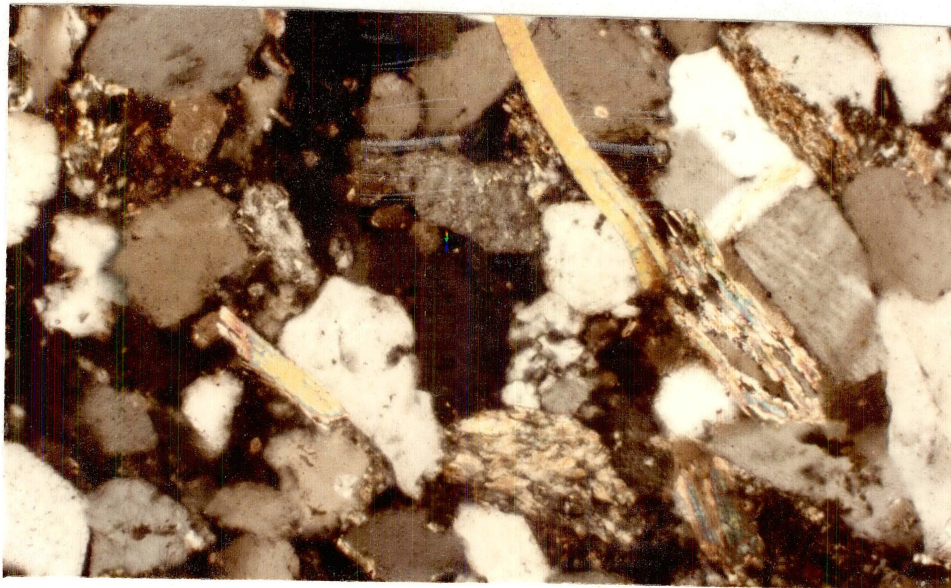


Figure 34. Photomicrograph of Several Low-Rank Metamorphic-Rock Fragments. 100X, CN, Gulf McClung, Depth: 4166 ft.

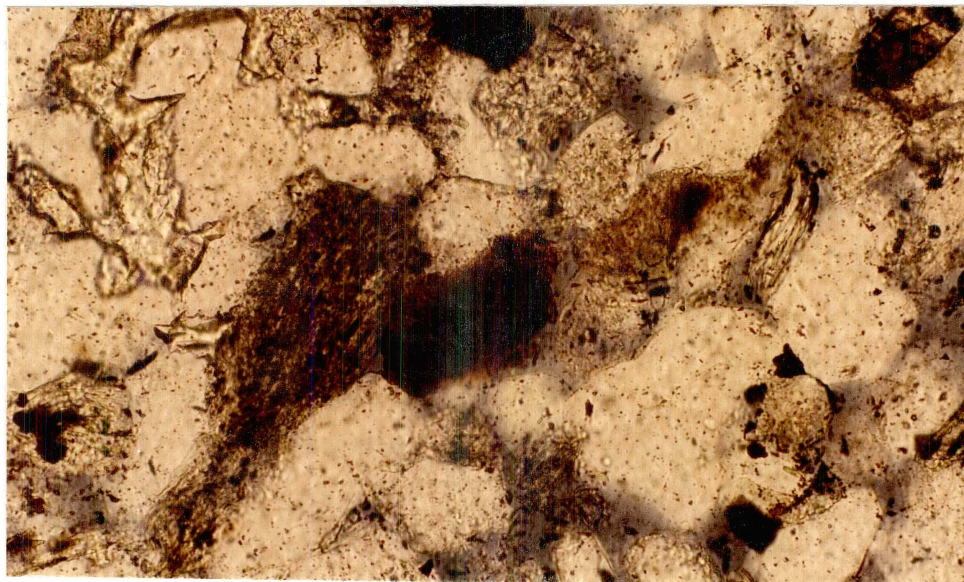


Figure 35. Photomicrograph of Sedimentary Rock Fragment. 200X, PP, Shell Bedell, Depth: 4453 ft.

Micas are fairly abundant averaging just under 5% of the total rock (Figure 36). Opaque mineral grains (Figure 37) constitute just under 1% of the total rock and chert (Figure 38) also averages under 1%. Other detrital constituents that are present only in trace amounts are glauconite (Figure 39), zircon (Figure 40), tourmaline, hornblende, and fossil fragments (Figure 41).

The detrital matrix is composed mainly of coarse grained illitic material and fine grained micas (Figure 42). The detrital matrix averages about 3% of the total rock.

Diagenetic Constituents

Syntaxial quartz overgrowths are in almost all of the samples. The calculated average percentage for overgrowths is less than 1%. However, it is thought that the actual value for quartz overgrowths is much higher because of a lack of dust rims which prohibited distinction of the overgrowths. Quartz overgrowths appeared to be very abundant upon scanning electron microscope examination (Figure 43).

Calcite cement is the most abundant cement of the Laverty-Hoover Sandstone averaging over 7% of the total rock (Figure 44). Siderite is fairly common and exists primarily in the detrital matrix and fine grained zones (Figure 45), and lining the edges of calcium carbonate cement (Figure 46). Dolomite was seen only in one sample

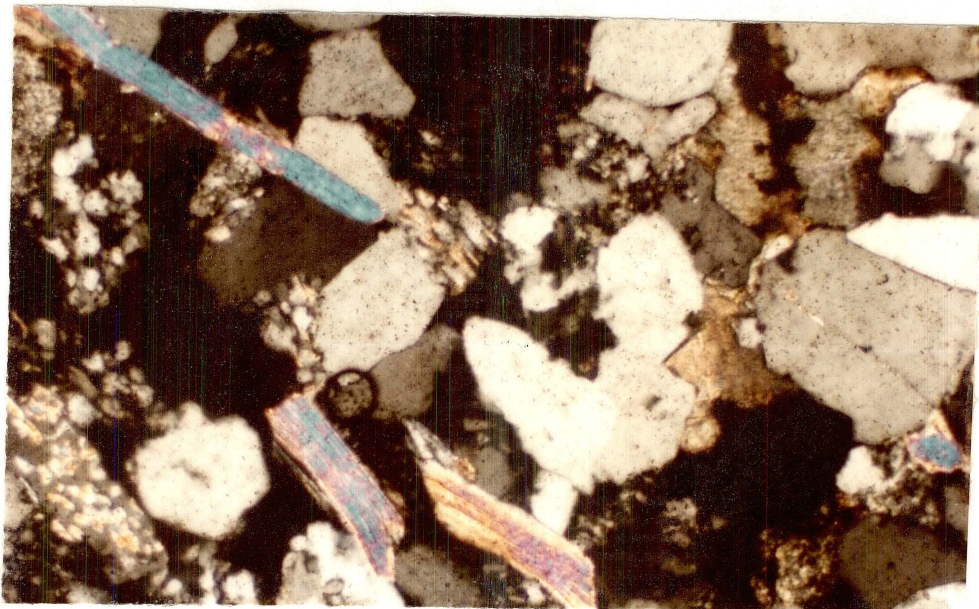


Figure 36. Photomicrograph of Several Detrital Mica Grains. 100X, CN, Gulf McClung, Depth: 4221 ft.

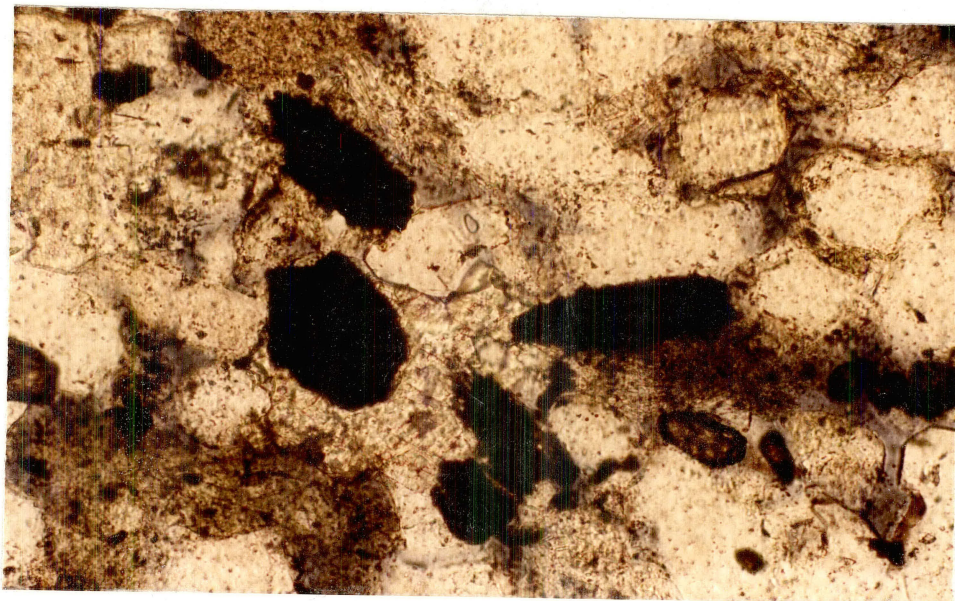


Figure 37. Photomicrograph of Opaque Mineral Grains. 100X, PP, Shell Bedell, Depth: 4434 ft.

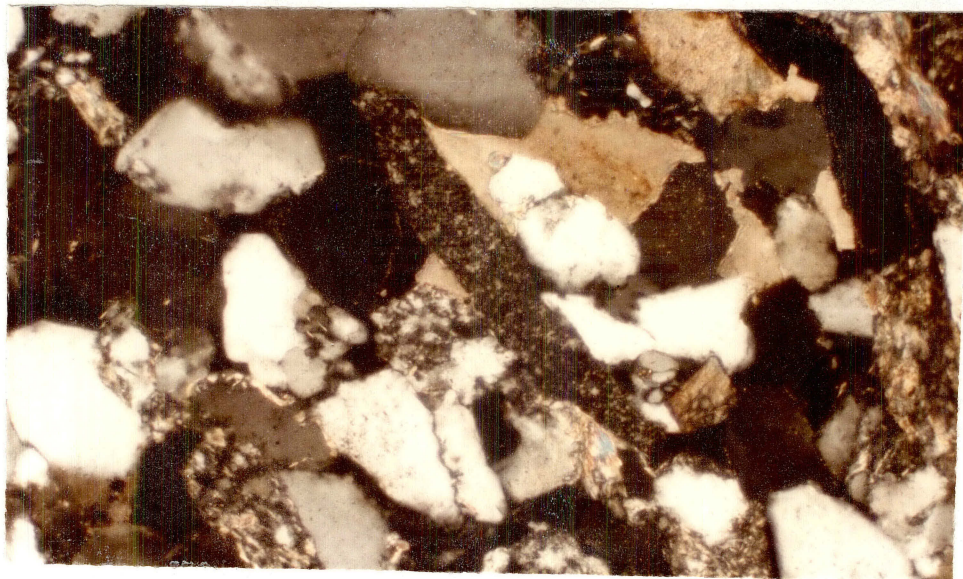


Figure 38. Photomicrograph of an Elongate Detrital Chert Grain. 100X, CN, Gulf McClung, Depth: 4171 ft.

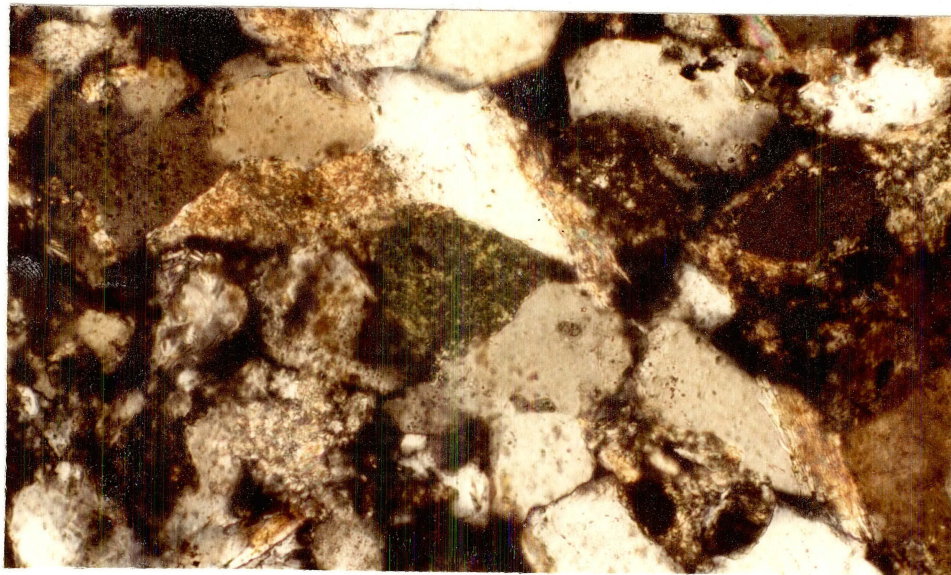


Figure 39. Photomicrograph of a Glauconite Grain. 200X, CN, Shell Bedell, Depth: 4430 ft.

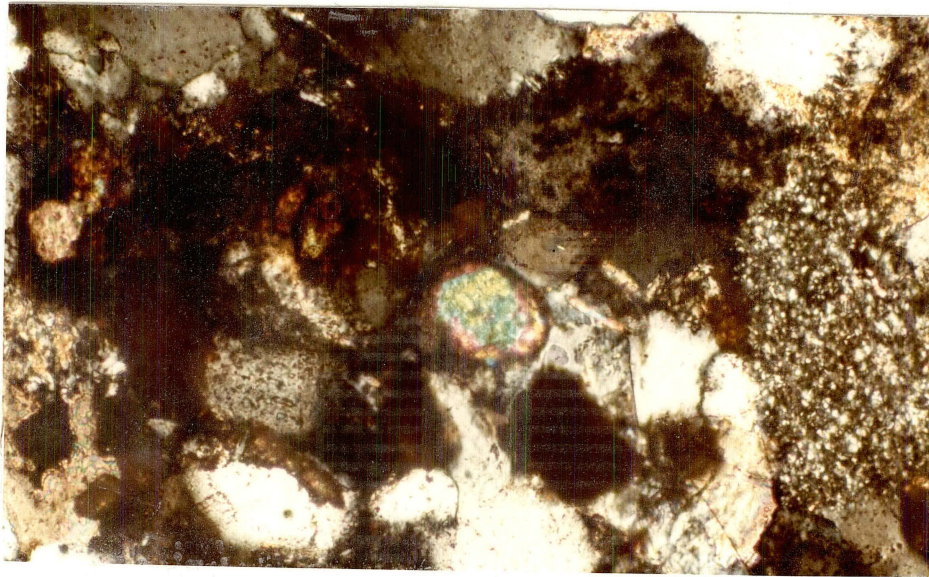


Figure 40. Photomicrograph of Detrital Zircon. 200X, CN, Shell Bedell, Depth: 4419 ft.

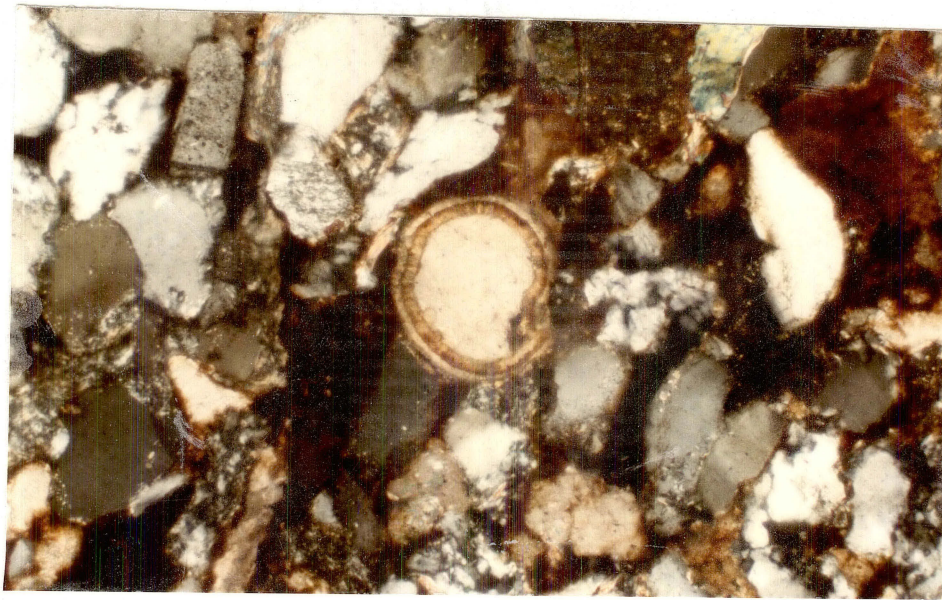


Figure 41. Photomicrograph, Fragment of a Fossil. 100X, CN, Gulf McClung, Depth: 4171 ft.

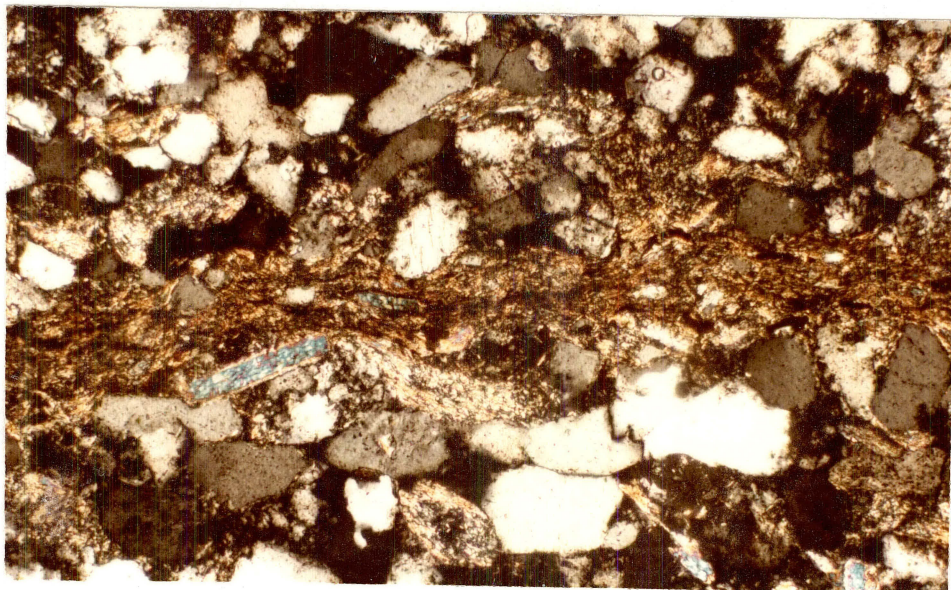


Figure 42. Photomicrograph of Detrital Matrix Material.
100X, CN, Shell Bedell, Depth: 4417 ft.

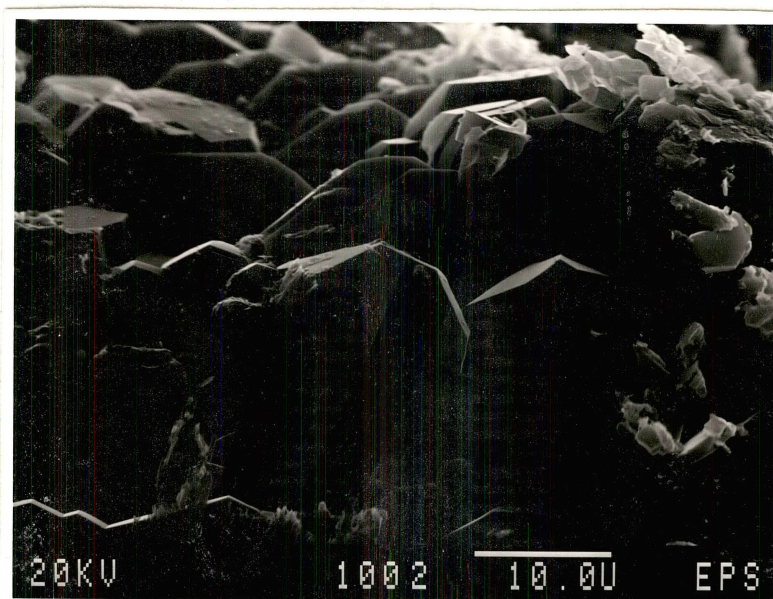


Figure 43. SEM Micrograph Showing Abundance of Quartz
Overgrowths. 2000X, Gulf McClung, Depth:
4250 ft.

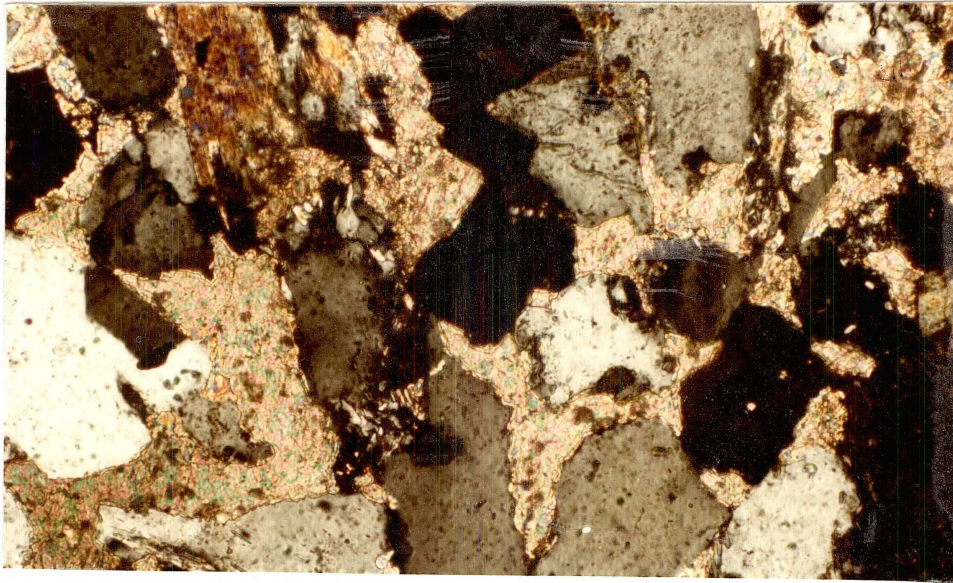


Figure 44. Photomicrograph of Calcium-Carbonate Cement.
200X, CN, Shell Bedell, Depth: 4404 ft.

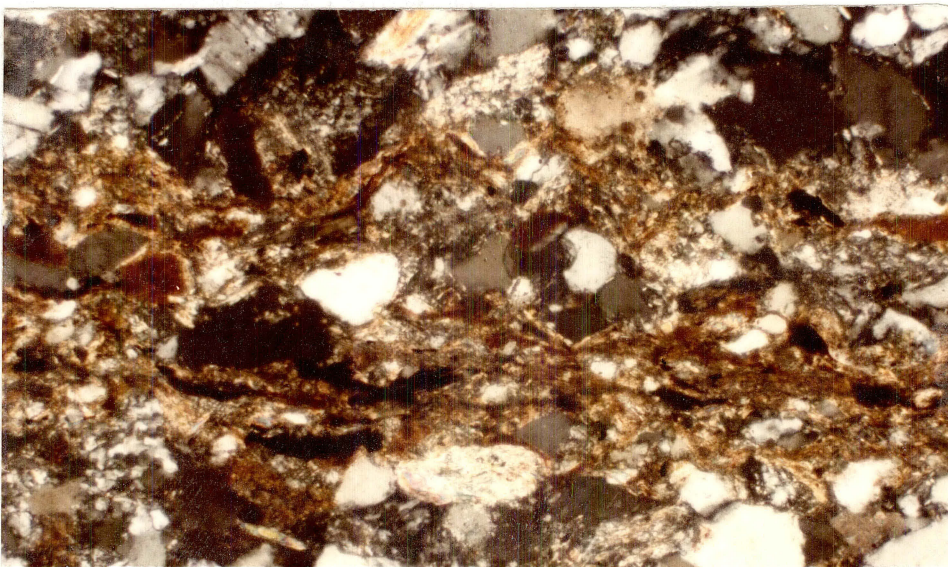


Figure 45. Photomicrograph of Siderite Concentrated in
Detrital Matrix. 100X, CN, Gulf McClung,
Depth: 4184 ft.

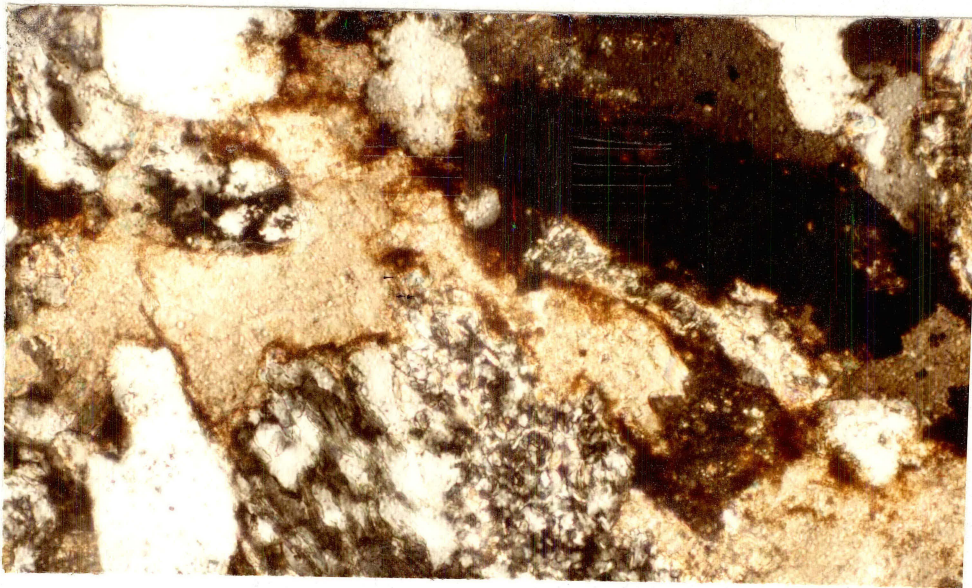


Figure 46. Photomicrograph of Siderite Lined Edges of Calcite Cement. 200X, CN, Gulf McClung, Depth: 4171 ft.

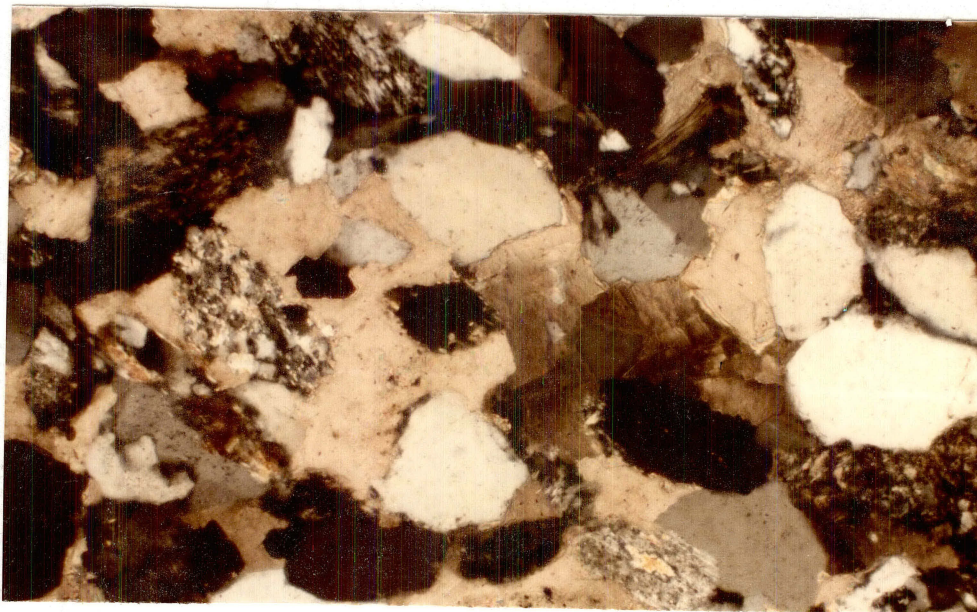


Figure 47. Photomicrograph of Dolomite Surrounded Detrital Grains. 100X, CN, Gulf McClung, Depth: 4166 ft.

at the top of the Gulf McClung No. 1 well at a depth of 4166 feet (Figure 47).

Iron oxides are present in the Lavery-Hoover Sandstone and they average just over 1% of the total rock (Figure 48). Framboidal pyrite was observed in trace amounts during thin section examination, and appeared to be fairly abundant under the scanning electron microscope (Figure 49).

Authigenic clays can be recognized in all of the samples and make up about 5% of the total rock. Authigenic kaolinite exists in booklets and constitutes just under 2% of the total rock (Figure 50). Authigenic illite is present in all of the samples accounting for just under 3% of the rock, and is commonly seen as needlelike projections lining the detrital grains (Figure 51). Authigenic chlorite can be recognized in most of the samples that were examined, but is not extremely abundant averaging less than .3% of the rock. Smectite is present in the Lavery-Hoover Sandstone, but only in trace quantities.

Pseudomatrix material consists primarily of low rank metamorphic rock fragments which have been squeezed into available pore spaces during compaction (Figures 52, 53 and 54). Pseudomatrix material accounts for about 2.4% of the total rock.

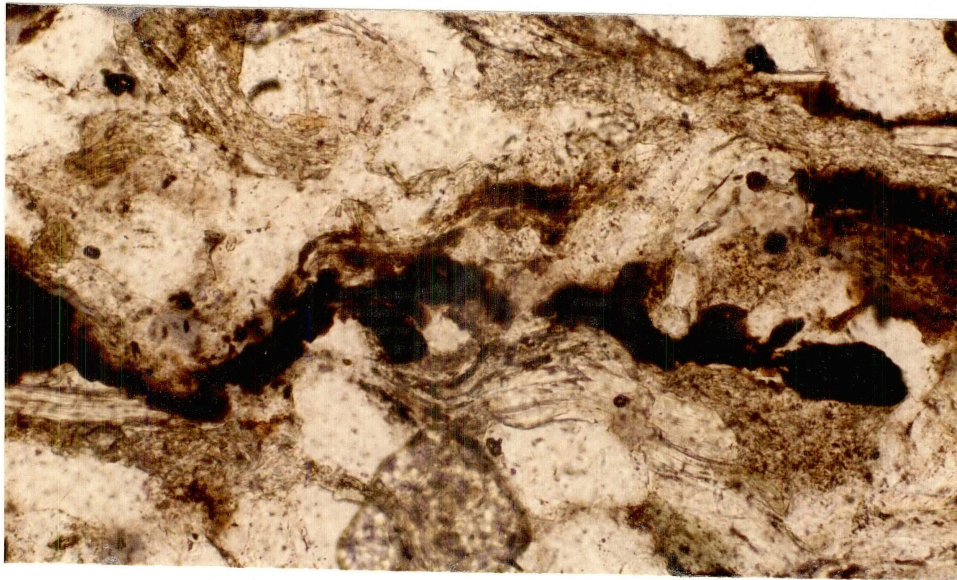


Figure 48. Photomicrograph of Iron Oxides. 100X, CN, Gulf McClung, Depth: 4231 ft.

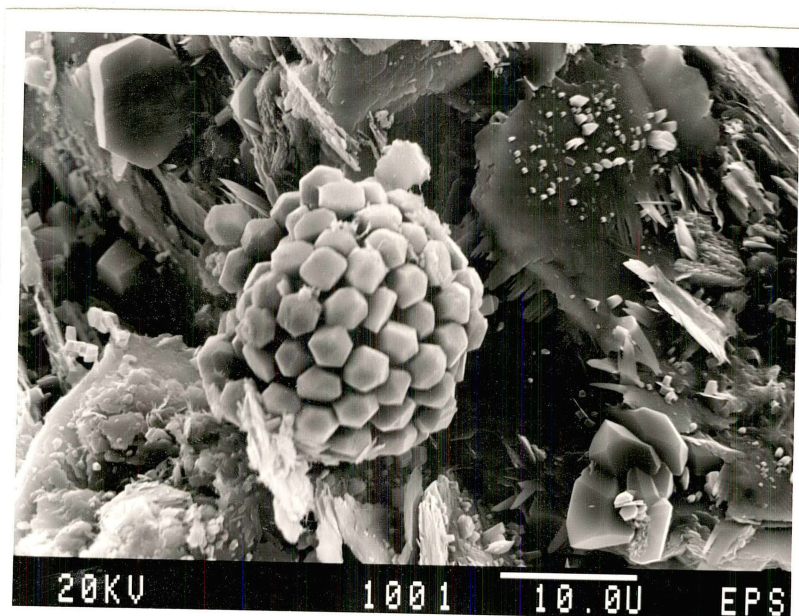


Figure 49. SEM Micrograph of Framboidal Pyrite. 2000X, Gulf McClung, Depth: 4266 ft.

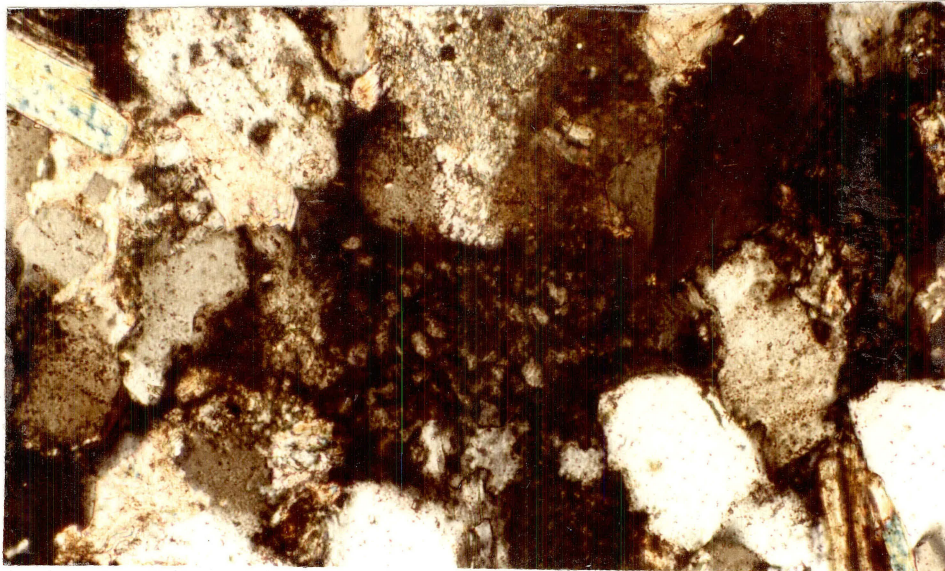


Figure 50. Photomicrograph of Pore-Filling Kaolinite. 200X, CN, Shell Bedell, Depth: 4418 ft.

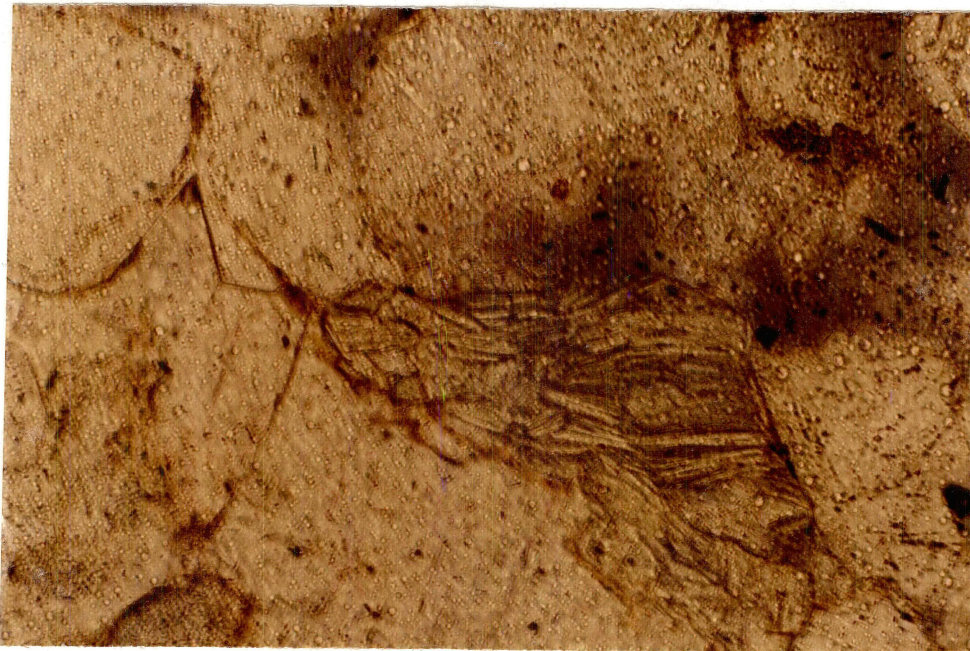


Figure 51. Photomicrograph of Detrital Grains Coated with Authigenic Illite. 200X, PP, Gulf McClung, Depth: 4171 ft.

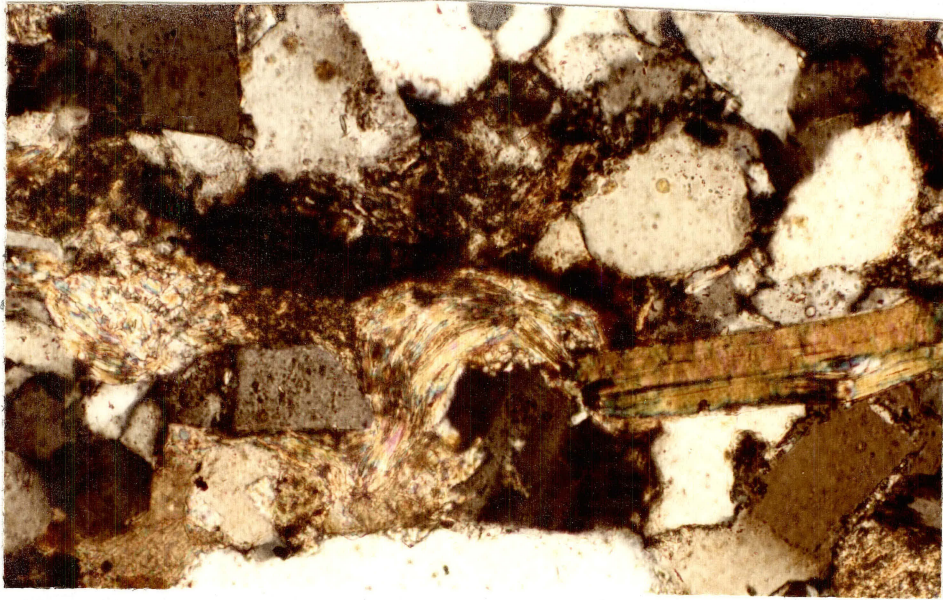


Figure 52. Photomicrograph of Pseudomatrix Material. 200X,
CN, Shell Bedell, Depth: 4426 ft.

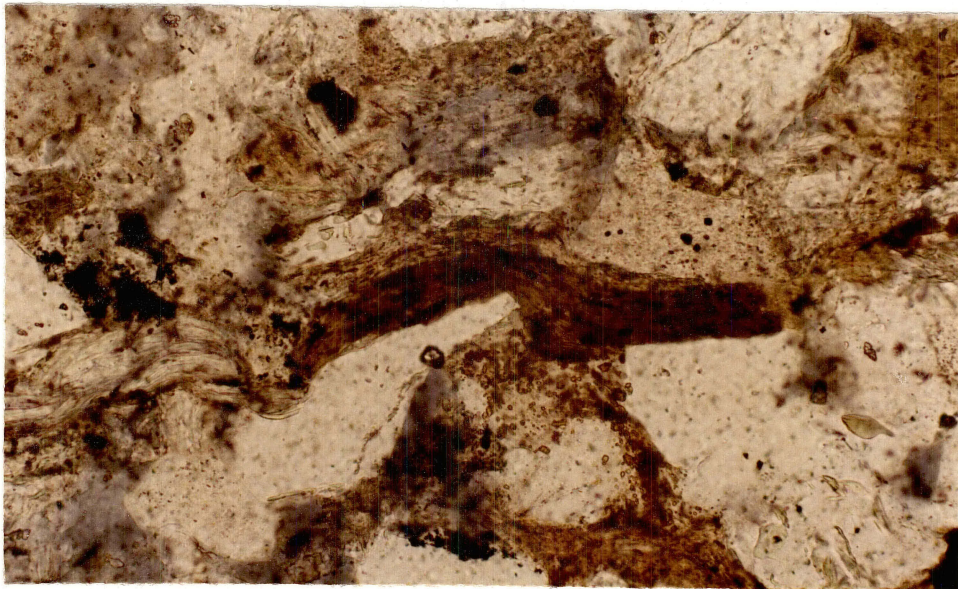


Figure 53. Photomicrograph of Pseudomatrix Material. 100X,
PP, Gulf McClung, Depth 4266 ft.

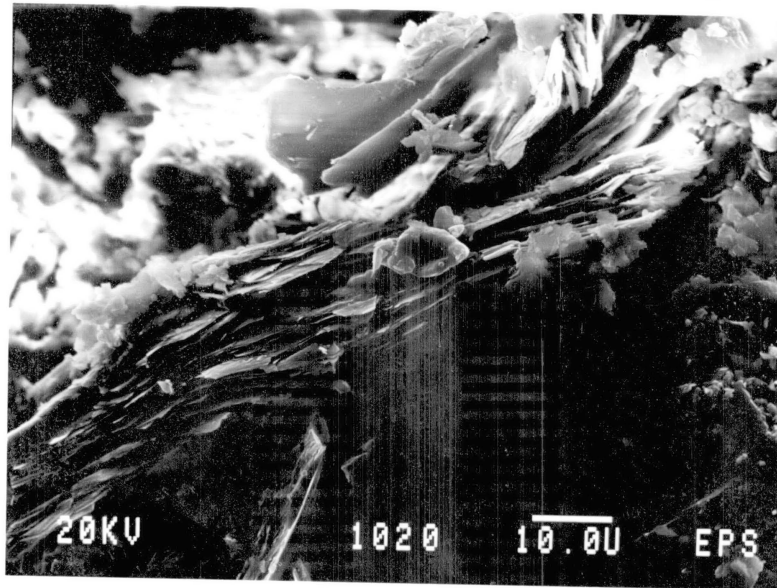


Figure 54. SEM Micrograph Showing Ductile Deformation of Micaceous Material. 1200X, Shell Bedell, Depth: 4446 ft.

CHAPTER VII

DIAGENESIS

Introduction

The Laverty-Hoover Sandstone has been greatly affected by diagenetic processes. Several diagenetic features have been recognized using thin section petrography, scanning electron microscopy, and x-ray diffraction techniques. These diagenetic events and the relative time frame in which these events occurred will be discussed in this chapter.

Silica

Quartz grains are sutured together by syntaxial quartz overgrowths which are present in almost all of the samples. These quartz overgrowths can be recognized in many grains by dust rims which outline the original shape of the detrital grain. The overgrowths appear varved-like under the scanning electron microscope which suggests that the quartz overgrowths were stacked upon each other in thin layers, the precipitation of quartz overgrowths being controlled by the pH of the pore fluids.

The quartz overgrowths surrounding the detrital grains

are commonly corroded around the edges (Figure 55). The corrosion of the quartz overgrowths is believed to be associated with carbonate precipitation (Figure 56), and the event was probably aided by alkaline pore fluids.

Dissolution of Feldspar

The complete and partial dissolution of feldspar grains was an important diagenetic event, giving rise to a large amount of secondary porosity in the rock. Complete dissolution of feldspar is evidenced by grain molds which allow recognition of the former detrital grain's shape (Figure 57). Many feldspars show partial dissolution and are preferentially dissolved along cleavage planes (Figures 58, 59, 60, 61, and 62).

Dissolution of Detrital Matrix

The detrital matrix was preferentially dissolved in a few areas and can be recognized by elongate, thin, porous zones (Figure 63). These zones were probably leached by acidic pore waters along weak bedding planes which provided permeable pathways for the migrating fluids.

Carbonates

Calcium carbonate is the most abundant cementing agent in the Lavery-Hoover Sandstone. It commonly occurs in small clusters, as large, well-developed crystals. In a few samples, calcite cement dominates the rock, and has

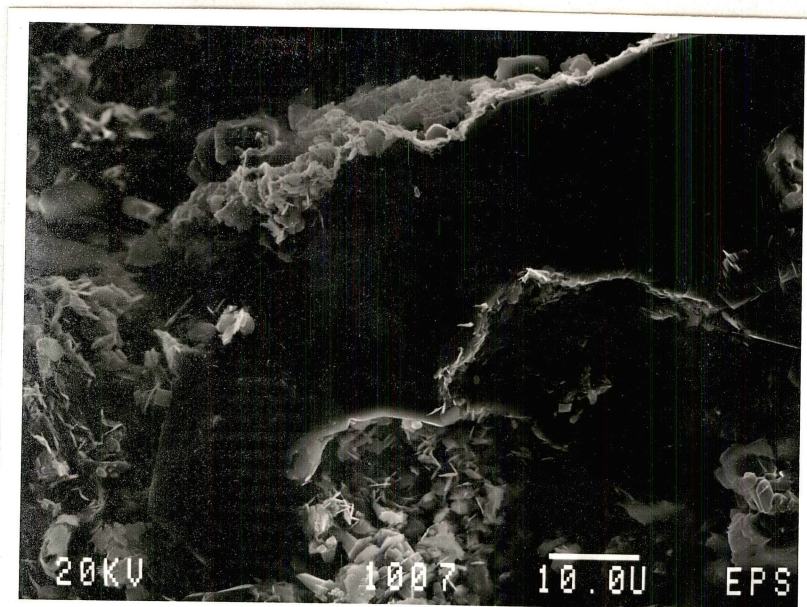


Figure 55. SEM Micrograph of a Corroded Quartz Grain Lined with Authigenic Clays. 1300X, Shell Bedell, Depth: 4428 ft.

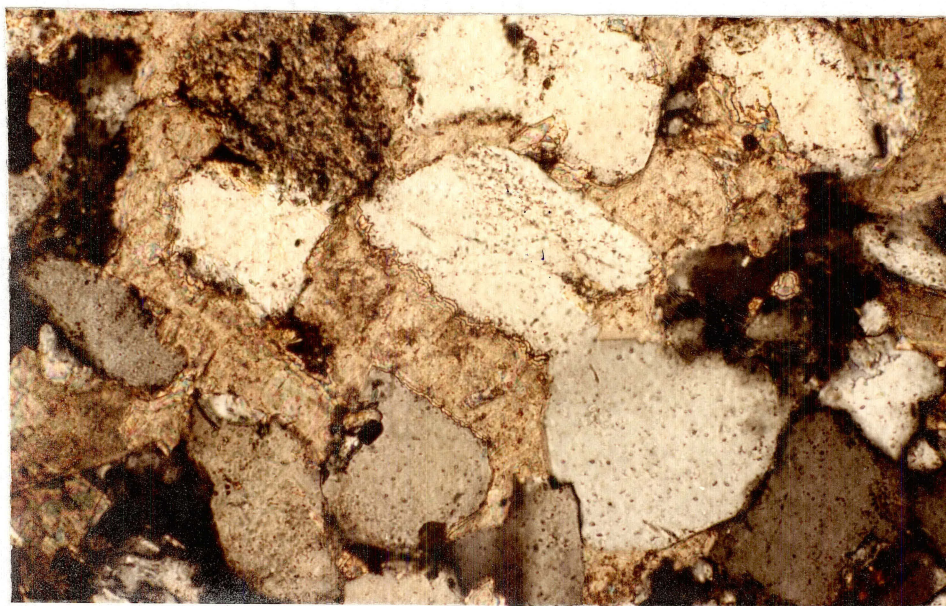


Figure 56. Photomicrograph of Calcite Invaded Detrital Grains. 200X, CN, Shell Bedell, Depth: 4413 ft.

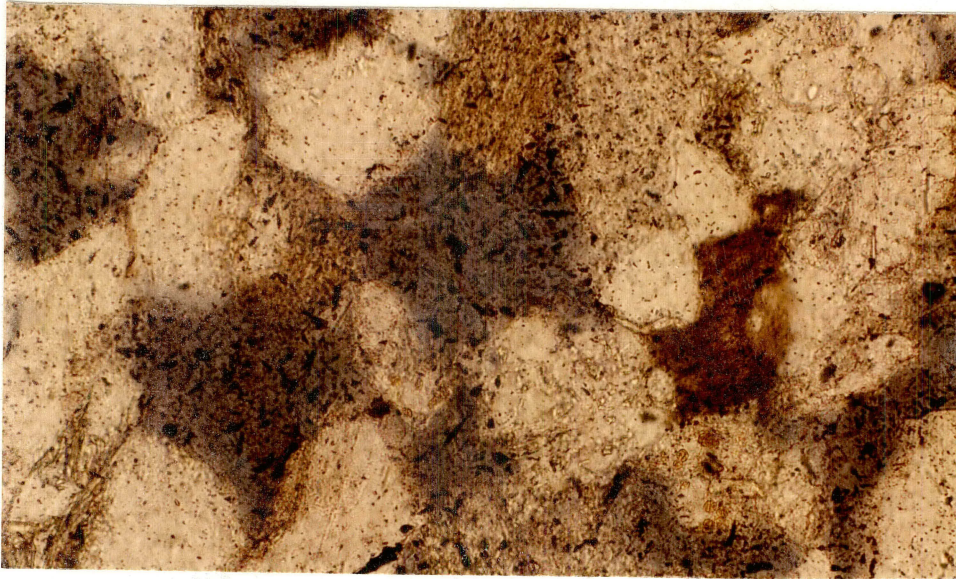


Figure 57. Photomicrograph of Grain Molds. 200X, PP, Shell
Bedell, Depth: 4434 ft.

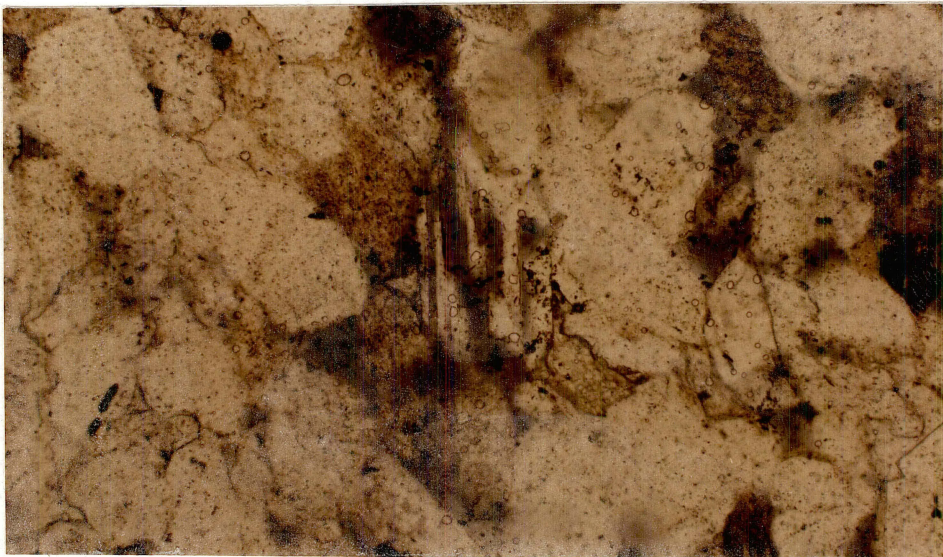


Figure 58. Photomicrograph of Partly Dissolved Feldspar.
100X, PP, Gulf McClung, Depth: 4266 ft.

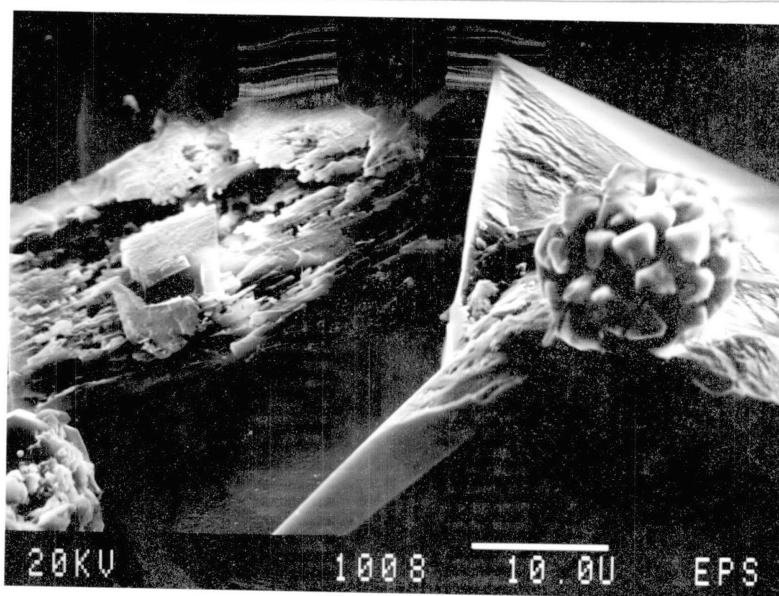


Figure 59. SEM Micrograph of Quartz Overgrowth, Feldspar Dissolution, and Framboidal Pyrite. 2000X, Gulf McClung, Depth: 4184 ft.

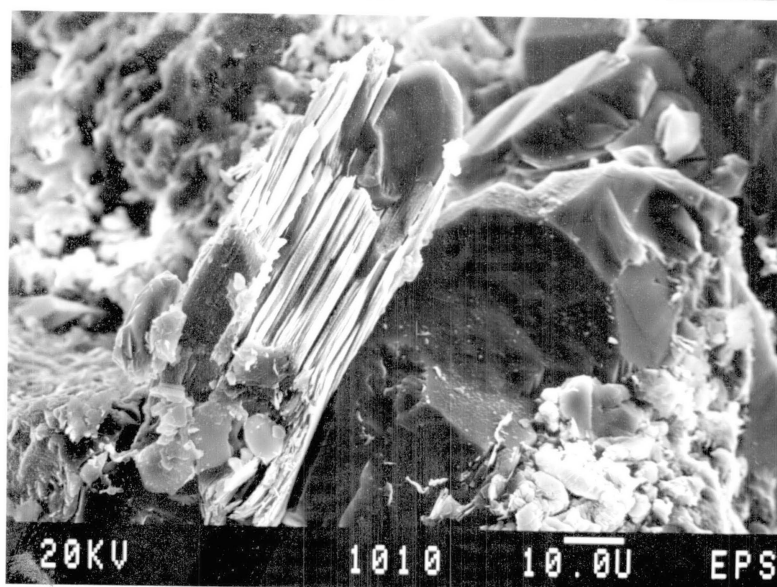


Figure 60. SEM Micrograph of Partially Dissolved Feldspar Grain. 860X, Gulf McClung, Depth: 4245 ft.

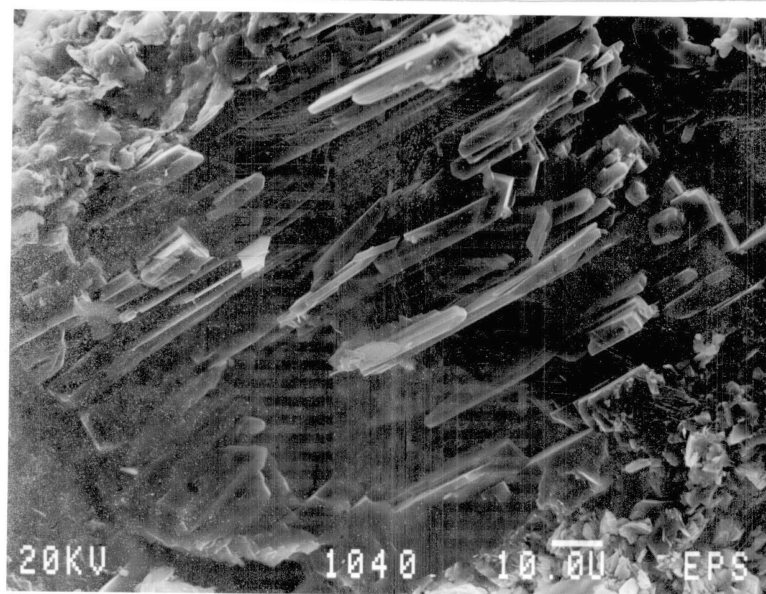


Figure 61. SEM Micrograph of Dissolved Feldspar. 720X, Shell Bedell, Depth: 4465 ft.

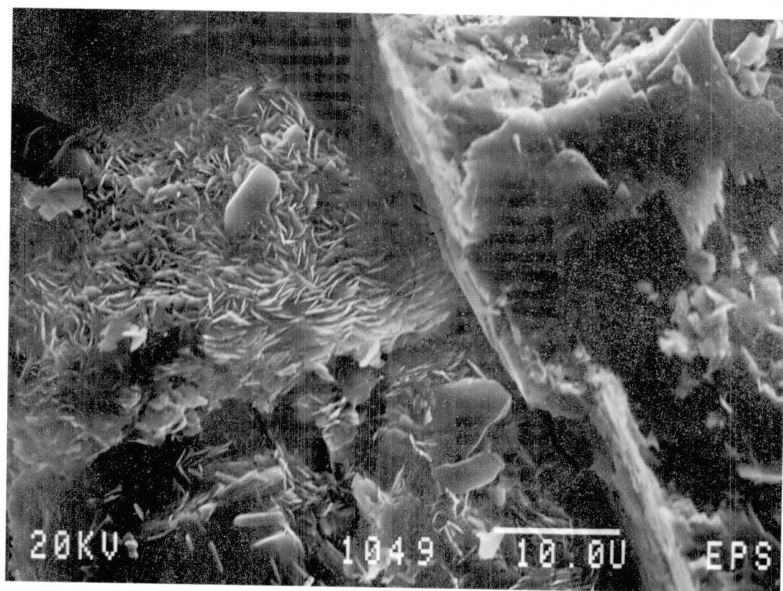


Figure 62. SEM Micrograph of Partly Dissolved Feldspar and Authigenic Chlorite. 1800X, Shell Bedell, Depth: 4465 ft.

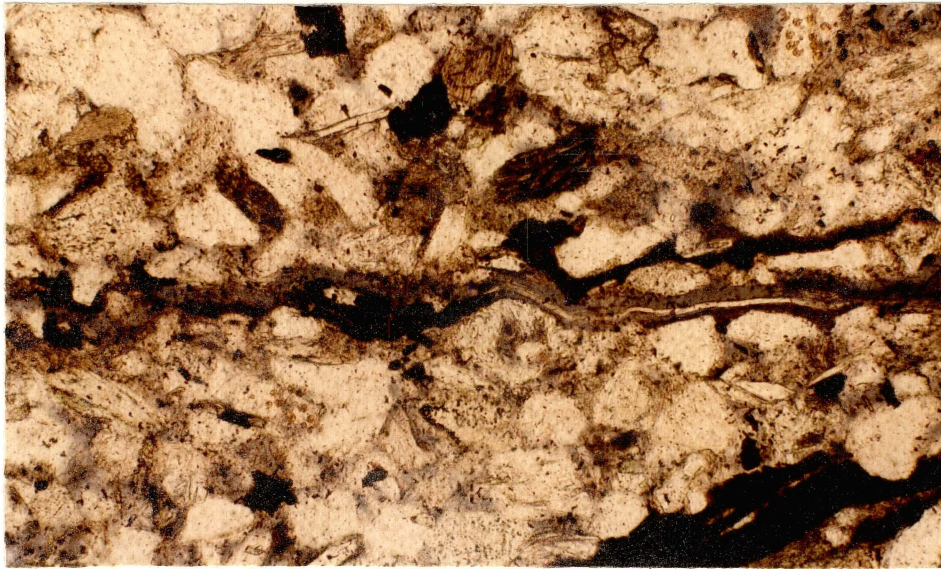


Figure 63. Photomicrograph of Dissolved Detrital Matrix.
100X, PP, Shell Bedell, Depth: 4455 ft.

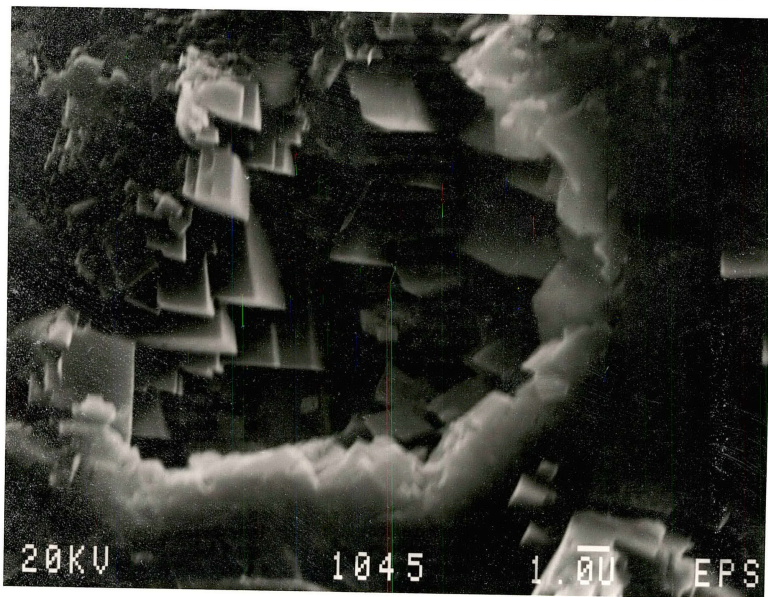


Figure 64. SEM Micrograph Showing Evidence of Dissolution
of Silica by Calcite. 3600X, Shell Bedell,
Depth: 4465 ft.

replaced a large amount of the detrital constituents.

It is believed that calcium carbonate once occupied nearly all the available pore spaces of the Lavery-Hoover Sandstone. The calcite was later dissolved by acidic pore fluids creating a large amount of secondary porosity (Figure 64).

Siderite can be recognized in two areas. It can be seen as small bands, from a few millimeters to a few centimeters thick, especially concentrated in the fine grain sediments (Figure 45). This type of siderite is believed to have formed shortly after deposition. The normal pH, low Eh, and low sulphur activity necessary for this process are all present in a rapidly developing delta system. Siderite may also be found lining the edges of calcite (Figure 46). This type of siderite is believed to have formed diagenetically, replacing calcite along its outer boundaries shortly after calcite dissolution.

Dolomite was seen only at the top of the Gulf McClung well (Figure 47). Dolomitization of calcium carbonate is believed to have taken place in the later stages of diagenesis.

Authigenic Clays

Thin section examination, scanning electron microscopy, and x-ray diffraction techniques allowed the identification of authigenic kaolinite, illite, and chlorite. The abundance and relative positions of the

clays within the pore spaces are very important. These clays were observed lining, filling and bridging pore spaces and throats, which create microporosity, decrease macroporosity, and reduce effective permeability.

Authigenic kaolinite is very abundant in the Lavery-Hoover Sandstone, and exists as stacked, pseudo-hexagonal booklets, which commonly fill secondary pore spaces (Figures 50, 65, 66, 67, 68, and 69). Kaolinite is believed to have been derived as a dissolution and alteration product of feldspar. Kaolinite appeared much more abundant under the scanning electron microscope than in the thin sections.

Authigenic illite is also very abundant in the Lavery-Hoover Sandstone. Illite most commonly occurs as pore bridging or pore lining clay. It can often be seen lining a corroded quartz grain or overgrowth (Figures 49, 68, 69, 72, and 73). The authigenic illite is believed to have been derived from the alteration of feldspar grains and the breakdown of fine grained micaceous material located in metamorphic rock fragments and the detrital matrix.

Authigenic chlorite is less abundant than kaolinite and illite. It is usually seen either lining or bridging secondary pore spaces, and also, occasionally present as pore filling clay (Figures 62, 74, 75, and 76). Chlorite's presence as a pore filling clay could possibly be explained by the complete alteration of illite or

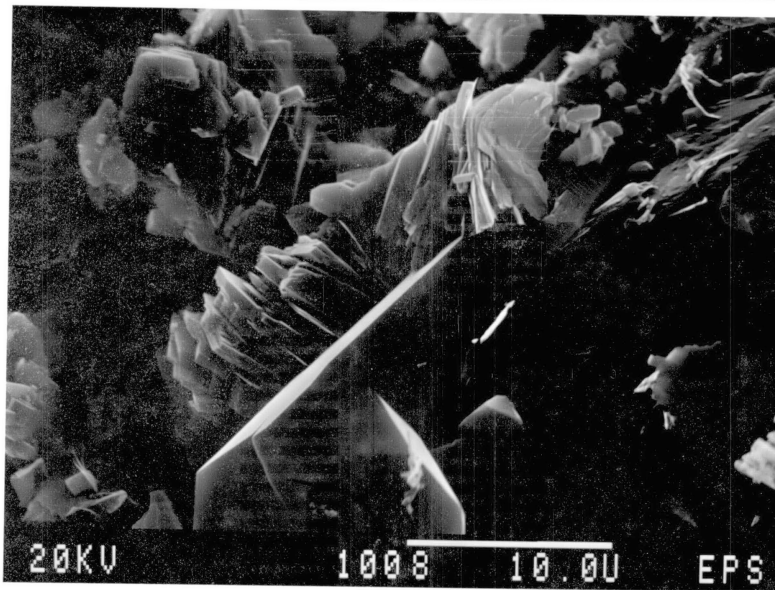


Figure 65. SEM Micrograph of Authigenic Pore-Filling Kaolinite. 3000X, Shell Bedell, Depth: 4465 ft.

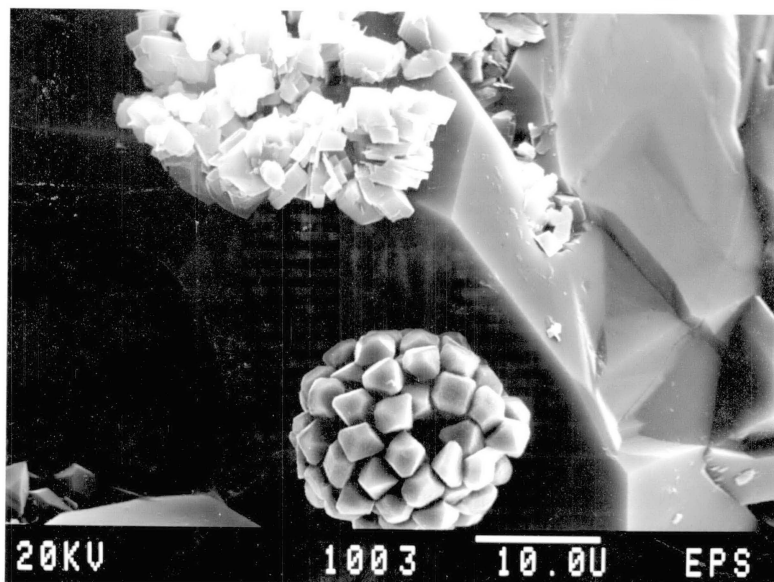


Figure 66. SEM Micrograph of Quartz Overgrowth, Authigenic Kaolinite, and Framboidal Pyrite. 1800X, Gulf McClung, Depth: 4204 ft.

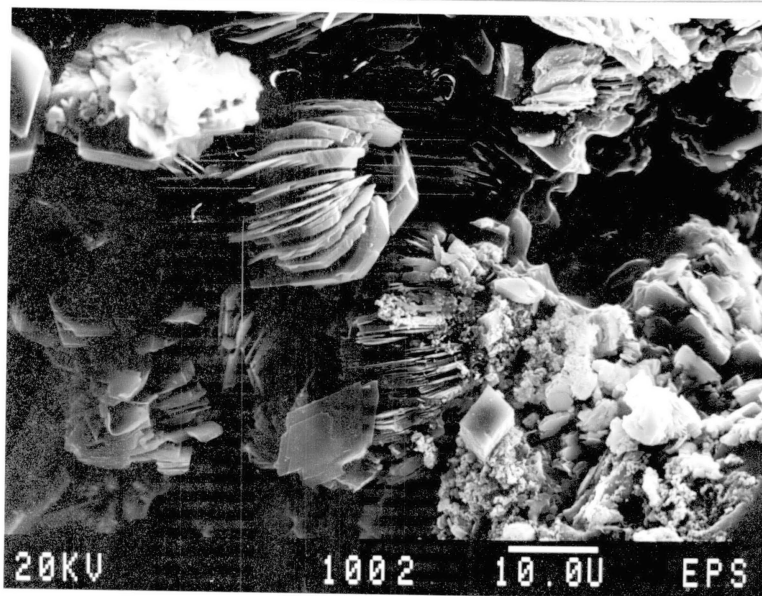


Figure 67. SEM Micrograph of Pore-Filling Authigenic Kaolinite. 1300X, Gulf McClung, Depth: 4204 ft.

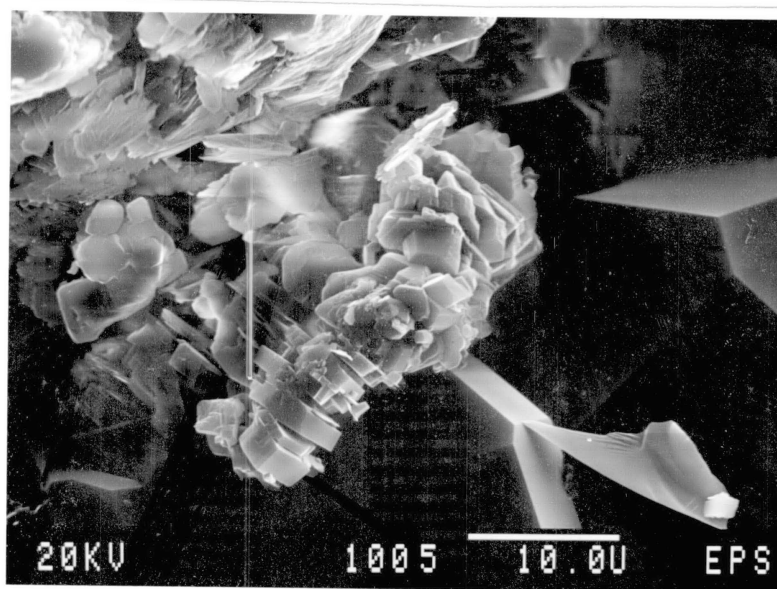


Figure 68. SEM Micrograph of Pore-Filling Kaolinite and Quartz Overgrowths. 2200X, Gulf McClung, Depth: 4266 ft.

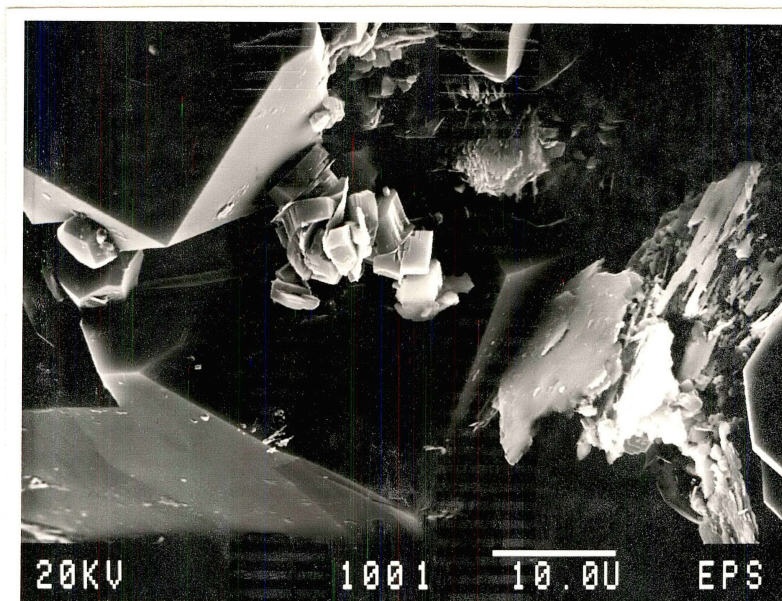


Figure 69. SEM Micrograph of Pore-Filling Authigenic Kaolinite and Quartz Overgrowths. 1800X, Gulf McClung, Depth: 4204 ft.

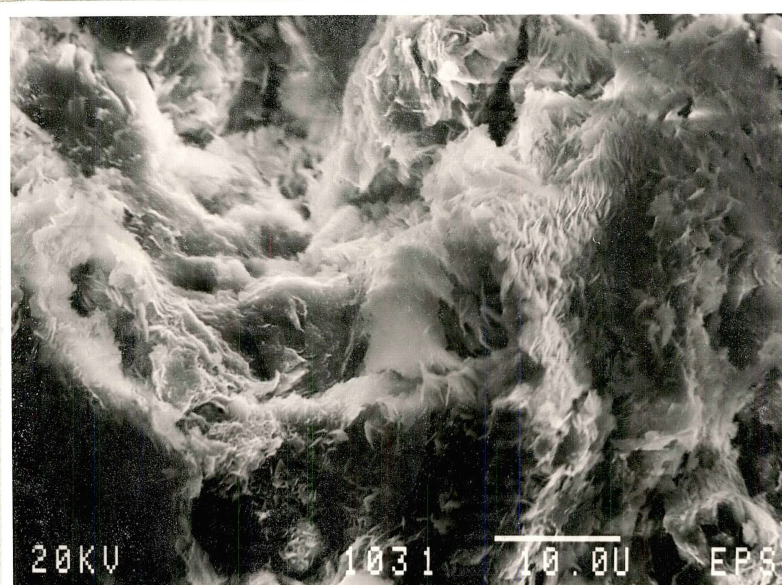


Figure 70. SEM Micrograph of Grain-Coating Authigenic Illite and Chlorite. 1800X, Shell Bedell, Depth: 4452 ft.

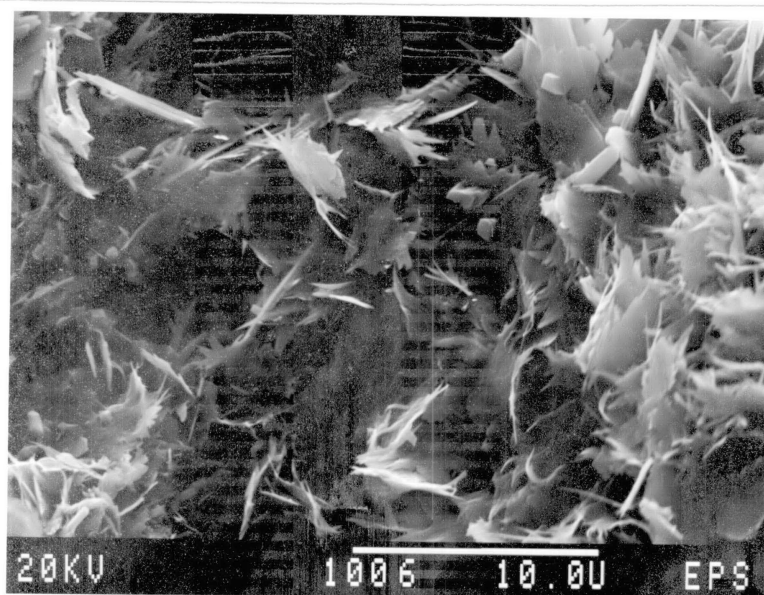


Figure 71. SEM Micrograph of Authigenic Illite. 3600X, Gulf McClung, Depth: 4259 ft.

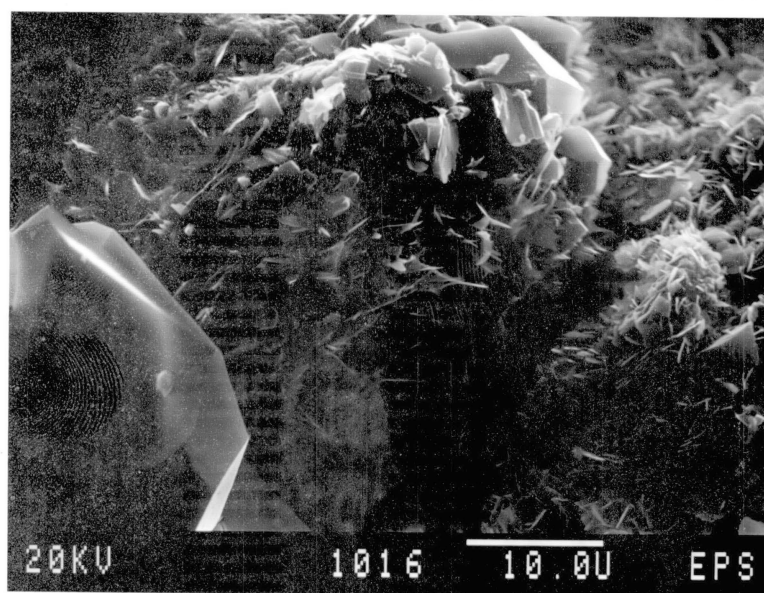


Figure 72. SEM Micrograph of Illite-Lined Quartz Grain and Chlorite Bridged Pore Space. 2000X, Shell Bedell, Depth: 4413 ft.

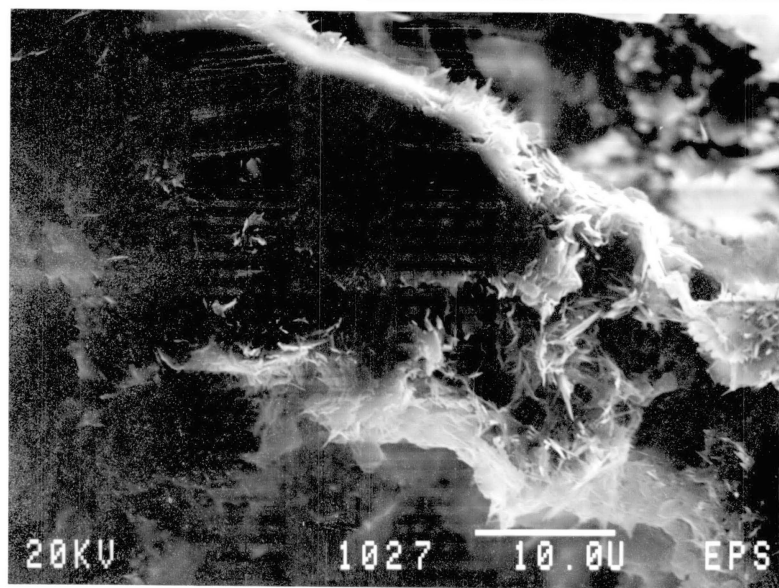


Figure 73. SEM Micrograph of Illite-Lined Corroded Quartz Grain. 2000X, Shell Bedell, Depth: 4446 ft.



Figure 74. SEM Micrograph of Authigenic Chlorite. 2400X, Shell Bedell. Depth: 4436 ft.

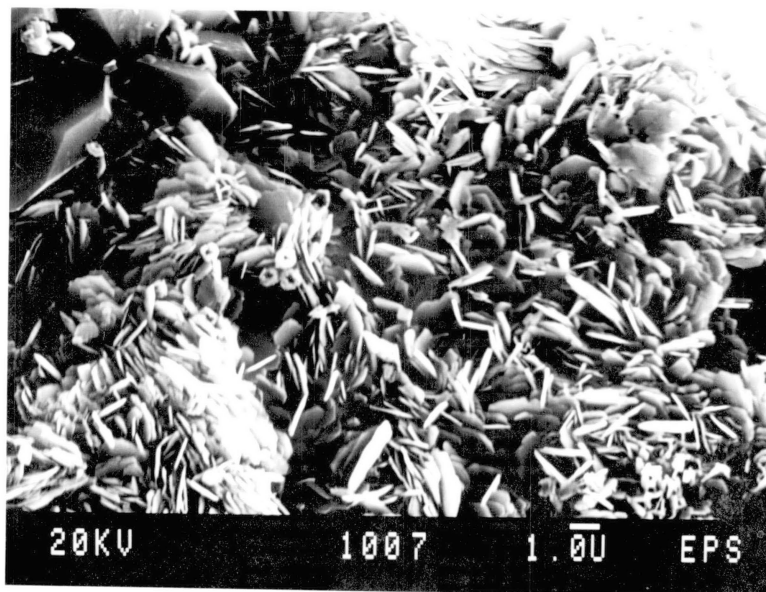


Figure 75. SEM Micrograph of Authigenic Chlorite.
4400X, Gulf McClung, Depth: 4184 ft.

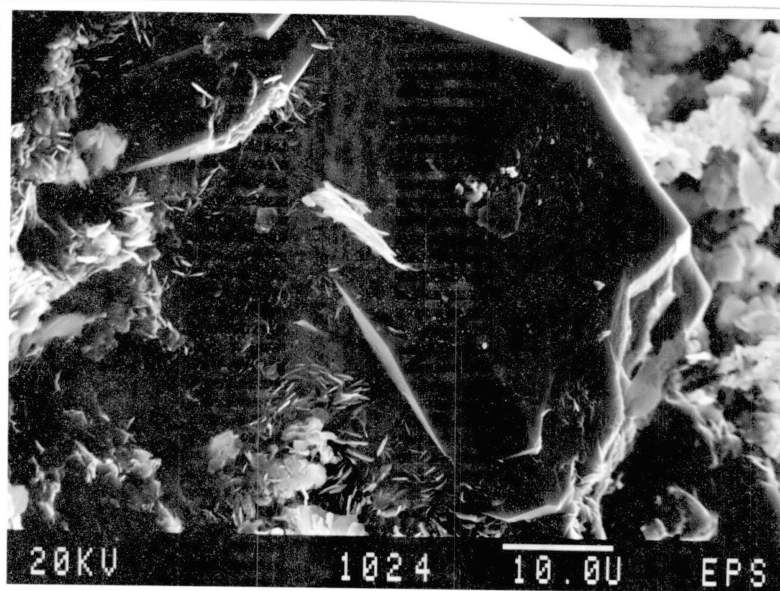


Figure 76. SEM Micrograph of Quartz Overgrowth and
Authigenic Chlorite Occupying Pore Space.
1600X, Shell Bedell, Depth: 4418 ft.

kaolinite to chlorite.

Other Diagenetic Constituents

Authigenic framboidal pyrite appeared to be fairly abundant upon scanning electron microscope examination of the samples (Figures 49, 59, and 64). The pyrite is usually found in association with carbonaceous matter, hematite, and fine grained detrital sediment.

Hematite is also present among the finer sediments. It is believed to be the oxidized alteration product of pyrite, an event that occurred in the late stages of diagenesis.

Diagenetic History

Detailed thin section analysis and scanning electron microscopy were the basis for determining the sequence of diagenetic events effecting the Laverty-Hoover Sandstone. Figure 76 shows the diagenetic history of the rock.

Early in the burial history of the rock, mechanical compaction caused the ductile deformation of micas and low rank metamorphic rock fragments, reducing primary porosity. Shortly afterwards, quartz overgrowths and silica precipitation took place.

After precipitation of the quartz overgrowths, the pH of the pore fluids became slightly basic resulting in the precipitation of calcium carbonate. The calcite invaded and corroded the earlier precipitated quartz overgrowths.

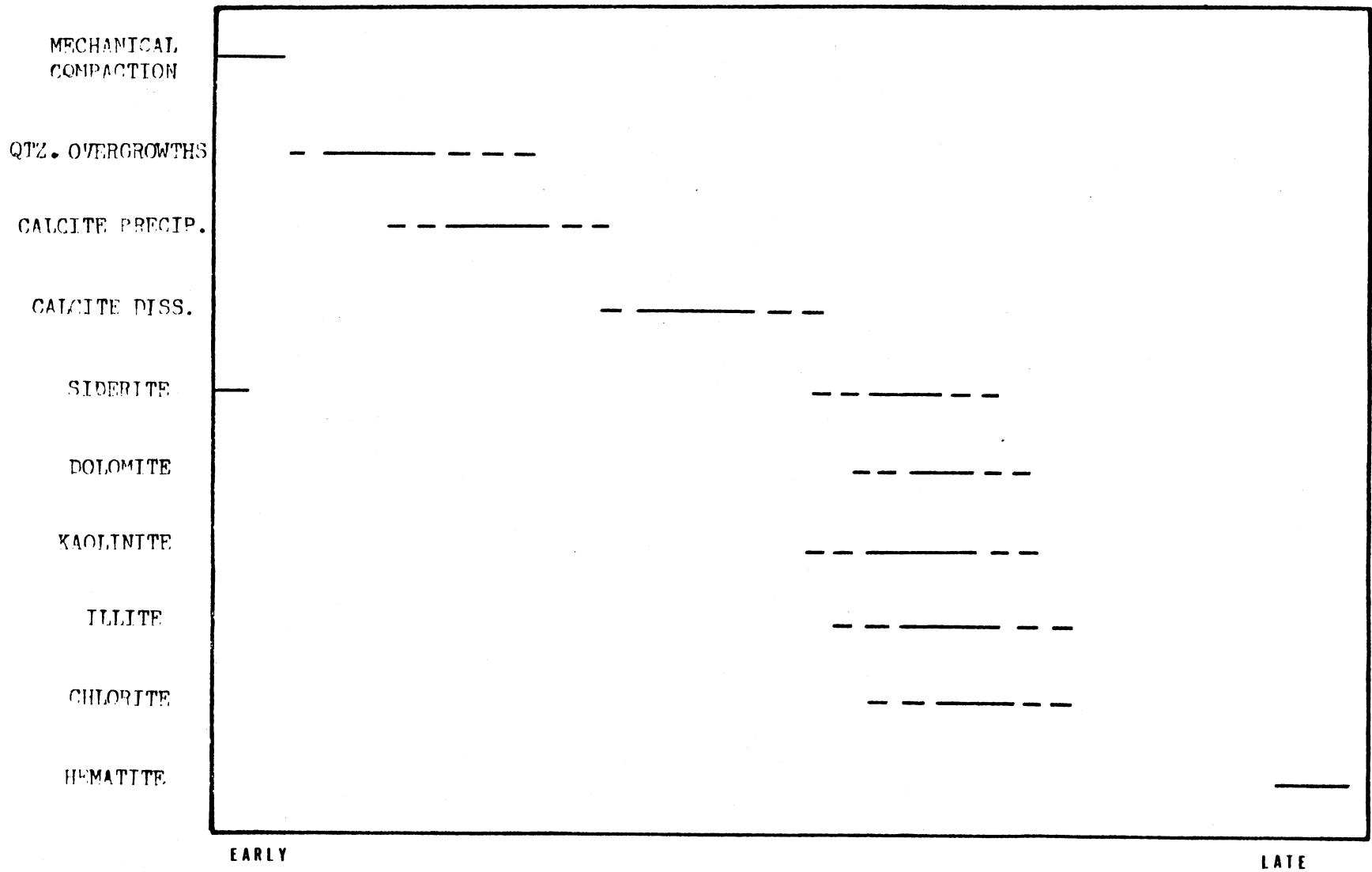


Figure 77. Diagenetic History of the Lavery-Hoover Sandstone.

Increasing depth of burial and temperature led to the maturation of nearby organic matter, which resulted in the production of carbonic acid. The acid dissolved much of the calcite and created a large amount of secondary porosity. Shortly after calcite dissolution, siderite precipitated along the outer boundaries of the remaining calcite. Conditions became favorable for the dolomitization of calcite in some areas.

Dissolution of feldspars and other unstable detrital constituents occurred shortly after calcite dissolution. Authigenic clays were formed during this time as a result of the dissolution of these unstable constituents.

Hematite formed late in the diagenetic sequence, and was probably an oxidized alteration product of pyrite.

CHAPTER VIII

POROSITY

Introduction

Porosity abundance and types of the Lavery-Hoover Sandstone were determined by thin section examination. Both primary and secondary types of porosity were recognized. Primary intergranular porosity is not extremely abundant, accounting for about 4.4% of the total rock in the samples that were examined. Secondary porosity is the most abundant porosity type in the rock averaging about 7.5% of the total rock in the samples that were examined. The purpose of this chapter is to describe the various types of primary and secondary porosities present in the Lavery-Hoover Sandstone.

Primary Porosity

Intergranular primary porosity, resulting from original depositional processes, is not abundant in the Lavery-Hoover Sandstone. Of the estimated 4.4% primary intergranular porosity, it is probable that a significant amount of these pore spaces were once occupied by authigenic calcite cement.

Secondary Porosity

As previously stated, secondary porosity is the most abundant porosity type accounting for 7.5% of the total rock. The bulk of this porosity is considered to have been created by the dissolution of authigenic calcite cement and feldspar grains.

A significant amount of primary intergranular porosity has been reduced by syntaxial quartz overgrowth cementation. The reduced intergranular pores are easily recognized and are usually triangular shaped (Figure 78). Syntaxial quartz cementation has reduced the effective porosity of the Lavery-Hoover Sandstone.

A much larger percentage of the primary intergranular pore spaces have been enlarged (Figure 79). It is believed that during the early stages of diagenesis, calcite cement occupied nearly all the available pore spaces in the rock. The calcite selectively replaced the less stable detrital material. In the later stages of diagenesis, the calcite cement was dissolved creating enlarged secondary pore spaces.

The dissolution of feldspar grains has also created a significant amount of secondary porosity in the Lavery-Hoover Sandstone. Some feldspars have been partially dissolved and honeycombed grains allow petrographic recognition (Figure 58). Grain molds are abundant and provide good evidence for complete dissolution of some

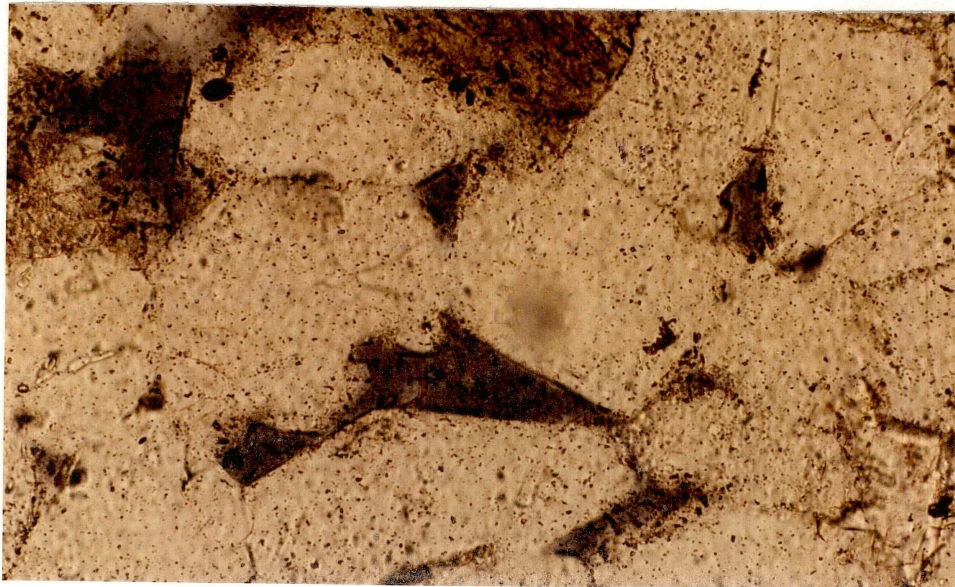


Figure 78. Photomicrograph Showing Reduced Primary Intergranular Porosity. 200X, PP, Shell Bedell, Depth: 4419 ft.

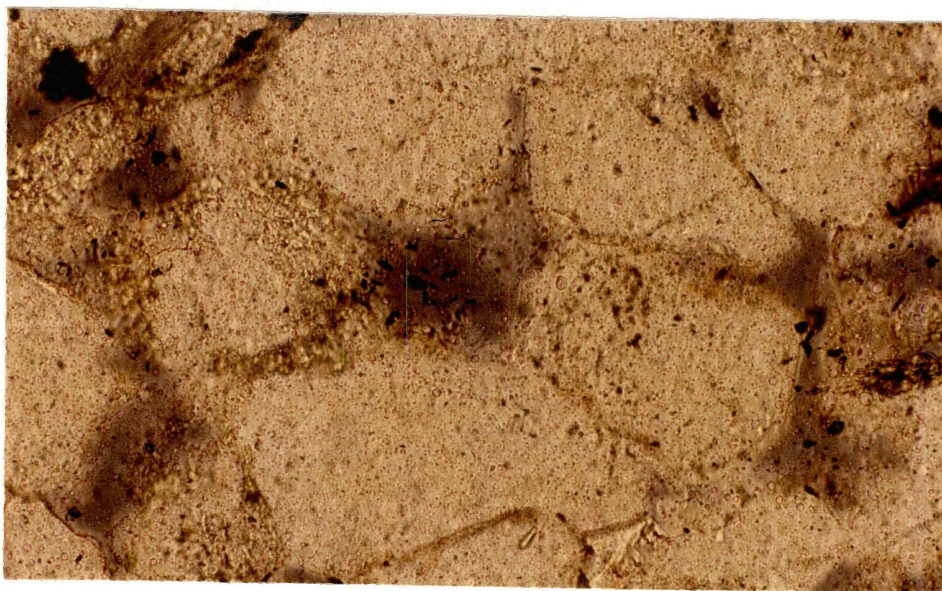


Figure 79. Photomicrograph of Enlarged Intergranular Porosity. 200X, PP, Gulf McClung, Depth: 4171 ft.

feldspar grains (Figures 57 and 80).

Dissolution of the detrital matrix is not extremely abundant, however, in some areas it has created thin, elongate, porous zones (Figures 63 and 81). Apparently, the fine grained matrix material was selectively removed along bedding planes in many areas. The dissolution of metamorphic rock fragments can be recognized throughout the rock. Secondary porosity created from this event is of minor importance.

Microporosity exists in the Lavery-Hoover Sandstone in almost every sample that was examined. The pore apertures of this type of porosity are too small to contribute to the effective porosity of the rock. Microporosity is seen most often in association with authigenic clays, especially between kaolinite booklets (Figure 82). Occasionally, this type of porosity may be seen within the detrital matrix of the Lavery-Hoover Sandstone.

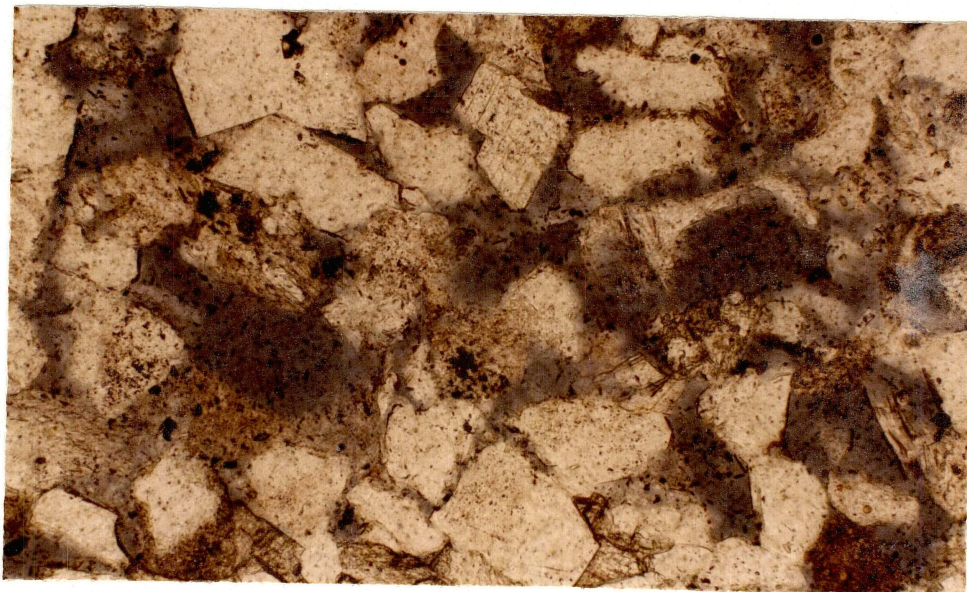


Figure 80. Photomicrograph Showing Grain Molds. 100X, PP, Gulf McClung, Depth: 4204 ft.

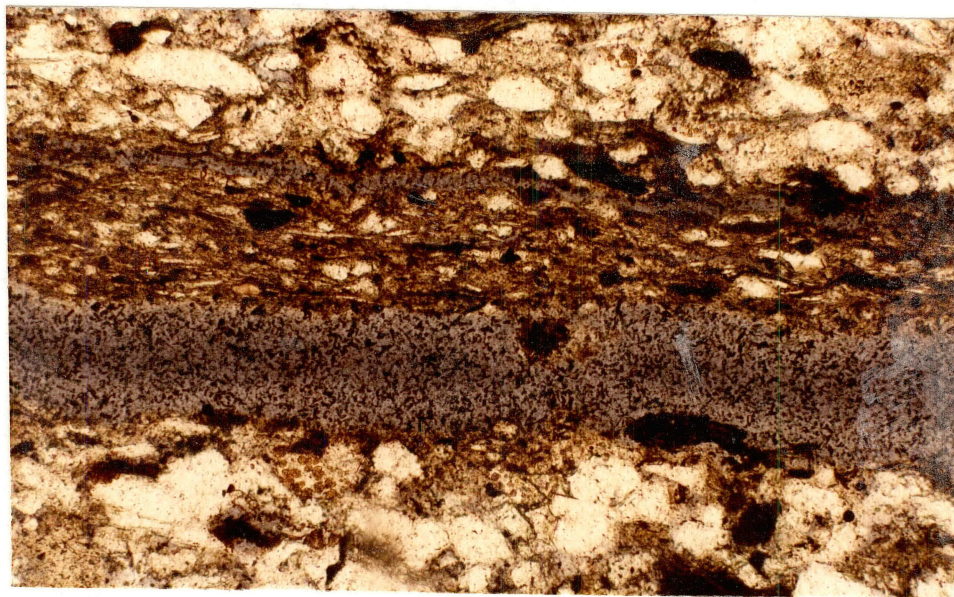


Figure 81. Photomicrograph Showing Dissolved Detrital Matrix. 100X, PP, Shell Bedell, Depth: 4408 ft.

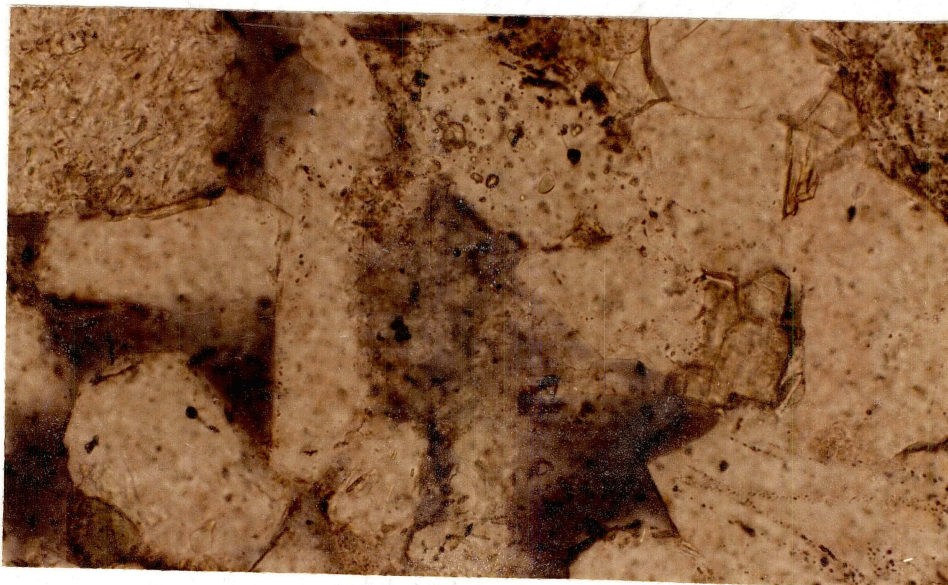


Figure 82. Photomicrograph of Microporosity. 200X, PP,
Gulf McClung, Depth: 4204 ft.

CHAPTER IX

CONCLUSIONS

The following conclusions may be made from this study:

1) The area of study is on the Northern shelf of the Anadarko Basin, and the east-west oriented sand body is tilted to the south creating an ideal stratigraphic trap along the northern limits of the sand.

2) P.V.U. 4 represents one complete transgressive-regressive cycle of sedimentation. In the transgressive phase, conditions were favorable for limestone deposition on the shelf and basin. In the following regressive phase, a fluvial-deltaic clastic system prograded into the basin.

3) The clastic material is considered to have been derived from the Ouachita foldbelt.

4) The delta front seems to have been reworked by wave action. The delta may best be classified as a high constructive lobate delta.

5) Most of the samples examined may be classified petrologically as sublitharenites. The sand is dominated by quartz, contains a small amount of feldspar, and contains abundant low rank metamorphic rock fragments.

6) The diagenetic history of the Laverty-Hoover Sandstone may be summarized as follows: (a) reduction of

primary porosity by mechanical compaction and silica precipitation shortly followed by calcite cementation, (b) dissolution of calcite cement and chemically unstable detrital constituents (primarily feldspars), (c) precipitation of authigenic clays and siderite and dolomitization of calcite, and (d) alteration of pyrite to hematite.

7) Most of the original primary intergranular porosity has been destroyed. Secondary porosity is more abundant than primary porosity in the Laverty-Hoover Sandstone. Dissolution of calcite cement and detrital feldspar grains has created most of this secondary porosity.

SELECTED BIBLIOGRAPHY

- Al-Shaieb, Z., and Shelton, J. W., 1981, Migration of Hydrocarbons and Secondary Porosity in Sandstones: Amer. Assoc. of Petr. Geol. Bull., V. 55, No. 11, pp. 2433-2436.
- Al-Shaieb, Z., 1984, Personal Communication.
- Brown, L. F. Jr., Cleaves, A. W. II, and Erxleben, A. W., 1973, Pennsylvanian Depositional Systems in North Central Texas: A Guide for Interpreting Terrigenous Clastic Facies in a Cratonic Basin: Texas Univ. Bur. Econ. Geol. Guidebook 14, 122 p.
- Brown, L. F. Jr., 1979, Deltaic Sandstone Facies in the Midcontinent, in Pennsylvanian Sandstones of the Midcontinent: Tulsa Geol. Soc. Spec. Pub. No. 1, pp. 35-63.
- Busch, D. A., 1971, Genetic Units in Delta Prospecting: Amer. Assoc. Petr. Geol. Bull., V. 55, pp. 1137-1154.
- Fisher, W. L., Brown, L. F. Jr., Scott, A. J., and McGowen, J. H., 1969, Delta Systems in the Exploration for Oil and Gas: Bur. Econ. Geol., Univ. of Texas at Austin, Texas. pp. 1-22.
- Fisher, W. L., 1969, Gulf Coast Basin Tertiary Delta Systems, in Delta Systems in the Exploration for Oil and Gas: Bur. Econ. Geol. Univ. of Texas at Austin, Texas. pp. 30-39.
- Fisher, W. L., and Brown, L. F. Jr., 1972, Clastic Depositional Systems--A Genetic Approach to Facies Analysis: Bur. Econ. Geol. Univ. of Texas at Austin, Texas. 211 p.
- Forgotson, J. M. Jr., 1957, Nature, Usage, and Definition of Marker Bed Defined Vertically Segregated Rock Units: Amer. Assoc. Petr. Geol. Bull. V. 41, pp. 2108-2113.

- Frezon, S. E., and Dixon, G. H., 1975, Texas Panhandle and Oklahoma, in Paleotectonic Investigations of the Pennsylvanian System., Part I: Introduction and Regional Analysis of the Pennsylvanian System. McKee, E. D., and Crosby, E. J. (Eds.), pp. 175-195.
- Gibbons, K. E., 1960, Pennsylvanian of the North Flank of the Anadarko Basin. Unpublished Masters Thesis, Univ. of Okla.
- Gibbons, K. E., 1962, Pennsylvanian of the North Shelf of the Anadarko Basin. The Shale Shaker Digest. V. 12, No. 5, pp. 2-19.
- Hayes, J. B., 1979, Sandstone Diagenesis--The Hole Truth. in Aspects of Diagenesis: SEPM Spec. Pub. No. 26, pp. 127-139.
- Huffman, G. G., 1958, Geology of the Flanks of the Ozark Uplift, Northeastern Okla.: Okla. Geol. Sur. Bull., No. 77.
- Jordan, L., Pate, J. D., and Williamson, S. R., 1959, Petroleum Geology of Harper County, Oklahoma: Okla. Geol. Sur. Bull. 80, pp. 69-92.
- Jordan, L., 1967, Geology of Oklahoma: Okla. Geol. Notes, V. 27, pp. 215-228.
- Klein, G., 1980, Sandstone Depositional Models for Exploration for Fossil Fuels: Burgess Publishing Co., 149 p.
- Lane, S. D., 1978, Relationships of the Carbonate Shelf and Basinal Clastic Deposits of the Missourian and Virgilian Series of the Pennsylvanian System in Central Beaver County, Oklahoma: Unpublished Masters Thesis, Oklahoma State Univ.
- Pate, J. D., 1962, Laverne Gas Area, Beaver and Harper Counties, Oklahoma, in Natural Gases of North America: Amer. Assoc. Petr. Geol. Memoir 9., Vol. 2, pp. 1509-1524.
- Pittman, E. D., and Wilson, M. D., 1977, Authigenic Clays in Sandstones: Recognition and Influence on Reservoir Properties and Paleoenvironmental Analysis: Jour. of Sed. Petr., V. 47, No. 1, pp. 3-31.
- Pittman, E. D., 1979, Porosity, Diagenesis, and Productive Capability of Sandstone Reservoirs in Aspects of Diagenesis: SEPM Spec. Pub. No. 26, pp. 159-173.

- Rascoe, B. Jr., 1962, Regional Stratigraphic Analysis of Pennsylvanian and Permian Rocks in Western Midcontinent Colo., Kansas, Okla., Texas: Amer. Assoc. of Petr. Geol. Bull., V. 46, No. 8, pp. 1345-1370.
- Rascoe, B. Jr., 1978, Sedimentary Cycles in the Virgilian Series of the Anadarko Basin; The Shale Shaker Digest. V. 28, pp. 120-123, 144-149.
- Rascoe, B. Jr., Genetic Units in Petroleum Exploration. Unpublished.
- Rascoe, B. Jr., and Adler, F. J., 1983, Permo-Carboniferous Hydrocarbon Accumulations, Midcontinent, U.S.A.: Amer. Assoc. Petr. Geol. Bull., V. 67, No. 6, pp. 979-1001.
- Rascoe, B. Jr., 1982-1984, Personal Communication.
- Schmidt, V., and McDonald, D. A., 1979, The Role of Secondary Porosity in the Course of Sandstone Diagenesis: SEPM Spec. Pub. No. 26, pp. 175-207.
- Schmidt, V., and McDonald, D. A., 1979, Texture and Recognition of Secondary Porosity in Sandstones: SEPM Special Pub. No. 26, pp. 209-225.
- Stewart, G. F., 1975, Kansas, in Paleotectonic Investigations of the Pennsylvanian System, Part 1: Introduction and Regional Analysis of the Pennsylvanian System: McKee, E. D., and Crosby, E. J. (Eds.), pp. 155-173.
- Swanson, D. 1980, Handbook of Delta Facies: Lafayette Geological Society, Subsurface Clastic Facies Workshop. 81 p.
- Totten, R. B., 1956, General Geology and Historical Development, Texas and Oklahoma Panhandles: Bull. Amer. Assoc. Petr. Geol., V. 40, No. 8, pp. 1945-1967.
- Wilson, J. L., 1975, Carbonate Facies in Geologic History: N.Y. Heidelberg Berlin Springer Verlag. 471 p.

VITA \

Douglas Lynn Yelken

Candidate for the Degree of
Master of Science

Thesis: DEPOSITIONAL ENVIRONMENT, PETROLOGY, AND DIAGENESIS
OF THE LAVERTY-HOOVER SANDSTONE IN BEAVER, HARPER,
ELLIS, AND WOODWARD COUNTIES, OKLAHOMA AND
LIPSCOMB COUNTY, TEXAS

Major Field: Geology

Biographical:

Personal Data: Born in Bartlesville, Oklahoma, the
son of Jack and Leola Yelken.

Education: Received Bachelor of Science degree in
Geology, December, 1982, from Oklahoma State
University; completed requirements for the
Master of Science degree at Oklahoma State
University in May, 1985.

Professional Experience: Seismic Crew Laborer in the
summer of 1980 for Phillips Petroleum Co.
Geophysicist, in the summers of 1981 and 1982 for
Phillips Petroleum Co., Geologist for Phillips
Petroleum Co. in the summers of 1983 and 1984 for
Phillips Petroleum Co. (Bartlesville, Oklahoma).

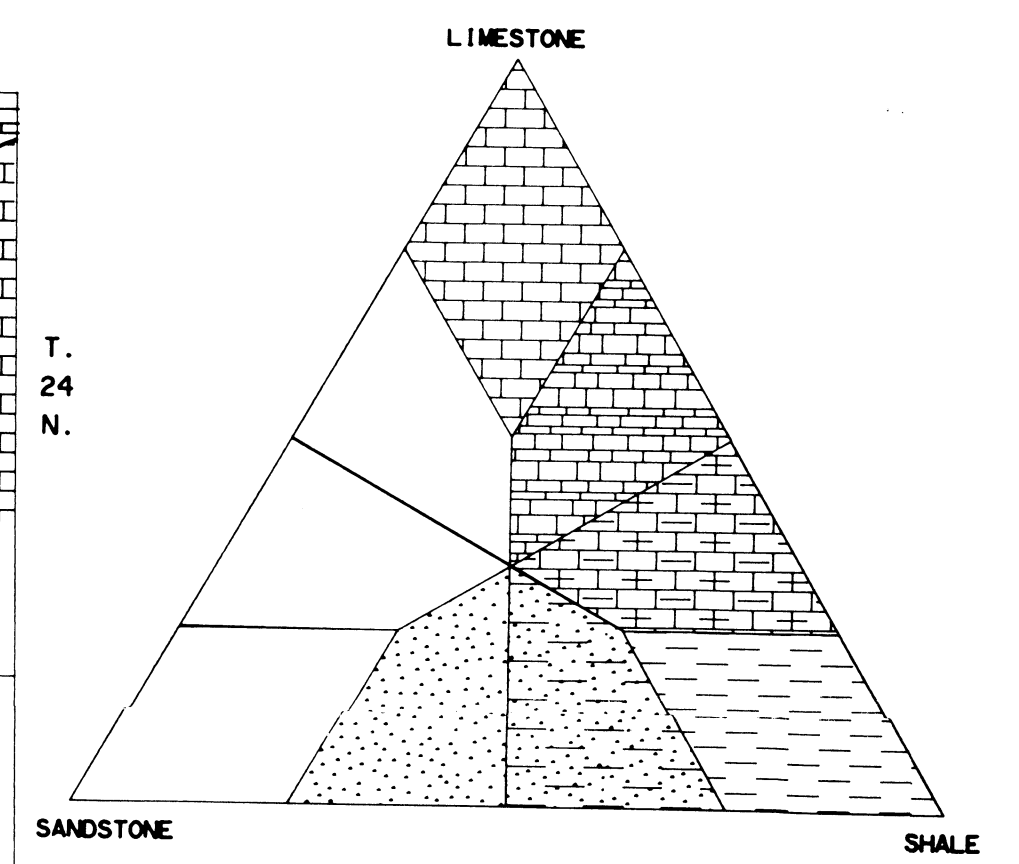
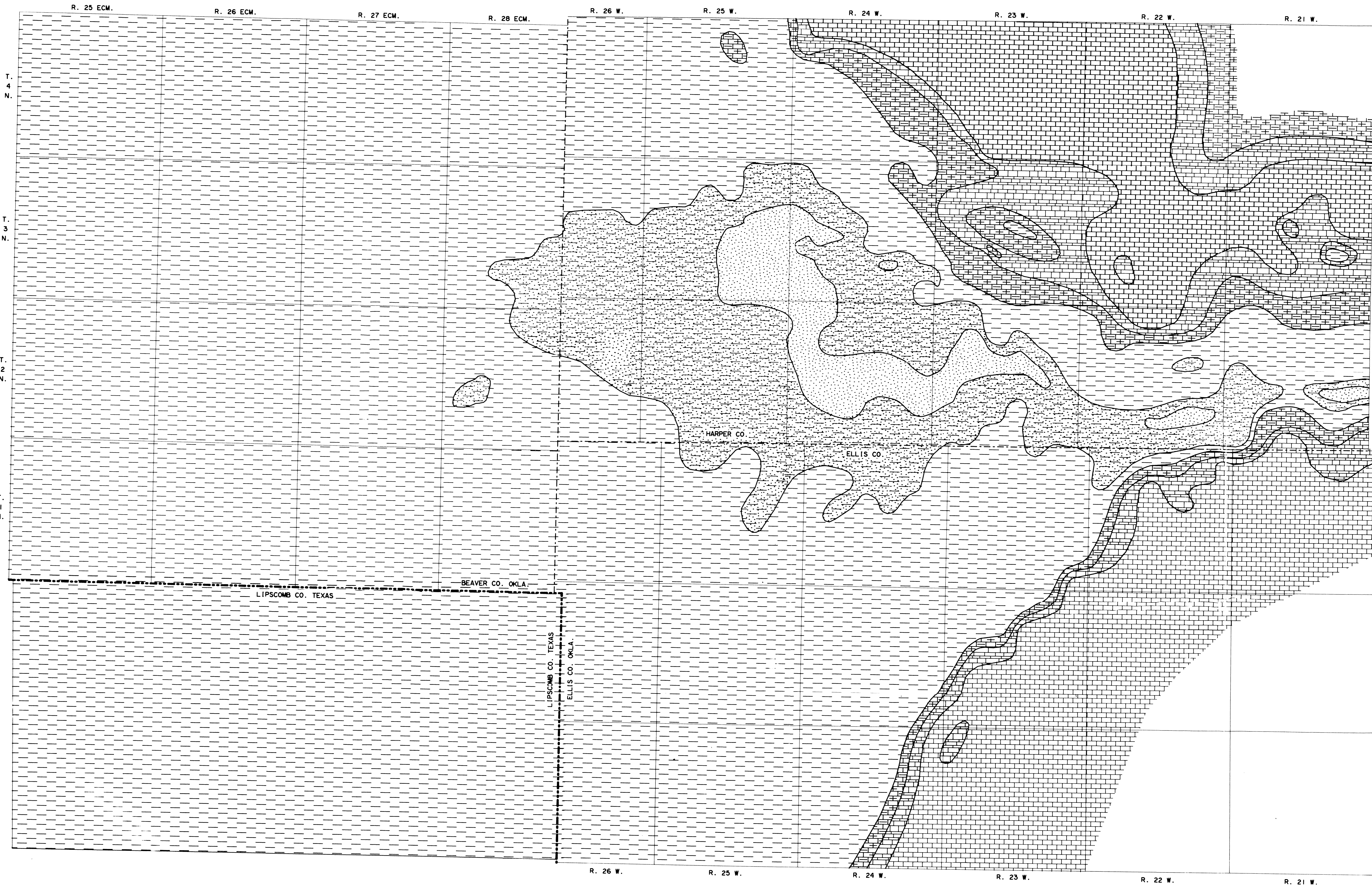


PLATE I
LITHOFACIES MAP OF P.V.U. 4
CONTAINING THE
LAVERY-HOOVER SANDSTONE
PLATE I
0 1 2
MILES
BY: DOUG YELKEN 1984

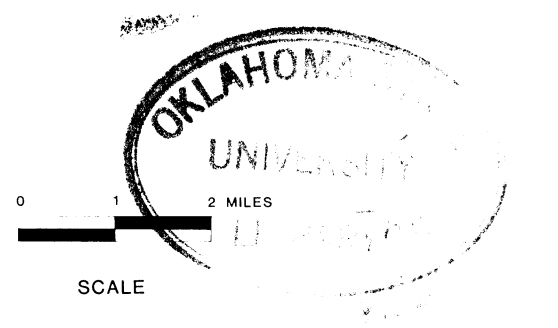
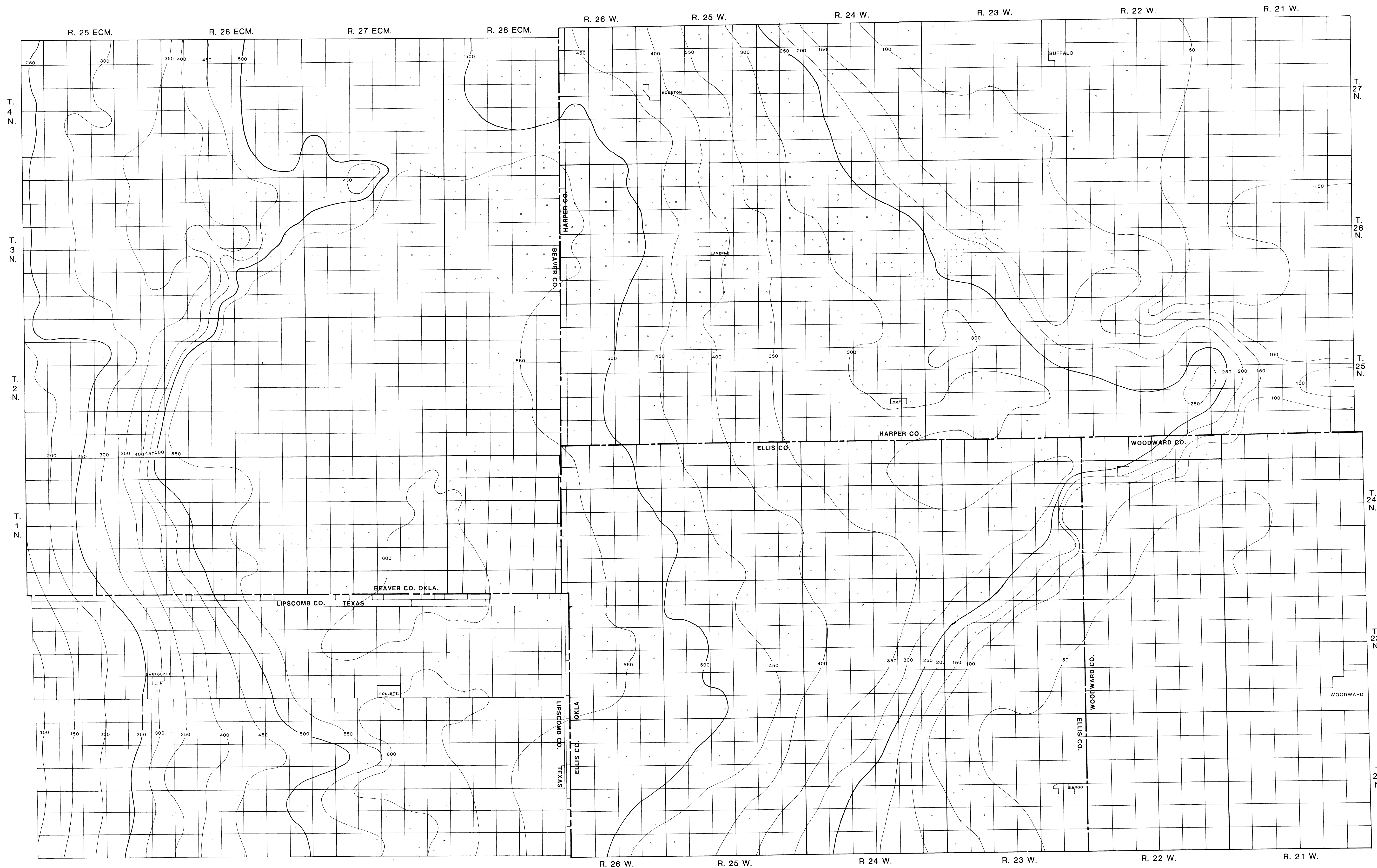


PLATE II
 ISOPACH MAP OF P.V.U. 4
 CONTAINING THE
 LAVERTY - HOOVER SANDSTONE
 C. I. : 50 FEET
 BY: DOUG YELKEN 1984

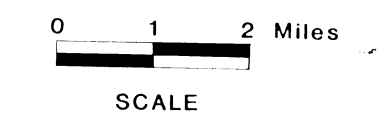
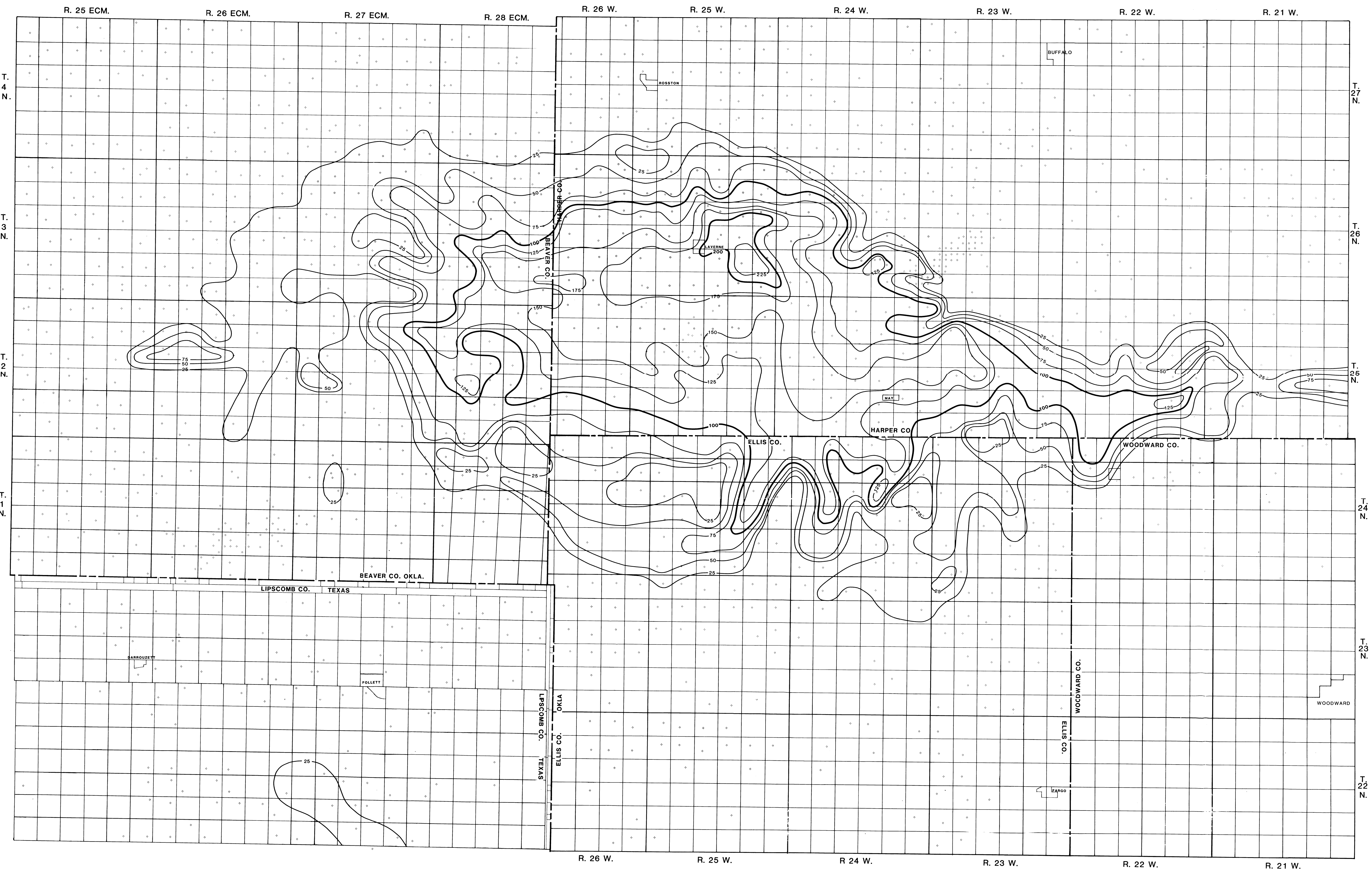
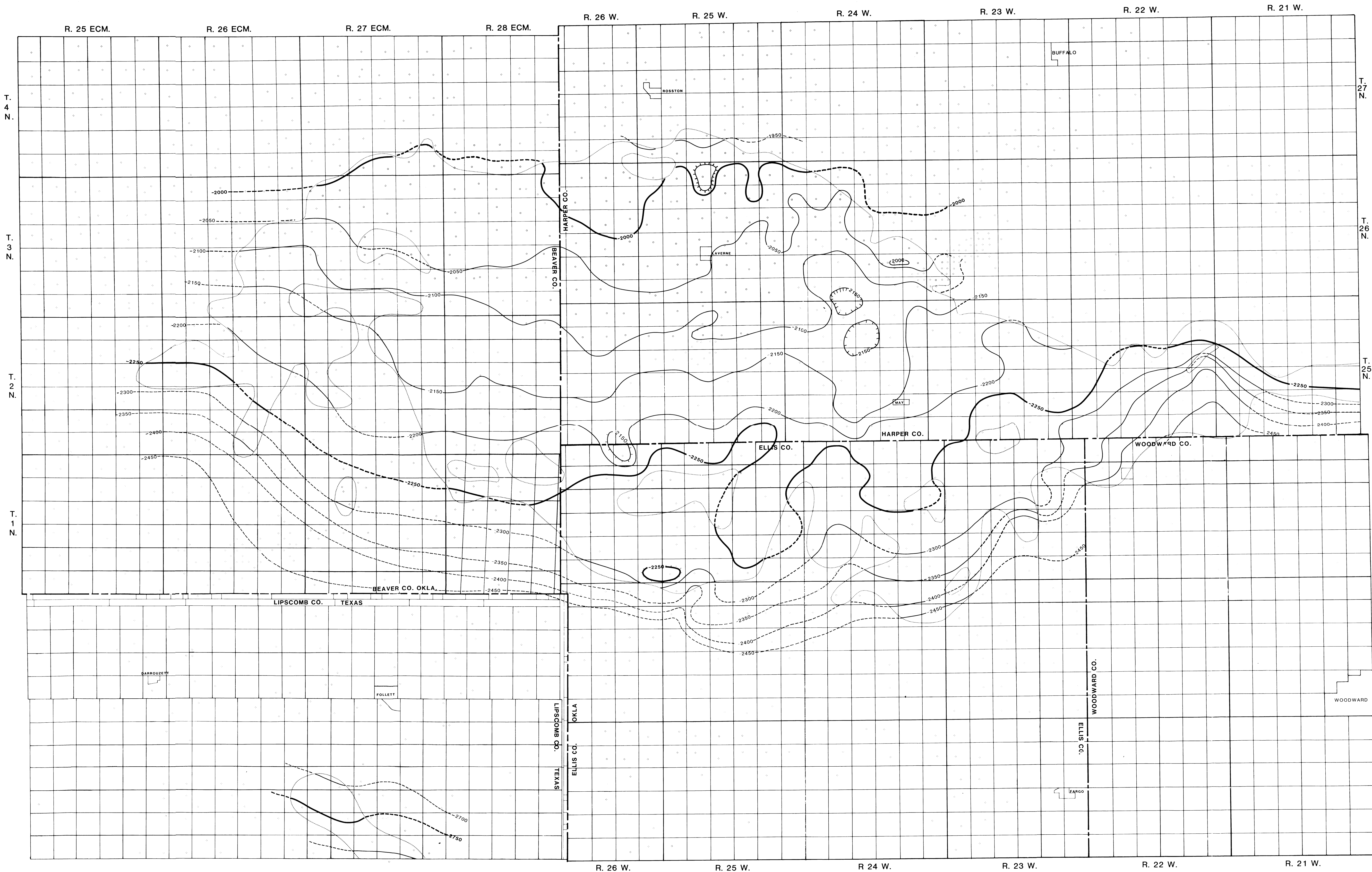


PLATE III
 SANDSTONE ISOLITH MAP
 OF THE
 LAVERTY - HOOVER
 SANDSTONE
 C.I.: 25 FT
 BY: DOUG YELKEN 1984



- SAND < 25' THICK
- - - - - STRUCTURAL CONTOUR < 25' OF SAND
- STRUCTURAL CONTOUR > 25' OF SAND

STRUCTURAL CONTOUR MAP
 OF THE
 LAVERY-HOOVER SANDSTONE
 PLATE IV
 0 1 2
 MILES

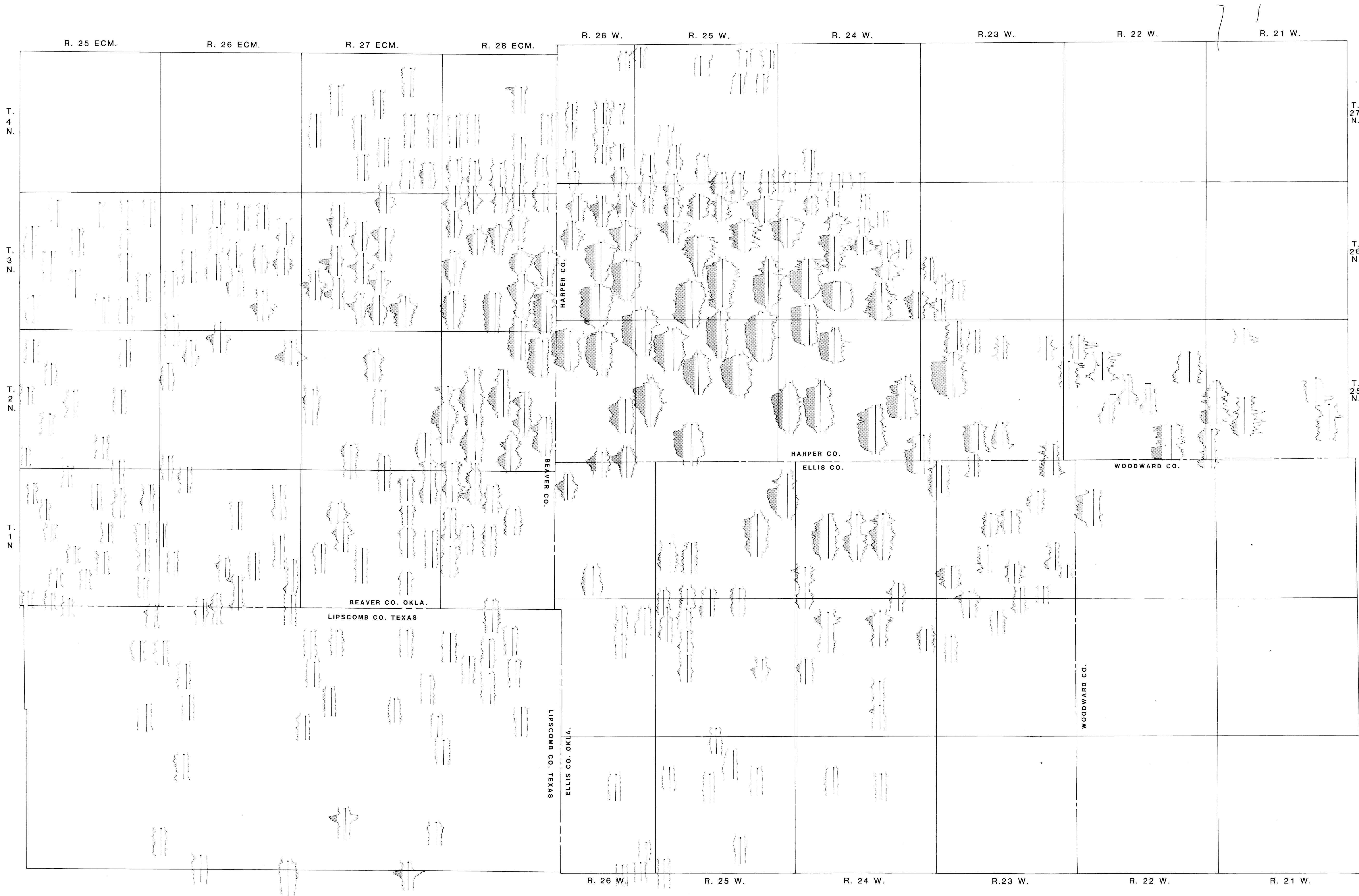


PLATE V
 SP - RESISTIVITY
 CHARACTERISTICS
 OF THE
 LAVERTY - HOOVER SANDSTONE

BY: DOUG YELKEN 1984



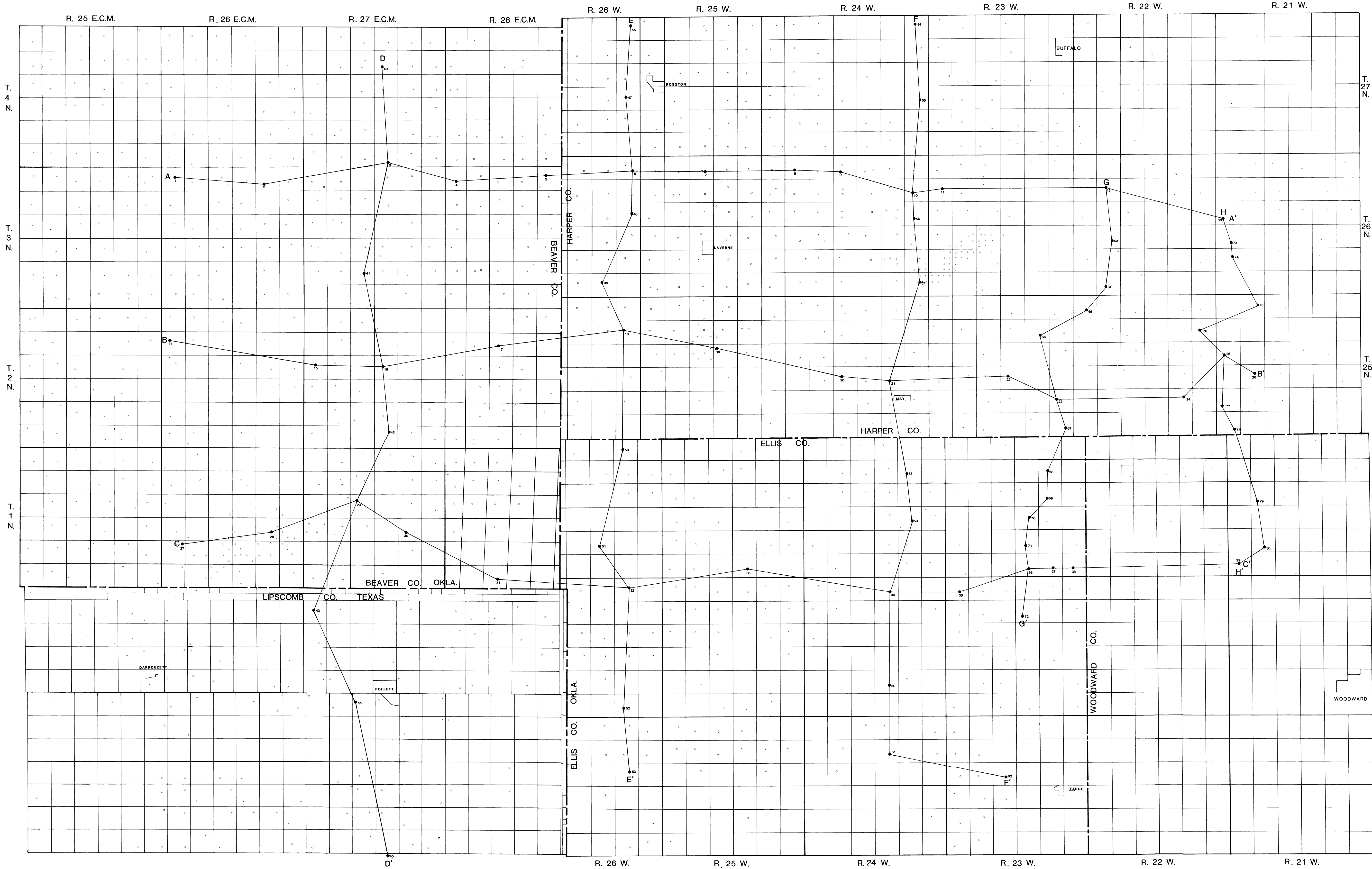


PLATE VI

CROSS-SECTION

LOCATION MAP

BY: DOUG YELKEN 1984

(80 wells - total)



PLATE VII

EAST-WEST STRATIGRAPHIC CROSS SECTION






PLATE IX

EAST - WEST STRATIGRAPHIC CROSS SECTION

C

C'


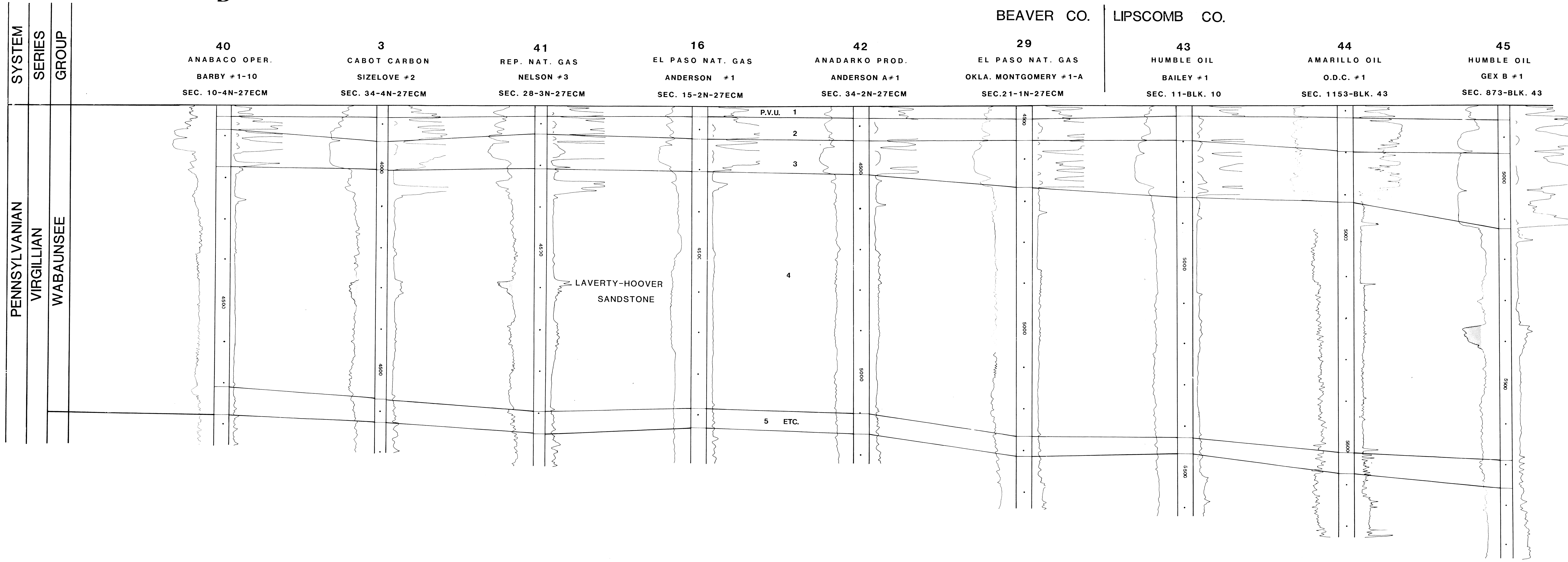




PLATE X

NORTH-SOUTH STRATIGRAPHIC CROSS SECTION

	BEAVER CO.					LIPSCOMB CO.				
D	40 ANABACO OPER. BARBY #1-10 SEC. 10-4N-27ECM	3 CABOT CARBON SIZELOVE #2 SEC. 34-4N-27ECM	41 REP. NAT. GAS NELSON #3 SEC. 28-3N-27ECM	16 EL PASO NAT. GAS ANDERSON #1 SEC. 15-2N-27ECM	42 ANADARKO PROD. ANDERSON A#1 SEC. 34-2N-27ECM	29 EL PASO NAT. GAS OKLA. MONTGOMERY #1-A SEC. 21-1N-27ECM	43 HUMBLE OIL BAILEY #1 SEC. 11-BLK. 10	44 AMARILLO OIL O.D.C. #1 SEC. 1153-BLK. 43	45 HUMBLE OIL GEX B #1 SEC. 873-BLK. 43	D'



SYSTEM
SERIES
GROUP

PENNSYLVANIAN
VIRGILLIAN
WABAUNSEE



PLATE XI

NORTH-SOUTH STRATIGRAPHIC CROSS SECTION

HARPER CO. | ELLIS CO.

E

E'

SYSTEM
SERIES
GROUP
PENNSYLVANIAN
VIRGILLIAN
WABAUNSEE

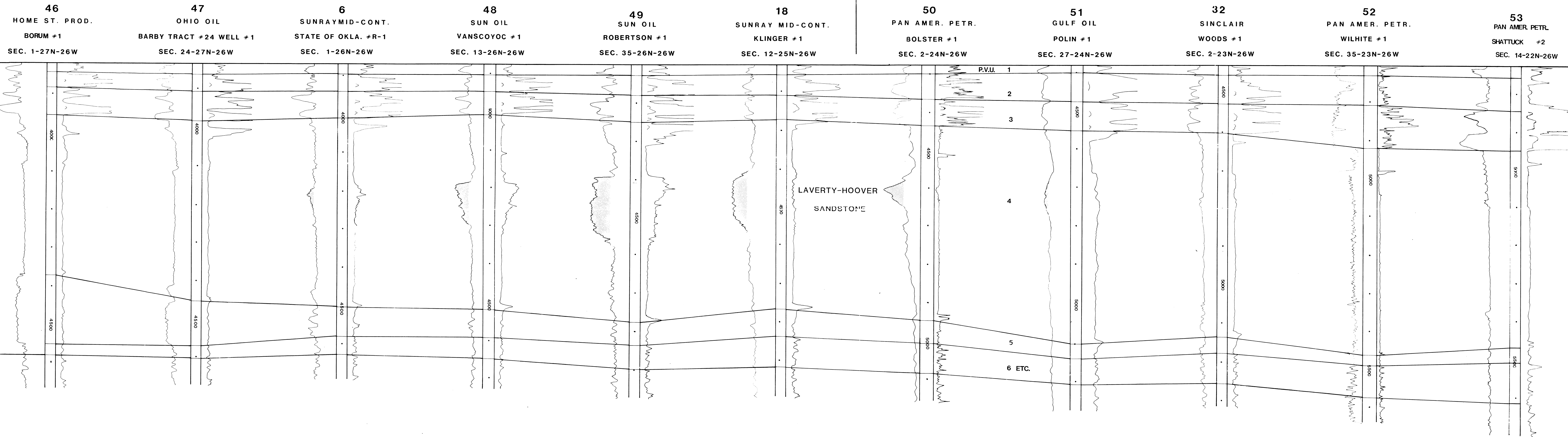




PLATE XII

NORTH-SOUTH STRATIGRAPHIC CROSS SECTION

HARPER CO. | ELLIS CO.

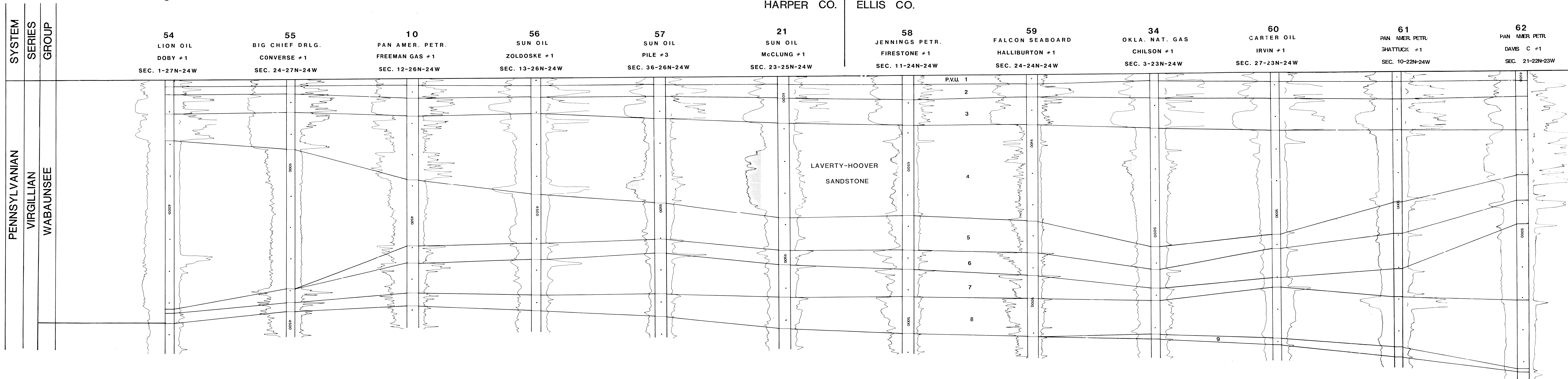





PLATE XIII

NORTH-SOUTH STRATIGRAPHIC CROSS SECTION

G

G'



PENNSYLVANIAN
VIRGILLIAN
WABAUNSEE

LAVERTY-HOOVER
SANDSTONE

P.V.U. 1

2

3

4

5

6

7

8

9



PLATE XIV

NORTH-SOUTH STRATIGRAPHIC CROSS SECTION

HARPER CO. | WOODWARD CO.

H

H'

